UNIVERSITY OF VERONA

DEPARTMENT OF DIAGNOSTIC AND PUBLIC HEALTH

PH.D. SCHOOL OF NATURAL SCIENCES AND ENGINEERING

PH.D. IN

NANOSCIENCE AND ADVANCED TECHNOLOGIES

Scholarship funded by the University of Verona

CYCLE / YEAR of initial enrolment: XXXIV / 2018

ENZYMATIC AND MODERN MECHANICAL APPROACHES TO ISOLATE, AND CHARACTERIZE STROMAL VASCULAR FRACTION TO STUDY ADIPOGENESIS *IN VITRO* AND *IN VIVO* FOR ITS POSSIBLE APPLICATION IN RECONSTRUCTIVE AND REGENERATIVE MEDICINE

S.S.D. (Disciplinary Sector): BIO/16 – Anatomia Umana

Coordinator: Prof. Dr Adolfo Speghini

Signature:

Tutor: Prof. Dr Andrea Sbarbati

Signature:

Ph.D. Candidate: Dr. Reetuparna Biswas:

Doctoral Thesis by Dr Reetuparna Biswas

Submitted to U-GOV University Research Catalogue

Verona, 30 November 2021

ISBN

Sommario

Cellule staminali mesenchimali e loro procedure di estrazione: il tessuto adiposo (grasso corporeo) è fondamentale per la salute e un'importante fonte di MSC. Insieme alle cellule adipose e staminali, il tessuto adiposo contiene numerose cellule nervose e vasi sanguigni. Si ritiene che le MSC siano un elemento chiave per l'adipogenesi che può essere isolata dal grasso corporeo dopo la liposuzione. Nella medicina rigenerativa e negli interventi di chirurgia plastica, il grasso della liposuzione viene elaborato in diversi meccanismi per isolare la SVF che viene poi rimessa all'uomo per diversi scopi di trattamento.

Materiale e metodo: nel nostro esperimento, abbiamo mostrato tre nuove procedure meccaniche e una enzimatica per elaborare il grasso, che richiedono meno tempo e sono più efficienti rispetto ad altre procedure esistenti. Nelle tre procedure, una è Rigenera® che impiega circa 12 minuti per essere processata mentre le altre due sono Hy-Tissue SVF e Hy-Tissue Nanofat di Fidia Pharmaceuticals che impiegano circa 10 minuti per processare il grasso. Dopo l'elaborazione meccanica è stata raccolta la SVF, di cui una parte è stata assegnata al monitoraggio della crescita in vitro e alla differenziazione in diverse linee cellulari. Un'altra parte è stata assegnata al test di citometria a flusso per vedere il contenuto di cellule staminali presenti al passaggio 0. Nel caso di Rigenera, la SVF ottenuta è stata sottoposta al ginocchio del cane per osservarne la capacità di differenziazione. Nel caso di Hy-Tissue SVF, una parte di SVF raccolta è stata iniettata per via sottocutanea a topi con/senza scaffold semi-liquido (HA) per osservare l'adipogenesi. Per il processo enzimatico, è stato eseguito solo il test di tossicità in vitro confrontando con la procedura di digestione dei grassi esistente, ovvero la digestione con collagenasi di tipo I.

Risultati: Tutto il processo meccanico ed enzimatico ci ha dato buoni risultati positivi. Abbiamo osservato l'adipogenesi sia in vitro che *in vivo* con la SVF che abbiamo isolato dalle procedure meccaniche.

Conclusione: queste nuove tecniche e dispositivi sono pronti per sostituire alcune vecchie tecniche che richiedono molto tempo. I nostri esperimenti hanno mostrato un miglioramento vitale nell'elaborazione del grasso e nell'isolamento delle MSC, che è economico e potrebbe essere facilmente utilizzato nei trattamenti rigenerativi da chiunque senza alcuna precedente esperienza in questo campo.

Abstract

Mesenchymal stem cells and their extraction procedures: Adipose tissue (body fat) is crucial for health and an essential source of MSCs. Along with fat & stem cells, adipose tissue contains numerous nerve cells and blood vessels. MSCs are essential for adipogenesis that can be isolated from body fat after liposuction. In regenerative medicine and plastic surgeries, Liposuctioned fat is processed in different mechanisms to isolate SVF and then put back into humans for different treatment purposes.

Material & method: In our experiment, we have shown three new mechanical and one enzymatic procedure to process the fat, which is less time-consuming and more efficient than other procedures. Of the three procedures, one is Rigenera® which takes around 12 min to process, whereas the other two are Hy-Tissue SVF and Hy-Tissue Nanofat from Fidia Pharmaceuticals, taking about 10 min to process the fat. After mechanical processing, the SVF was collected, of which one part was assigned to *in vitro* growth monitoring and differentiation to different cell lines. Another part was assigned to the flow cytometry test to see the stem cell content at passage 0. In the case of Rigenera, the SVF obtained was subjected to the knee of the dog to observe its differentiation ability. In the case of Hy-Tissue SVF, a part of collected SVF was injected subcutaneously to mice with/ without semi-liquid scaffold (HA) to observe adipogenesis. For the enzymatic process, only in vitro toxicity test was compared with the existing gold stand procedure of fat digestion, i.e., Collagenase Type-I digestion.

Results: The mechanical and enzymatic process has given us good positive results. We have observed adipogenesis both in vitro and *in vivo* with the SVF we isolated from the mechanical procedures.

Conclusion: These new techniques and devices are ready to replace some old time-consuming methods. Our experiments have shown vital improvement in fat processing and isolating MSCs, which are cheap and could be easily used in regenerative treatments by anyone without any previous expertise.

Acknowledgements

First and foremost, I want to thank my PhD tutor Andrea Sbarbati to give me the chance of entering the doctoral school at the University of Verona. I appreciate all his contributions of time and ideas to make my PhD experience productive and stimulating. I am also thankful for the excellent example of a successful biologist and professor.

The members of the Sbarbati group have initially contributed immensely to my personal and professional time at Verona. I am incredibly grateful to Elena Dai Pre for her advice, mentorship and teaching me how to work in a research lab whenever needed. I want to acknowledge the contribution of Silvia Manucci, Alice Busato, Ilaria Scambi, Paolo Bernardi, Prof. Patricia Lievens, Emanuela Grandis, and Laura Marcazzan for their immense support and advice from the very beginning to the end of my doctoral study. I thank Dr Michele Riccio, Francesco De Francesco, and Carlo Soranzo for their frequent transfer of adipose tissues and the necessary devices. I appreciate Samantha Solito and Giulio Fracasso's help in their time to process our samples in the Flow cytometer. I thank my lab-mate friends, Alice, Elena, Silvia, Nidula, Vikas, Mathieu, Molakun & L. A. Q. Sierra, for their support during my lab days. I especially thank Martina Loro for her help regarding my accommodation in Verona.

I am thankful to Prof. Federica Bortolotti, Prof. Franco Tagliaro, and Prof. Adolfo Speghini for their official support and the absolute authority of the University of Verona for granting me funds for my summer school at the University of Pisa and the internationalisation award to spend a period abroad at the Harvard Medical School.

I would like to especially thank Professor Dr Shiv Pillai from Harvard Medical School to bless me with the opportunity of working under his supervision with all his laboratory members, especially Dr Vinay Mahajan during my period at the Ragon Institute of MGH, Harvard & MIT of my Doctoral study where I started loving almost 12 hours period in the lab with learning different molecular and microbiological techniques. Their mentorship helped me know 'how to think' and blessed me with exposure to the world of immunology, which taught me to embrace biological science to better develop my career.

Lastly, I would like to thank my family and soulmate Arghya for supporting me in all my pursuits from the beginning to the end of my doctoral years. Thank you!

Reetuparna Biswas
Kolkata, India
September 2022

Abbreviations

AT - Adipose Tissue
FB - Fibroblasts
CFU-F - Colony-Forming Unit-Fibroblast
CFE - Colony-Forming-Efficiency
ED - Enzymatic Digestion
Fat-ED - Fat Enzymatic Digestion
ADSCs - Adipose-Derived Stromal Cells
ASCs - Adipose Stem cells
MSCs - Mesenchymal Stem Cells
OA - Osteoarthrosis
ECs - Endothelial Cells
HA - Hyaluronic Acid
RT – Room Temperature
FDFC - Fidia Collagenase Digested Cells
APM - Arrector Pili Muscle
BM - Bone Marrow
DWAT - Dermal White Adipose Tissue
EP - Epidermis
ESG - Eccrine Sweat Gland
HF - Hair Follicle
PC - Panniculus Carnosus
h – hour/ hours
min – minute/ minutes

TPT -Tissue Processing Time
RPM - Revolution Per Minute
ml - Milliliter
PPC - Peri-Prosthetic Capsule
CC - Capsular Contracture
ACM - Acellular Matrix
ECM - Extracellular Matrix
HBSS - Hank's Balanced Salt Solution
BSA - Bovine Serum Albumin
DMEM - Dulbecco's Modified Eagle's Medium
P/S - Penicillin/Streptomycin
MRI - Magnetic Resonance Imaging
ROI - Region of Interest
VEGF - Vascular Endothelial Growth Factor

Coll. I - Collagenase Type I
Coll. III - Collagenase Type III
PL - Porous Layer

CL - Compact Layer
CF - Cytoplasmatic Flaps
WPM - Wrinkled Plasmatic Membrane
H&E - Hematoxylin and Eosin
MT - Mallory's Trichrome

Contents

1

Introduction

i) Tissue regeneration: State of Art

Biology of regeneration

In biology, regeneration is the process of restoration, renewal, and tissue growth that makes genomes, cells, organisms resilient to events that cause a disturbance, damage, or natural fluctuations [1]. From bacteria to humans, every species can regenerate [2, 3]. Stem cells are specialised cells capable of renewal. They can differentiate into different cell types in the human body, which populate to form tissue, i.e., they possess information that allows them to become any cell in the body or a restricted cell type with a specialised function. These abilities make stem cells extremely useful for biomedical applications and regenerative medicine and have become the primary molecular tool. For example, skeletal muscles can regenerate and form new muscle tissue, while cardiac muscle cells do not regenerate. Smooth muscle cells have the most significant ability to regenerate.

Regenerative medicine

This new branch of medicine tries to study the regenerating tissues and organ systems that fail due to age, genetic defects, disease, tissue engineering, or damage. Regenerative medicine has quickly become one of the promising treatment options for patients with tissue failure. 'Regenerative medicine' and 'Tissue engineering' have become highly interchangeable, with the field hoping to focus on treatments rather than complex and often chronic disease treatments. However, tissue engineering is an emerging biomedical field aimed at helping to restore physical tissue defects to the point of self-repair and replacing the biological functions of damaged and injured members using cells with differential and reproductive abilities.

Tissue engineering technology has evolved from developing biological materials (biomaterials), which combine scaffolds, cells, and biologically active molecules of functional tissues. Tissue engineering aims to gather structures that restore, maintain, or improve damaged tissues or whole organs. Artificial engineered cartilage and skin tissues have been recently authorised by the FDA [4]. When scaffolds are created, cells with or without a 'mix' of growth factors can be introduced. Then, assuming that the environment is appropriate, the tissue grows.

Sometimes, cells, growth factors, and scaffolds are mixed simultaneously, allowing the tissue to ‘self-assemble’.

The scaffold uses different ways to create a new fabric or tissue. The donor tissue or organ cells are stripped, and the maintained collagen scaffold forms new tissue. A new tissue has been created in the biological engineering of the rat's heart, liver, lungs, and kidney tissues. This approach holds great promise for using scaffolds from human tissues discarded during surgery and integrated with the patient's cells for the work of dedicated members that the immune system cannot reject. The tissue needs a good "draining and plumbing system" (veins or arteries) to feed cells and carry waste. Without blood supply or any similar mechanism, cells die quickly. Ideally, scientists would like to create engineered tissue using a plumbing system that has already been built (lattices). New hope for the bum knee: cartilage has been challenging if it is not impossible to repair since cartilage lacks a blood supply to promote regeneration. The gel/adhesive combo successfully regenerated cartilage tissue following surgery in a recent clinical trial of patients [4].

The present scaffold uses different ways to create a new fabric or tissue. The donor tissue or organ cells are stripped, and the maintained collagen scaffold is used to form new tissue. A new tissue has been created in the biological engineering of the heart, liver, lungs, and kidney tissues. This approach holds great promise for using scaffolds from human tissues discarded during surgery and integrated with the patient’s cells for the work of dedicated members that the immune system cannot reject.

The main goal of the tissue regeneration study

The main goal of tissue regeneration studies is to acquire knowledge to enhance the new wide range of regenerative medicine. This information may include evidence to stimulate stem cell activity, structural engineering of better scaffolds or direct initiation of biologic regeneration programs. Scientists already understand some forms of regeneration enough to manipulate and modify major events for therapeutic reasons. For example, the common practice of bone marrow transplantation is to guide hematopoietic cells to regenerate blood cells properly. However, research has begun to acquire knowledge and techniques for most innovative models to selectively ban or enhance selective steps during renewal.

Cell-based therapeutic strategies have been developed to treat and reverse such disorders in the past decades. Stem cells are appealing in the field, being a responsive undifferentiated population, with the ability to self-renew and differentiate into different lineages. Mesenchymal stem cells can be obtained from

several adult tissues, including the synovial membrane. Synovia-derived mesenchymal stem cells can be found in individuals of any age and are associated with intrinsic regenerative processes through paracrine and cell-to-cell interactions, thus contributing to host healing capacity. Studies have demonstrated the potential benefit of synovia-derived mesenchymal stem cells in these regenerative processes in both human and veterinary medicine.

Structure of dermis

The dermis is the mesenchymal component of the skin, separated from the epidermis by the basement membrane.

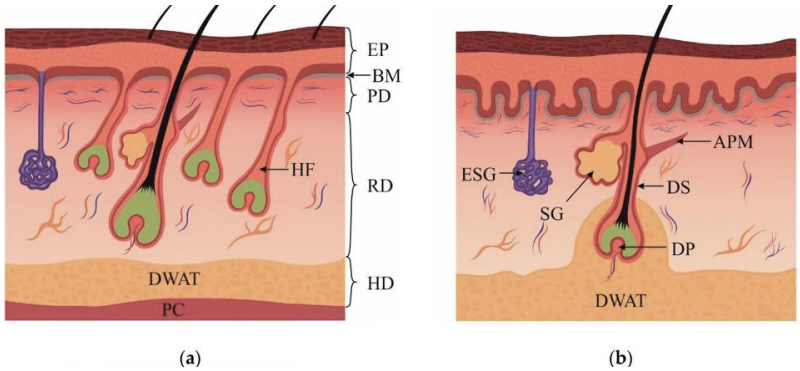

Figure 1. Skin structure: (a) murine skin structure. The mouse back skin has four types: guard (tylotrich) and awl, auchene, and zigzag HFs (non-tylotrich). The panniculus carnosus (PC) is under the hypoderm. (b) Human skin structure. Human skin structure differs from that of murine. The epidermis is thicker and forms ingrowths called rete ridges. Accordingly, the papillary dermis forms dermal papillae.

WAT & BAT:

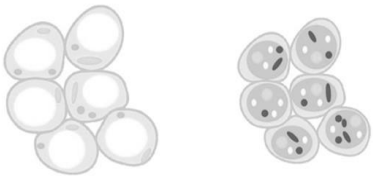

	WHITE ADIPOSE TISSUE	BROWN ADIPOSE TISSUE
Localization	• Subcutaneous • Intra-abdominal • Epicardial • Gonadal	• Interscapular • Paravertebral • Perirenal • Cervical • Supraclavicular
Morphology	Spherical	Elliptical and smaller than white
Cell composition	• Single lipid droplet • Few mitochondria • Flattened peripheral nucleus • Little endoplasmic reticulum	• Multiple small lipid droplets • Large number of mitochondria • Oval central nucleus
Function	Storing energy	• Expending energy and heat production (non-shivering thermogenesis)
Uncoupling protein	Undetectable	Positive

Table 1: Differences between White & Brown Adipose tissue

Adipose tissue and wound healing

Adipose tissue (AT) can be classified into three groups: white (WAT), brown (BAT) and beige (BeAT). WAT is the most common one. It represents a storage of lipids and a source of adenosine triphosphate (ATP) derived from the release of fatty acids during the β-oxidation process. Recent studies have identified a new type of white adipose tissue, DWAT, which plays a vital role in various methods: wound healing, the immune response, HF homeostasis, and thermoregulation [12]. It has been shown that intradermal adipocytes are necessary and sufficient for HF stem cell activity. PDGF (platelet-derived growth factor) expression in immature adipocytes regulates follicular stem cell activity and activation of HF growth. Data from Festa et al. indicated that adipocyte lineage cells form the niche of epithelial stem cells, positively regulate their activity, and induce HF regeneration [13]. In mouse skin, DWAT is located between the dermis and panniculus carnosus (Figure 1a). DWAT is deposited around single pilosebaceous units in human skin, including the HF bulb with a hair shaft, a sebaceous gland, and erector pili muscles. DWAT engulfs HFs in the form of a cone (Figure 1b) [12]. Interestingly, in humans, the cone-shaped structures of DWAT are found only in areas of the body that are prone to scarring

(for example, the abdomen, neck, chest, etc.) and are not pronounced in areas associated with reduced scarring (scalp, forehead, or early fetus) [14].

It is reported that adiponectin-positive dermal progenitor cells can differentiate into Fibroblasts (FBs). During the induction of fibrosis by bleomycin in mouse skin, adiponectin-positive precursors, whose presence is usually limited to DWAT, distributed over the entire damaged dermis over time, lost their adipocyte-specific markers and expressed FB markers [15]. Reduction of adipogenesis and the loss of DWAT are consistent features of cutaneous fibrosis. At the same time, DWAT can be replenished since the regeneration of adipocytes from FBs is possible [16].

FBs are the most abundant cells in the dermis. A characteristic feature of these cells is synthesising and remodelling the extracellular matrix (ECM). Remodelling is supported by the synthesis of the cleaving metalloproteinases and their inhibitors. Collagen synthesis is the primary and unifying typical feature of FBs [5]. FBs of the dermis are a heterogeneous population of cells, the specificity of which is determined mainly by their location relative to the dermis layers. Interactions between the epithelium and mesenchyme are critically important for the development and regeneration of the epidermis.

Wound healing in the skin depends on the coordinated collective activity of several cell types. Keratinocytes and FBs migrate into the wound to restore skin structure. Furthermore, other cells participate in the process, including hemopoietic, endothelial, immune, neural, white fat cells, pericytes, Schwann cells, tissue-specific stem cells, and progenitors. FBs and mesenchymal cells play a pivotal role in wound healing, mediate fibrosis, participate in inflammatory networks, synthesise matrix, and modulate immune cell functions.

Shortly after wounding, the wound is populated with FBs from the reticular dermis and cells from the hypodermis [6]. FBs of the reticular dermis can produce thick and well-organized collagen fibres compared to papillary FBs that are attracted later (during epithelialisation) and synthesise poorly organised ECM. Reticular FBs generate a collagen matrix typical for fibrosis [6, 7, 8]. Rognoni and colleagues [9] reflect a model where the lack of ability to form HFs by postnatal wounded skin is associated with an increase in the activation of WNT/β-catenin signalling in the wound bed, which in turn increases the number of reticular FBs unable to induce HF formation. When injured, the density of papillary FBs decreases, and the β-catenin activity in the dermis increases with age, which is linked to an increase in reticular FB expansion. In this case, the expansion of FBs takes place with minimal proliferation. Repair of postnatal skin wounds occurs quickly by attracting reticular FBs but at the cost of losing the regeneration of HFs at the wound site [9]. It can be supposed that specific epithelial-mesenchymal interactions occur between the

epidermis and the upper layer of the dermis represented by its papillary part, and maintenance of this interaction is vital for scarless healing and the generation of new appendages. Reticular FBs fail to provide valuable clues for skin morphogenesis.

Moreover, they organise the matrix typical for fibrosis in the wound. Therefore, the papillary dermis may provide reparative regeneration of the skin. Interestingly, in clinical practice, surgeons have learned to destroy the upper layer of the skin down to the interface between the papillary and reticular dermis to improve acne scars. However, it's known that one should not go deeper to prevent permanent scarring [10].

Collagen I is the dominant component of the ECM in the dermis and accounts for approximately 70% of its dry weight. Moreover, in intact adult skin, collagen I to collagen III is approximately 4:1, whereas it is approximately 1:1 in neonatal skin. In mature skin, less hyaluronic acid (HA) is secreted. Therefore, the amount of collagen III temporarily increases when the skin is injured and during the formation of the new dermis. The collagen I and III ratios are about 1:1 in neonatal skin in newly healed human skin. At the same time, in response to a wound, fetal skin shows a higher amount of collagen III and HA and lower collagen I [10, 11].

ii) Adipose tissue and SVF

Stromal Vascular Fraction (SVF) is a heterogeneous collection of cells within adipose tissue traditionally isolated using enzymes such as collagenase. With removing adipose cells, connective tissue, and blood from lipoaspirate comes the SVF, a mixture of mesenchymal stem cells, endothelial precursor cells, T regulatory cells, macrophages, smooth muscle cells, pericytes, and preadipocytes. Aside from their use in chronic conditions, SVF enrichment of fat grafts has proven a significant advance in maintaining fat graft volume and viability. Many SVF studies are currently in preclinical phases or are moving to human trials. Overall, regenerative cell therapy based on SVF is at an early investigative stage, but its potential for clinical application is enormous.

In tissue engineering and regenerative medicine, adipose tissue has emerged as an attractive cell source because it can be easily isolated and enriched with stem/progenitor cell populations. The SVF derived from adipose tissue contains heterogeneous cell populations such as preadipocytes, endothelial cells, mesenchymal progenitor/stem cells, T cells, pericytes, and M2 macrophages. In vitro, SVF-derived mesenchymal progenitor/ stem cells can be easily expanded and create diverse lineages of cells. However, there are specific issues related to their

isolation and purification. SVF cells demonstrate regenerative potential in damaged tissues or organs through paracrine and differentiation mechanisms.

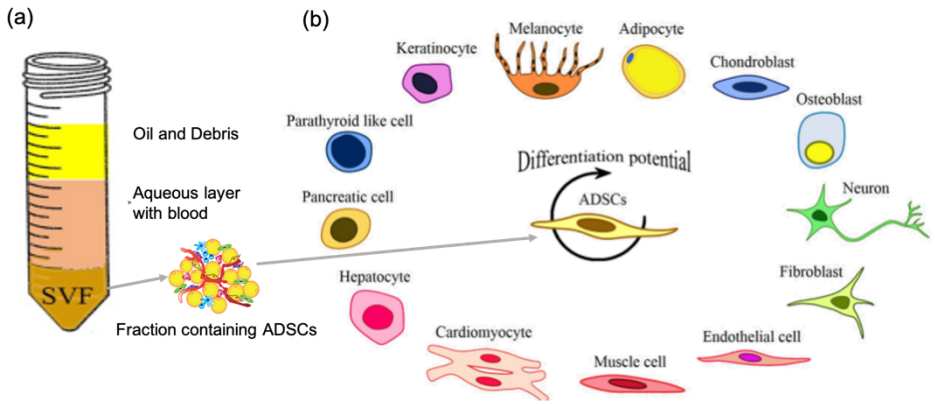

Figure 2: SVF containing ADSCs and their capability to differentiate into cell lines

iii) Fat grafting

Fat grafting is common in reconstruction and aesthetics. The lack of standardised protocols can partly explain reconstructive plastic surgery's unpredictable clinical outcomes of fat grafting for processing, harvesting, and transplanting adipose tissue (AT). Historically, plastic surgeons have relied on trial and error and clinical experience to develop fat grafting protocols [17].

In addition to vertical tissue descent, The process of ageing results from subcutaneous loss of volume. Surgeons emphasise soft tissue augmentation to achieve a natural, rejuvenated appearance in patients. Autologous fat grafting is now a commonly performed aesthetic procedure. Autologous fat grafting is a challenging procedure due to the fragile characteristic of adipose tissue. The viability of transplanted fat is the primary consideration when fat grafting is performed. Poor fat viability produces a preliminary result and thus is considered a complication of this procedure. Many studies have demonstrated that fat longevity depends on the handling and preparation of fat [18].

Therefore AFG, an autologous biological tissue containing several critical cellular components (adipocytes and mesenchymal stem cells), ECM, vessels, and nerves [19], can be considered either as 'bioactive material' when it is grafted into the

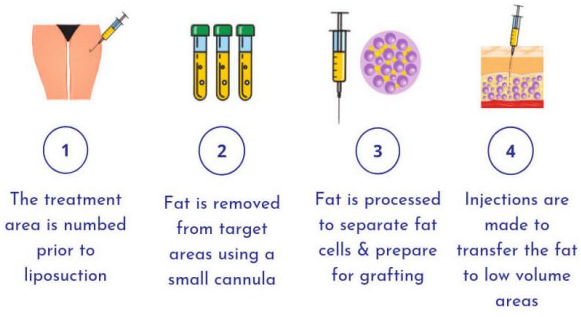

Figure 3: General fat grafting procedure

soft tissue defects aiming to improve the volume and tissue quality or as "bioactive scaffold" when ASCs enriches it. In this last case, AFG also acts as a scaffold for the ASCs, representing an autologous biological matrix (cellular and extracellular) to improve fat graft maintenance through an autologous regenerative approach based on adipogenesis and vascularisation improvement [19].

Harvesting

Autologous fat grafting is a surgical technique in which adipose tissue is transferred from one body area to another to reconstruct or regenerate damaged or injured tissues. To avoid inflammation and preserve graft viability before reinjection, adipose tissue must be purified from blood and cellular debris. For purification, different enzymatic and mechanical methods can be used. Autologous fat grafting has become increasingly used for multiple volume filling applications. However, the major obstacle to widespread clinical use is the lack of standardised guidelines during harvesting, processing, and implantation steps [20]. Indeed, many authors have recognised no universally accepted methodology for fat grafting [21, 22].

Fat is a delicate tissue and must be handled with maximal care to maintain its viability [23]. Therefore, the ideal methodology to approach autologous fat grafting has been a significant focus in the last years, but patient-related factors should also be considered when designing a study.

Distinct harvesting procedures lead to different outcomes of fat graft take. As aforementioned, details such as the best donor-site, what adipose tissue harvesting technique to use, what harvesting cannula diameter to choose, what pressure to apply to avoid the decrease of cell viability or the possibility of injecting a tumescent solution with anaesthetics before tissue collection are considered to get the highest cell viability and survival rates possible. Direct excision, syringe hand aspiration, and suction-assisted liposuction using various pressures (and different mechanisms to create that pressure) are some of the currently used techniques [24, 25, 26]. In addition, a liquid jet, ultrasound pulses, or laser energy can also assist liposuction [27, 28, 29].

Usual fat grafting areas

Chest (breast reconstruction), Butt, Face, Cheek, Lips, Scars across the body, Neck, Hollow areas around the eyes, Hands, Arms, and the other regions experiencing volume loss.

Processing

In the past years, AT has gained the attention of researchers for being an exciting source of adult stem cells for plastic surgery and regenerative medicine. The lipoaspirate is processed in many ways to collect SVF for autologous fat grafting purposes. In the mechanical procedure, the tissue is massaged manually (or blended inside the device in the case of Rigenera) to break down the collagen and then is centrifuged at a certain rpm to collect the SVF. In the enzymatic procedure, the tissue is incubated inside a rotating incubator for a specific time and then centrifuged.

iv) Goal and Findings

This work aimed to optimise an excellent device to isolate SVF (containing MSCs, which is thought to be one of the significant regenerative elements), its *in vitro* differentiation capability to confirm regenerative material inside, and application *in vivo* in contact with biomaterials to induce adipogenesis.

We have optimised three mechanical devices and one new collagenase to isolate SVF within a short period. These devices and the enzyme all are set to be used in any regenerative surgery. They have different time and handling measures to process the lipoaspirates without requiring previous expertise. Anyone can easily use these simple devices without any prior expertise, be transferred to any lab for research purposes and are ready to be used in fat-processing for stem cell therapy immediately after harvesting. We have successfully shown that the product generated after the fat processing is safe to use. We have applied the product subcutaneously in nude mice with HA, and yellowish adipose tissue was observed with naked eyes (after sacrificing the mice) and with 7T MRI; later, we confirmed induction of adipogenesis by examining the fat.

2

Mechanical isolation, characterisation of the regenerative element from lipoaspirates and its application

2.1. Introduction to Rigenera®

v) Introduction and overview of the machine

While adipose tissue has been considered a waste product for years, its essential role as a regenerative agent has only recently been recognised [30, 31]. Indeed, autologous fat grafting has many applications, including breast reconstruction following tumour therapies [32, 33], the treatment of burn scars and congenital and post-traumatic malformations [34, 35], and rejuvenation aims [36]. It is believed that the main agents responsible for regeneration are adipose-derived stem cells (ASCs), which are adult plastic-adherent mesenchymal stem cells abundant in, and easily isolable from adipose tissue [37-39]. They self-renew and are multipotent, which means that they can differentiate, under appropriate stimulation, into different mesodermal cell lineages, especially into adipocytes, osteocytes, and chondrocytes [40-45]. After liposuction, the processing of adipose tissue is a crucial step in avoiding inflammation and preserving the fat graft viability. The traditional purification method is enzymatic digestion, which involves using collagenase. This method consists of collagenase digestion, centrifugation, and washing steps to remove red blood cells, allowing adipocyte separation from dense cellular tissue, called the stromal vascular fraction (SVF) [46]. The SVF contains different cells, including ASCs, mesenchymal and endothelial progenitor cells, leukocytes, and pericytes. Although the enzymatic method is the most effective for SVF isolation, it is an expensive and time-consuming open system, requiring further enzyme purification. In addition, it destroys the stem-cell niche, known as the microenvironment, which surrounds the stem cell, allowing interactions with neighbouring cells that promote cell survival, proliferation, and differentiation.

Moreover, according to the Good Manufacturing Practice regulations of the European Parliament and Council (EC regulation no. 1394/2007), only minimal cell manipulation is allowed in a clinical setting. Therefore, enzymatic methods are forbidden [47, 48]. Furthermore, it is mandatory in clinics to purify the adipose tissue in the operating room immediately after the surgery without laboratory processing and in sterile conditions. For these reasons, many companies have developed

automatically closed devices based on mechanical methods [49-54]. One of these, named Rigenera® (HBW, Turin, Italy), composed of an engine and disposable sterile capsules, uses mechanical disaggregation operated by steel blades rotating at 80 rpm, followed by filtration through 70–80 µm pores, to produce immediately injectable micrograft. The present study aimed to *in vitro* characterises the product obtained by the Rigenera® device in terms of the cell viability and morphology, immunophenotyping, colony-forming unit, and differentiation potential. The study focused on adipose tissue isolated from the thigh and abdomen. We characterised *in vitro* the product of a closed automatic device based on mechanical disaggregation, named Rigenera®, focusing on two sites of adipose tissue harvesting.

vii) Optimising Rigenera and analysing its product

Adipose Tissue Sample Collection

The current non-enzymatic system (named Rigenera®, HBW, Turin, Italy) was designed to collect and prepare human disaggregated biological tissue, such as dental pulp [54], the dermis [55], scars [56], cartilage [48], and adipose tissue, for re-injection. This study harvested adipose tissue from nine women subjected to liposuction, aged between 41 and 69 years. According to the ethical guidelines set by the review board for human studies, consent was obtained before tissue collection. The tissue was subsequently processed with Rigenera® technology with 16 ml capsules, as De Francesco and colleagues [47].

Cell Isolation and Culture

Each adipose tissue sample was divided into two portions. In the Rigenera® capsule, 4 ml of lipoaspirate and 4 ml of the complete culture medium Dulbecco Minimum Essential Medium (DMEM) (Merck KGaA, Darmstadt, Germany) containing 10% Fetal Bovine Serum (FBS), 1% of a mix of penicillin/streptomycin 1:1 (GIBCO Life Technology, Monza, Italy), and 0.5% amphotericin B (GIBCO Life Technology, Monza, Italy) were added. The Rigenera® device was operated for 30, 45, or 60s. The collected cell pellet was withdrawn from the capsule by a syringe, filtered through a 70-µm nylon mesh, and centrifuged at 3000 rpm for 7 min. The supernatant was discarded, and the cell pellet was resuspended in 6 ml of complete medium, plated in a 25 cm^2 flask (BD FalconTM, Becton Dickinson, Milano, Italy), and incubated at 37 °C and 5% CO_2. The second portion of lipoaspirate was digested with collagenase following the collagenase protocol, as reported in [52]. Briefly, 4 ml was digested with 1 mg/ml type I collagenase (GIBCO life technology, Monza, Italy) in Hank's Balanced Salt Solution (HBSS) and 2% bovine serum

albumin (BSA) at 37 °C for 45 min. The enzymatic action was neutralised by adding a complete medium. Then, the sample was centrifuged at 3000 rpm for 7 min, the supernatant was discarded, and the cell pellet was incubated with 3 ml of 160 mM NH4Cl at room temperature for 10 min to lyse the erythrocytes. After centrifugation, the cells were resuspended in 6 ml of complete medium, filtered through a 70-µm nylon mesh, plated in a 25 cm^2 flask with complete culture medium, and incubated at 37 °C and 5% CO2. The medium was first changed after 72h and, successively, every 48h. At confluence, cells were detached by incubating them with trypsin-EDTA 1% (GIBCO Life Technology, Monza, Italy) at 37 °C for 5 min and re-plated in a 75 cm^2 flask.

Morphological Analysis: Scanning and Transmission Electron Microscopy

For transmission electron microscopy, the pellets of the product obtained after the treatment with Rigenera 60 min were fixed with glutaraldehyde 2% in Sorensen buffer pH 7.4 for 2h, post-fixed in 1% osmium tetroxide, in aqueous solution for 2h and dehydrated in graded concentrations of acetone. At the end of the dehydrating process, samples were positioned in a multi-well grid for electron microscopy and observed using an EM10 electron microscope (Zeiss, Oberkochen, Germany).
For scanning electron microscopy analysis, the pellets of the product obtained after the treatment with Rigenera 60 min were fixed to 2% glutaraldehyde in a phosphate buffer for 2–4 h, post-fixed in 1% osmium tetroxide in the same buffer for one hour and dehydrated in graduated acetone concentrations. The samples were then treated with a critical-point dryer (CPD 030, Balzers Vaduz, Liechtenstein), mounted on metal samples, and coated with gold (MED 010 Balzers). SEM imaging was performed with XL30 ESEM (FEI-Philips Eindhoven, The Netherlands).

Morphological Analysis and Cell Viability Test

Morphological analysis of the cells obtained with the three different Rigenera® operating timings and the enzymatic method visualised them under a light microscope from the two different harvesting sites (Optika Microscopes Ponteranica, Italy). In addition, the cell viability and growth rate were evaluated by the cell viability test with the trypan blue exclusion method.

Cell Colony-Forming Unit Assay

A colony-forming unit-fibroblast (CFU-F) assay was performed for cells treated with Rigenera® and enzymatic digestion. Briefly, cells isolated from the thigh and abdomen and treated with the Rigenera® device were plated in 6-well culture plates at a density of 3000 cells/cm^2 and cultured in the complete media. On the 15th day after plating, the total number of cell colonies (CFU-F, a cluster of at least 50

adhered and fibroblast-like cells) was stained with Toluidine Blue (Sigma) and counted.

Immunophenotyping

After isolation, cells were counted, and 2×10^5 cells were placed in a tube for cytofluorimetric analysis. The pellet was washed with 1 ml of 1% FBS in PBS and then labelled with fluorescent-dye conjugated antibodies in a final volume of 100 µl and incubated for 30 min in ice. The examined antibodies were APC-conjugated CD90 (dilution 1:5), PerCP-Cyt5.5-conjugated CD105 (dilution 1:20), BV421-conjugated CD73 (dilution 1:20), BV785-conjugated CD44 (dilution 1:20), PE-conjugated CD34 (dilution 1:5), FITC-conjugated CD29 (dilution 1:20), and BV650-conjugated CD45 (dilution 1:20). All antibodies were purchased from BD Biosciences (Becton Dickinson Italy S.p.A., Milan, Italy). Alexa Fluor-488-conjugated SEEA3 (dilution 1:20) was purchased from Aurogene (Aurogene S.R.L, Rome, Italy). After the incubation, the pellet was rinsed, resuspended in 300 µl of 1% FBS in PBS, and transferred to flow cytometry tubes. The immunophenotyping was performed through a FACS canto II (BD, Becton Dickinson, Italy).

Cell Differentiation Assay

The multilinear differentiation potential was evaluated by testing the ability of the product obtained after treatment with Rigenera (the 60s) and the enzymatic method to differentiate into adipocytes, chondrocytes, and osteocytes. Briefly, adipocyte differentiation was achieved after 16 days culture of MSCs with adipogenic medium, containing 10^{-6} M dexamethasone, 10 µg/ml insulin, and 100 µg/ml 3-isobutyl-1-methylxanthine (Sigma). Chondrocyte differentiation was achieved after 14 days of culture with the StemPro osteogenesis differentiation kit (GIBCO Life Technology, Italy). Osteoblast differentiation was achieved after 21 days of culture with the StemPro osteogenesis differentiation kit (GIBCO Life Technology, Italy). Oil Red O, Alcian blue, and Alizarin Red Stain were employed to identify adipocytes, chondrocytes, and osteocytes.

Adipogenic Differentiation

A total of 7000 cells were seeded on the slides in the 6-well plate. After 24h, the media was changed to an adipogenic medium. To confirm adipogenic differentiation, after 16 days, the cells were fixed with 4% paraformaldehyde (PFA) for 30 min, washed, and stained with a solution of Oil Red O (Bioptica) for 20 min and hematoxylin (Bioptica) for 2 min. They were then washed with distilled water. Images were obtained using optical microscopy.

Chondrogenic Differentiation

1×10^6 cells were seeded on the slides in the 24-well plate, and after 2h, the media was changed to a chondrogenic medium. To confirm chondrogenic differentiation, after 14 days, cells were fixed with 4% PFA for 30 min, and Alcian Blue 8GX (Sigma-Aldrich) was used to stain the extracellular matrix mucopolysaccharides and hematoxylin (Bioptica) for 2 min. The staining solution was prepared by dissolving 1% Alcian Blue 8GX in 0.1 N HCl. This solution was filtered and added to each culture well for 30 min, and the cells were then washed with distilled water. Images were obtained using optical microscopy.

Osteogenic Differentiation

In total, 5000 cells were seeded on the slides in the 12-well plate. After two h, the media was changed to an osteogenic medium. To confirm osteogenic differentiation, after 21 days, cells were fixed with 4% PFA for 30 min and incubated in 0.2% Alizarin Red S (Sigma-Aldrich) for 5 min and hematoxylin (Bioptica) for 2 min. Then, they were washed with PBS (Gibco), and images were obtained using optical microscopy. The control group cells were cultured with the ASC complete medium (Dulbecco's Modified Eagle Medium (DMEM), 10% FBS, and 1% penicillin/streptomycin). The cells were stained with hematoxylin to highlight the nucleus.

Statistical Analysis

Data were expressed as the mean ± standard deviation. Unpaired sample student's t-tests were performed, and differences between two groups were considered statistically significant when p-value < 0.05.

Although the enzymatic method, which has been used for 40 years in the laboratory to isolate cells, is the best available method, it is not compatible with clinics due to the long-lasting procedure and legal restrictions. Many efforts have been made to establish a mechanical method with a yield comparable to collagenases. Unfortunately, so far, none of them has displayed the same performance. In addition, to use it *in vivo*, a closed device is needed, and the method must be fast, safe, standardised, and autologous. Rigenera® addresses all these requirements. In this study, we characterised in vitro the Rigenera® product, focusing on two sites of adipose tissue harvesting. At first, we optimised the Rigenera® operating time, demonstrating that the 60s of treatments allows a higher cellular yield in terms of

the cell number and growth rate. This result optimises the mechanical disaggregation and can increase the final product's clinical efficiency. Then, comparing the thigh and abdomen, our results showed that the thigh provides a higher number of mesenchymal-like cells, with a faster replication rate and a higher ability to form colonies. Finally, the immunophenotypic analysis confirmed that a much higher yield of ASCs was obtained from thigh samples. We conclude that it is possible to get the most efficient product by collecting adipose tissue from the thigh and treating it with the Rigenera® device for the 60s. This should lead surgeons to prefer the thigh as a harvesting site, especially for surgeries requiring a small injectable volume.

The Rigenera® device is a technology that allows the mechanical disaggregation of a small amount of adipose tissue to obtain an autologous product that can promote regeneration. The procedure consists of tissue manipulation conducted by a ceramic blade and filtration (filter of 80 µm). After processing, the product is collected from the reservoir located at the bottom of the removable capsule of the Rigenera® device. At first, the composition of the product obtained from the mechanical disaggregation and harvested from two different anatomical sites—the thigh and abdomen—were examined at an ultrastructural level. In Figure 4, SEM and TEM images of the product obtained from adipose tissue of the thigh are shown. No difference was observed at an ultrastructural level between the two sites of adipose tissue collection (images not shown). The adipose tissue SEM images (Figure 4. a, b) show connective tissue fragments consisting of elastic fibres (see the black arrow in Figure 4. a), collagen fibres (white arrow in Figure 4. a, b), and different kinds of isolated cells (Figure 4. b). Among the isolated cells, mesenchymal-like cells (Figure 4. c), characterised by rough endoplasmic reticulum (see the black arrow in Figure 4. c) and small size lipidic droplets (white arrow, Figure 4. c) were visualised by TEM.

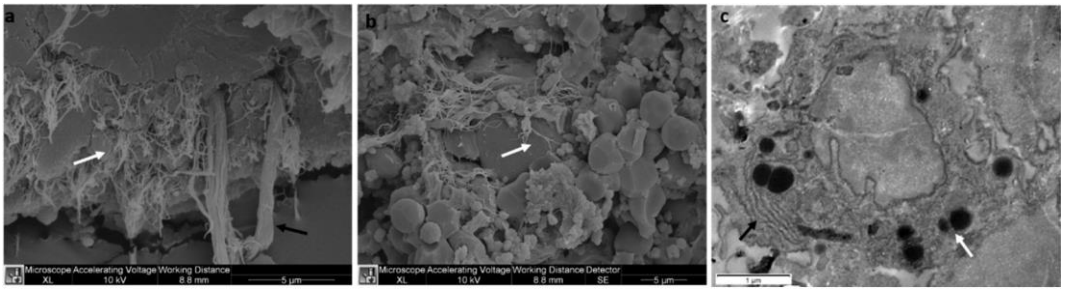

Figure 4. Representative SEM (a, b) and TEM (c) images of the Rigenera product were obtained from the thigh. The Rigenera® device provides fragments consisting of elastic fibres ((a) black arrow), collagen fibres ((a, b) white arrow), and different kinds of isolated cells (b), including mesenchymal-like cells (c), characterised by rough endoplasmic reticulum (black arrow) and lipidic droplets (white arrow). No differences at an ultrastructural level were found between the two sites of adipose tissue collection (thigh and abdomen).

To determine the mechanical processing time (seconds of sample treatment with ceramic blades) affects the cellular yield of the device, the number of ASCs, the growth rate, and the cell morphology were evaluated. Based on preliminary results [47], the best processing time was chosen among 30, 45, and 60s. At first, the cells were counted at passage 0 (Figure 5. a). The number of cells with 60s treatment was much higher compared to 45s and 30s (respectively, $15.16 \times 10^6 \pm 0.49$ compared to $6.84 \times 10^6 \pm 0.19$ and $4.13 \times 10^6 \pm 0.33$ for the abdomen and $21 \times 10^6 \pm 0.16$ compared to $9 \times 10^6 \pm 0.35$ and $7.2 \times 10^6 \pm 0.28$ for the thigh, as shown in Figure 5a). After one week, only cells capable of forming fibroblast-like colonies were attached to the flask and were countable. Compared to the 60s treatment, the thigh cell yield after the 45s treatment was about 42%, and after the 30s, it was about 20% (tab in Figure 5. b). In addition, the meantime of confluence was eight ± 2.8 days lower with 60s treatment than with 45s treatment. The 30s-treated cells grew very slowly and were discarded after 45 days (Figure 5. b). In the case of abdominal cell extraction, the cell yield of the 60s treatment was about 36% compared to the 45s treatment, whereas the 30s-treated cell yield was about 5%. The mean time of confluence was seven days less with 60s treatment than with 45s treatment (Figure 5. c). Additionally, the 30s treatment cells grew very slowly for abdomen samples and were discarded after 45 days (tab in Figure 5). By calculating the mean cell growth per day, 60s treatments showed a higher replication rate (29.23×10^3 and 7.27×10^3 for the thigh and abdomen, respectively), as reported in the table of Figure 5. The ASC micrographs in Figure 5(d-k) represent the cell morphology in the flask. The Rigenera® treatment did not affect the cell morphology compared to cells obtained from enzymatic digestion (g–k), exhibiting a homogeneous fibroblast-like morphology. Indeed, no suffering signal was observed, and the membranes and nuclei were well-preserved (Figure 5d-f, h-j) for the thigh and abdomen, respectively). By analysing the results obtained for the cell yield, several cells, and growth rate, the 60s treatment can be considered the most efficient for the Rigenera® method.

Thigh	Mean 10^5cells/ml (after 1week) ±SD	Mean time of confluence	Mean 10^5cells/ml (at	Mean cells growth per day
30 seconds	0.127± 0.05	>45	<0.5	1.127
45 seconds	0.842± 0.04	29±1.4	2.10±0.33	7.488
60 seconds	2.320± 0.14	21±1.4	6.05±0.64	29.237
Abdomen	Mean 10^5cells/ml (after 1week) ±SD	Mean time of confluence	Mean 10^5cells/ml (at	Mean cells growth per day
30 seconds	0.147± 0.05	>45	<0.5	1.134
45 seconds	0.305± 0.09	34±6.5	0.677±0.15	2.107
60 seconds	0.722± 0.13	27±3.7	1.93±4.20	7.272

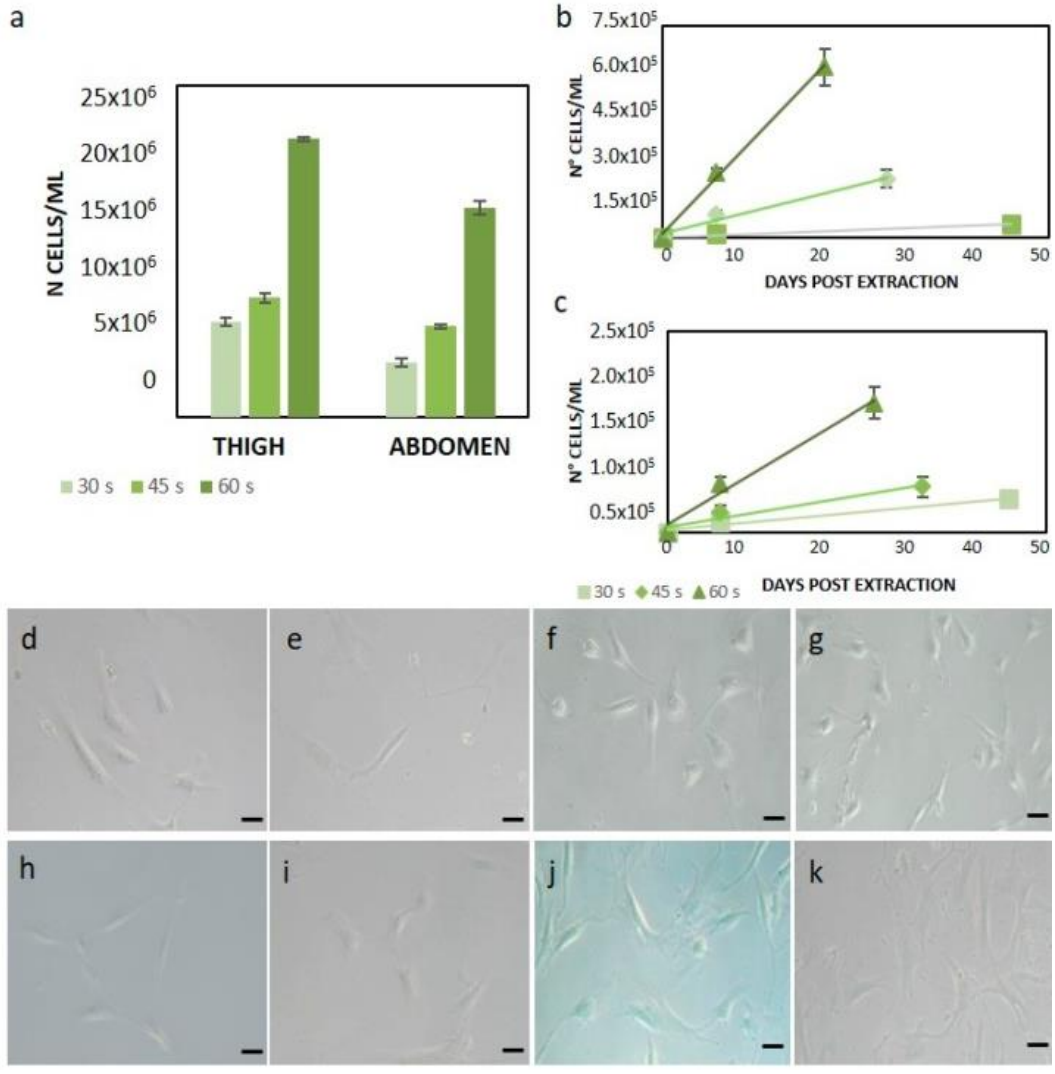

Figure 5. Rigenera® method optimisation. The tabs show all the results obtained. (a) Cell viability test with the trypan blue exclusion method. At passage 0, total cells were much higher with the 60 s Rigenera® treatment than the other timings (30 and 45 s). After one week, the number of pure adipose-derived stem cells (ASCs) was still higher with the 60s Rigenera® treatment in both the thigh (b) and abdomen (c). Microscopic images (resolution 10×) of cells extracted from the thigh (d–f) and abdomen (h–k) with the Rigenera® device operating at different timings of the 30s (d, h), 45s (e, i), and 60s (f, j), and the enzymatic method (g, k).

Next, the cells obtained from the 60s treatment were compared with those obtained with the enzymatic method. After one week of culture, the Rigenera® cell yield for the thigh was 62% and for the abdomen, was around 25%, compared to the enzymatic method (table in Figure 6)

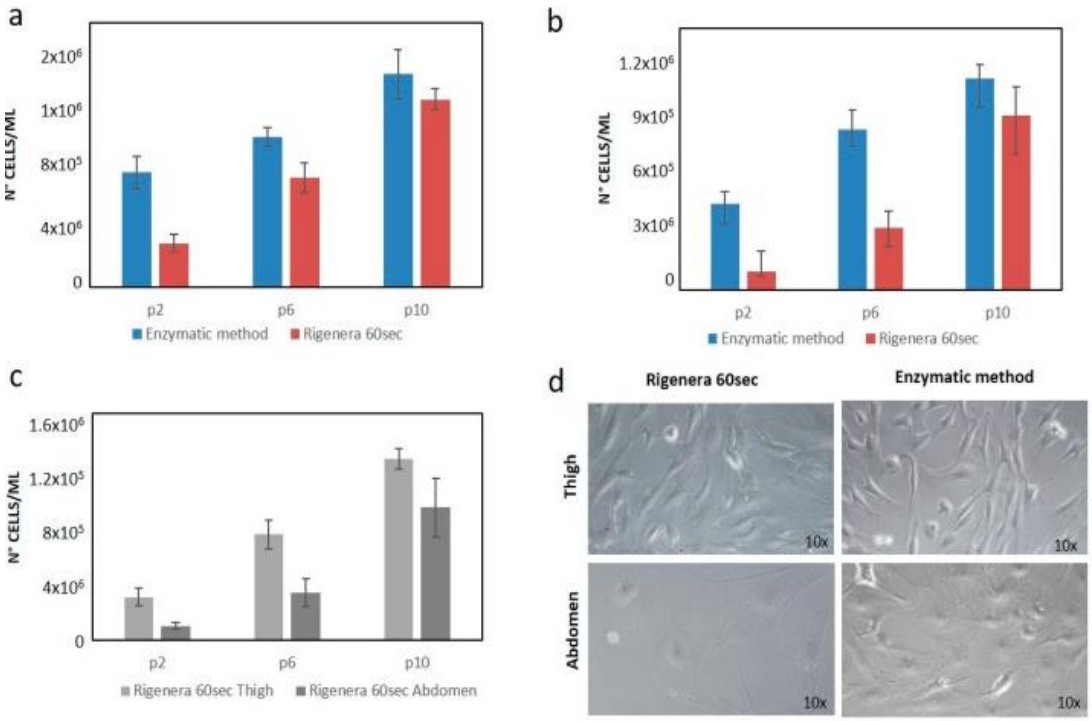

Enzymatic method vs Rigenera	Mean 10^5cells/ml (after 1week) ±SD	% of cells growth	Mean time of confluence	Mean 10^5cells/ml (at confluence)	Mean cells growth per day
Enzymatic Method Thigh	3.760± 0.71	100	13±3.5	8.07±0.75	67.710
Rigenera 60s Thigh	2.320± 0.14	62	21±1.4	6.05±0.64	29.237
Enzymatic Method	2.890± 1.10	100	12±2.30	5.81±0.98	46.591
Rigenera 60s Abdomen	0.722± 0.13	25	27±3.7	1.93±4.20	7.272

Figure 6. Comparison of Rigenera® and the enzymatic method. (a) Growth rate comparison of ASCs from Rigenera® extracted from the thigh and the enzymatic process. (b) Growth rate comparison of ASCs from Rigenera® extracted from the abdomen and the enzymatic method. (c) Growth rate comparison of ASCs extracted with Rigenera® from the thigh and abdomen. (d) Microscopic images (resolution 10×) of ASCs at high passages (p10). The tab shows all the results obtained.

Additionally, the replication rate was lower when using the Rigenera® device: extracted cells reached the confluence in 21 ± 1.4 and 27 ± 3.7 days with Rigenera® (for the thigh and abdomen, respectively), while, when using the

enzymatic method, they took 13 ± 3.5 and 12 ± 2.30 days (for the thigh and abdomen, respectively), as reported in the table of Figure 7.

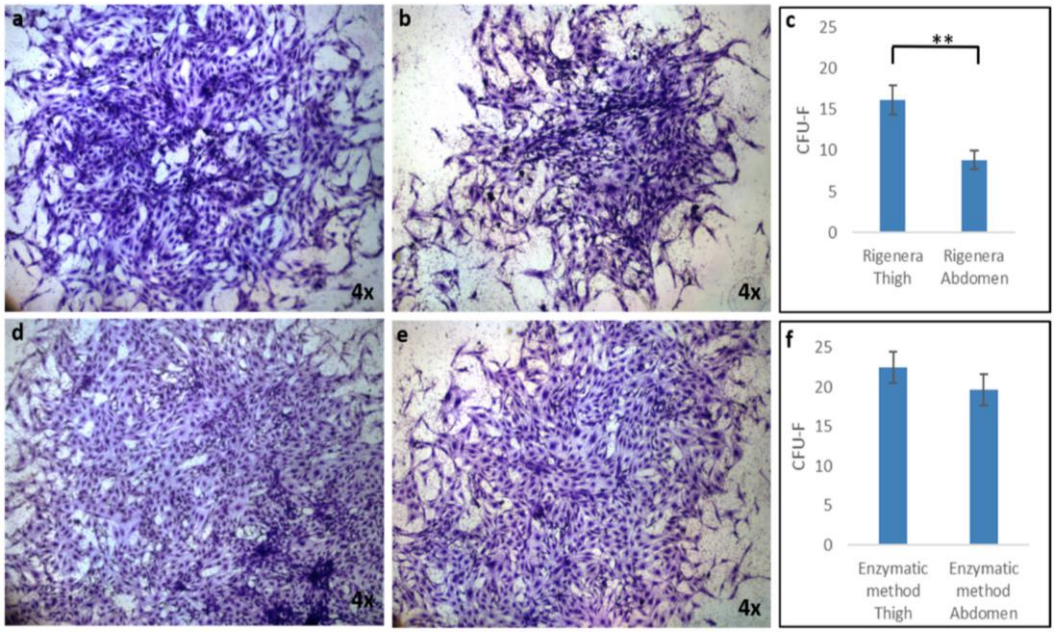

Figure 7. The colony-forming unit-fibroblast (CFU-F) assay of ASCs obtained by Rigenera® ((a) thigh and (b) abdomen) and the enzymatic method ((d) thigh and (e) abdomen). CFU-F values were determined at day 15 after plating using the Toluidine Blue staining method. ASCs extracted from the thigh (a–d) formed larger colonies containing more cells than those extracted from the abdomen (b–e); (c) CFU-F numbers at day 15 obtained by the Rigenera® device; CFU-F numbers showed significant differences between the two groups (thigh and abdomen). (f) The enzymatic method received CFU-F numbers on day 15; CFU-F numbers showed no significant differences between the two groups (thigh and abdomen). Data are presented as the mean ± SE, with n = 6 (** $p < 0.01$)

Comparing the two extraction sites, the cell yield for the abdomen was about 31% lower than that of the thigh. Moreover, the cells extracted from the thigh reached confluence six ± 2.3 days before the cells extracted from the abdomen (table in Figure 7), demonstrating a higher replicative rate.

The histograms in Figure 6. a, b show the number of cells from cellular passages 2 (p2), 6 (p6), and 10 (p10). Although the resulting rate of replication was higher with the enzymatic method, and the cells obtained with the enzymatic method were able to reach confluence faster than cells obtained with the Rigenera® method, at high passages (i.e., 10), no statistically significant difference in cell number was observed between the Rigenera®-obtained cells and Collagenase digestion (Figure 6a, b, *p*-value < 0.05). This means that, at these passages, the growth rate was comparable. Figure 6c compares the replication rate (in terms of the number of cells at passages 2–6 and 10) of the thigh and abdomen. The difference is evident at the low cellular passage (3.02×10^5 cells for the thigh and 9.92×10^4 cells of the

abdomen at passage 2). In contrast, the difference between the thigh and abdomen was not statistically significant after a long period of culture and many passages (such as at p10) (p-value < 0.05) (Figure 6.c). Finally, the morphological analysis highlighted a slight difference between the thigh and abdomen: for example, the cells obtained from the abdomen were flatter and more widely spread (Figure 6.d).

To compare the ability to form colonies of ASCs obtained from the thigh and abdomen, colony-forming unit-fibroblast (CFU-F) assays were performed. Figure 7 displays representative micrographs of CFU-F detected by Toluidine Blue staining after 15 days of Rigenera® treatment (Figure 7. a thigh, and b, abdomen) compared with enzymatic digestion (Figure 7.d, thigh, and b, abdomen). The images show that both ASCs treated with Rigenera® and isolated from the thigh and abdomen were able to grow to form clusters. Still, larger colonies (created by a higher number of cells) could be observed in samples obtained from the thigh compared to those from the abdomen (Figure 7. a, b). These differences are not evident in the samples treated with enzymatic digestion (Figure 7.d, e). Moreover, when the CFU-F numbers were counted, more colonies were detected in samples isolated from the thigh (16.17 ± 1.8) than the abdomen (8.83 ± 1.1), as reported in Figure 7. c. There were no statistical differences in the number of CFU-F between thigh and abdomen samples treated with enzymatic digestion.

To demonstrate the presence of ASCs in the Rigenera® product, an immunophenotypic assay at p0 (immediately after the treatments) was performed. Figure 8 shows a scatter plot that combines the signals obtained from the Forward Scatter (FSC) and Side Scatter (SSC). Based on the size, shape, and internal structure of cells, it was possible to select the mesenchymal-like cells presented in the scatter plot. In addition, the cytogram at p0 confirmed the much higher yield of stem cells for the enzymatic method (12.7% of ASCs from the thigh and 4.36% of ASCs from the abdomen) (Figure 8. a for the thigh, and b for the abdomen) compared to Rigenera® (0.92% of ASCs from the thigh and 0.15% of ASCs from the abdomen) (Figure 8.c for the thigh, and d for the abdomen).

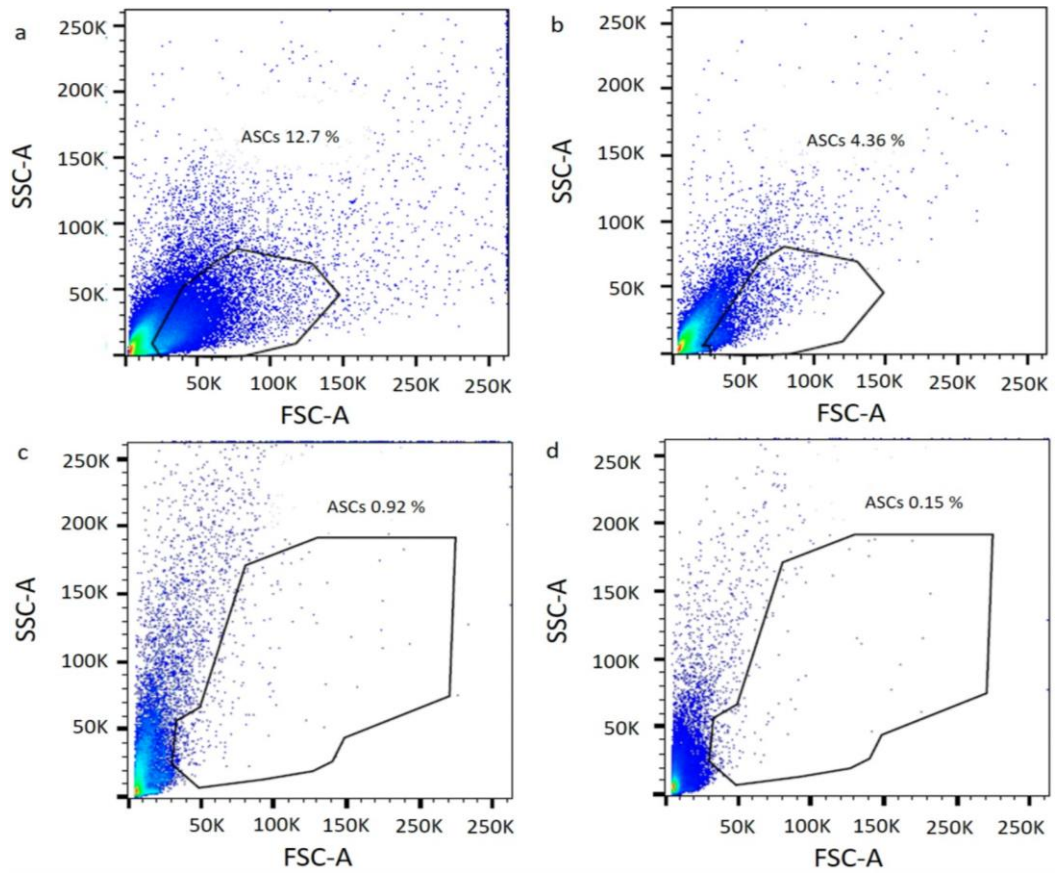

Figure 8. Cytograms of enzymatic digestion (a thigh; b, abdomen) and Rigenera® product (c, thigh; d, abdomen) at passage 0. Mesenchymal-like cells were selected based on Forward Scatter (FSC) and Side Scatter (SSC) information

Subsequently, specific single antigens or a combination of two antigens were tested on the previously selected cells. At p0, the ASCs isolated by the enzymatic method, including CD105, CD90, CD73, CD44, and CD29 (Figure 9 c–e), were expressed at a medium level. In contrast, the hematopoietic marker CD45 (Figure 9. a) was poorly expressed, and the hematopoietic marker CD34 was highly expressed (Figure 9).

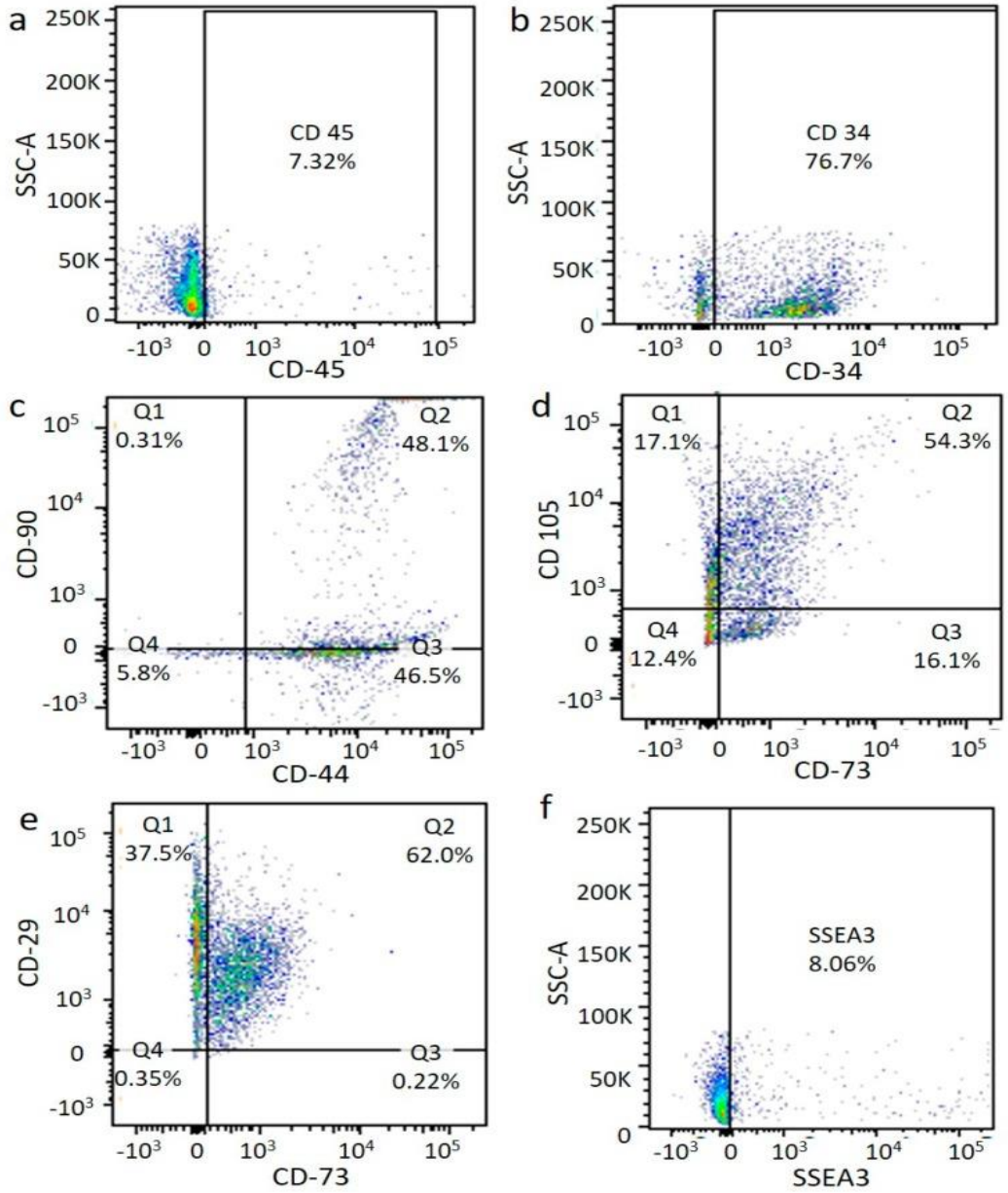

Figure 9. Flow cytometry after enzymatic digestion. Immunophenotyping analysis of ASCs at p0 from enzymatic digestion. Cell markers CD45 (a), CD34 (b), CD44/CD90 (c), CD73/CD105 (d), CD73/CD29 (e), and SSEA3 (f).

The ASCs obtained from the Rigenera® method at p0 showed a medium expression of mesenchymal stem cell markers (CD105, CD73, and CD29) (Figure 9. c–e) comparable with the results of the enzymatic method, confirming the presence of the ASC phenotype. In contrast, a different expression of the hematopoietic marker CD34 (Figure 9. b) was observed for the two techniques. Indeed, this antigen was more highly expressed after collagenase digestion, probably meaning that the Rigenera® method allowed the isolation of a purer cell population (see Figure 10). Finally, we also identified a generally low (8%) and medium (20.8%) presence of multi-lineage differentiating stress enduring cells (MUSE cells) for the enzymatic

and Rigenera® method, respectively (Figure 9. f and Figure 10. f). No differences in the marker expression level were found for the thigh and abdomen.

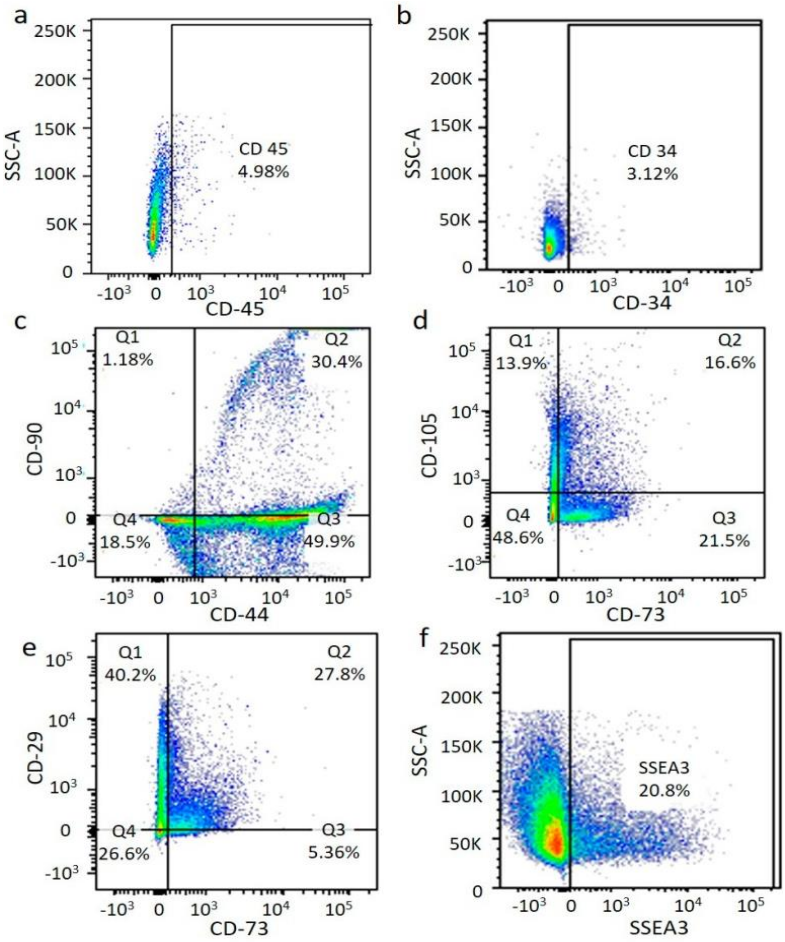

Figure 10. Flow cytometry after Rigenera® treatment. Immunophenotyping analysis of ASCs at p10 from Rigenera® treatment. The presence of the ASC phenotype is confirmed. Cell markers CD45 (a), CD34 (b), CD44/CD90 (c), CD73/CD105 (d), CD73/CD29 (e), and SSEA3 (f)

At a higher passage (p10), the antigen pattern was similar between cells obtained from the Rigenera® and enzymatic method, resulting in an increased expression of the mesenchymal stem cell surface marker and confirming phenotype maintenance. The immunophenotypic analysis at p10 also showed that the surface marker expression profiles of ASCs from the thigh and abdomen were comparable and preserved over time.

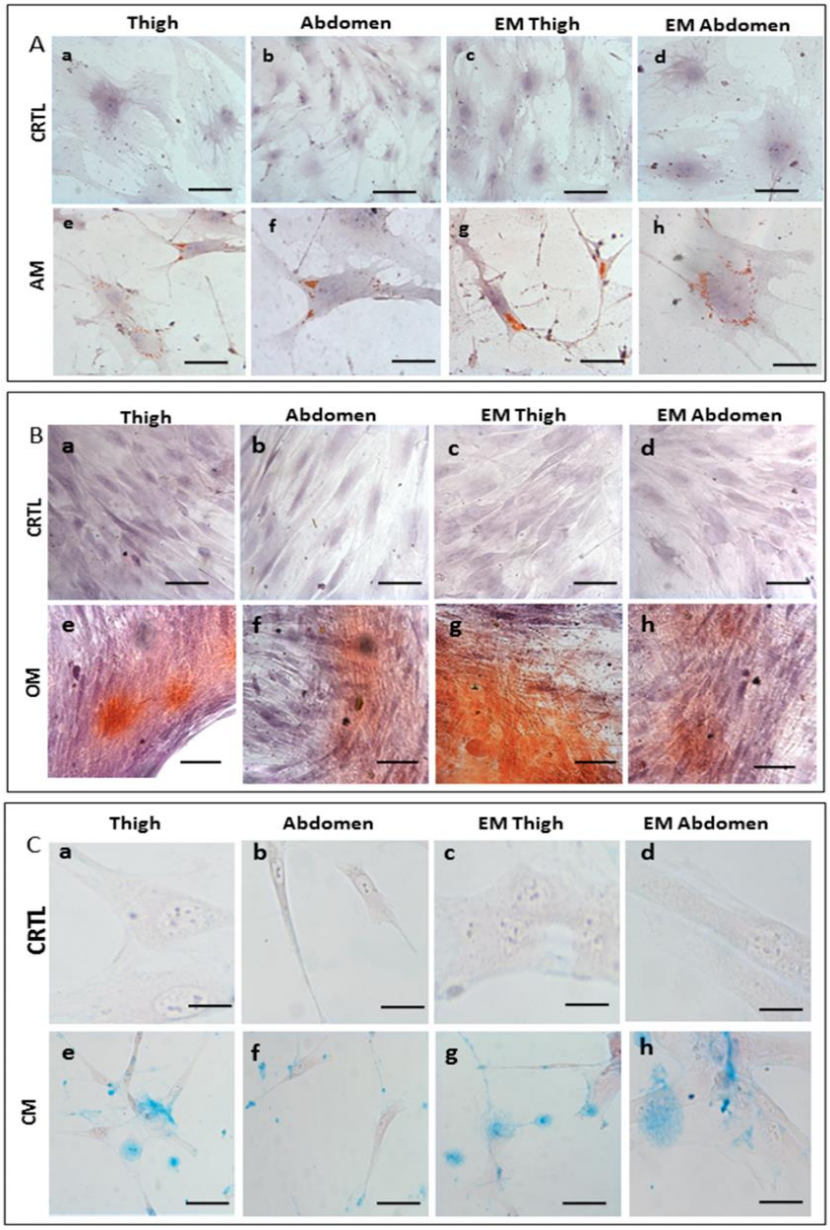

Figure 11. Cell differentiation assay. Multilineage differentiation potential of the ASCs from the thigh and abdomen after treatment with Rigenera® compared to enzymatic methods (EM). (A) Cells were cultured with complete ASC medium (CRTL) (a, b, c, scale bar 100 µm, d scale bar 50 µm) and adipogenic medium (AM) (e, f, g scale bar 100 µm, h scale bar 50 µm). In the adipogenic medium, adipogenesis was indicated by the accumulation of neutral lipid vacuoles stained with Oil Red O, while the nucleus was stained with hematoxylin. (B) Cells were cultured with complete ASC medium (CRTL) (a, b, c scale bar 100 µm, d scale bar 50 µm) and osteogenic medium (OM) (e, f, g, h scale bar 100 µm). In the osteogenic medium, osteogenesis was indicated by Alizarin Red S staining of extracellular matrix calcification, while the nucleus was stained with hematoxylin. (C) Cells were cultured with complete ASC medium (CRTL) (a, c, d scale bar 50 µm, b scale bar 100 µm) and chondrogenic medium (CM) (e, f, g scale bar 100 µm, h scale bar 50 µm). In a chondrogenic medium, chondrogenesis was shown by the deposition of sulphated proteoglycan-rich matrix stained with Alcian blue, while the nucleus was stained with hematoxylin.

To determine the multipotency of ASCs isolated from samples treated with Rigenera®, a differentiation assay for adipocyte, chondrocytes, and osteocytes was performed. In this experiment, we observed cellular differentiation macroscopically, and the results were compared with those of the enzymatic method and non-induced cells (Figure 11). The adipogenic differentiation of ASCs was confirmed by Oil Red O staining after 14 days of induction. Compared to the non-induced cells (Figure 11. A (a–d)), the cells stained with Oil Red O solution showed the formation of lipid droplets within the cytoplasm (Figure 11. A (e–h)). Moreover, there were no notable differences between ASCs isolated from the thigh and abdomen. The osteogenic potential was determined by Alizarin Red staining (Figure 11. B (e–h)) to indicate the extracellular matrix calcification. Both samples (thigh and abdomen) demonstrated positive staining in osteo-induced cells in contrast to the non-induced cells, indicating the osteogenic differentiation of ASCs. Finally, ASCs were chondrogenically cultured for three weeks and stained with Alcian blue. Chondrogenesis was observed in all samples by the deposition of the sulphated proteoglycan-rich matrix (Figure 11. C (e–h)). The differentiation potential between cells obtained with Rigenera® and enzymatic digestion was comparable. This result shows that ASCs obtained with Rigenera® treatment can differentiate towards multilineage cell fates.

viii) Application of Rigenera product *in vivo* (Dog)

Osteoarthrosis (OA) is a common degenerative, chronic, inflammatory, painful, and disabling condition which affects the joints. High rates of OA have been observed in dogs [74, 75,] and 20% of the canine population older than one year presenting OA across different stages [76, 77]. OA is one of the most disabling diseases in dogs [78-82] and is characterised by lameness, chronic pain, and functional impairment with a reduced quality of life. OA ultimately reduces mobility and can result in the complete loss of motor function [83]. Treatment of OA aims mainly to reduce pain and inflammation through drug administration, appropriate diets, and physiotherapeutic sessions. Typically, the non-operative approach is the most common. However, when this fails, surgical treatment can be performed [84-88].

OA is still the leading cause of non-traumatic euthanasia in dogs since pharmacological drugs mitigate articular pain without affecting OA progression. In recent years, scientific research has focused on substances able to slow down the progression of OA, regenerating the damaged tissues through local delivery instead of oral or parenteral drug administration, to avoid systematic side effects. For this purpose, oral visco-supplementation and intra-articular substances such as hyaluronic acid, platelet-rich plasma (PRP), and mesenchymal stem cells (MSC) have increased over time [89, 90]. MSCs are in the bone marrow, adipose tissue, synovial membrane, and muscular tissue, exerting an immunosuppressive, anti-inflammatory, and antifibrotic effect. Tissue engineering considers adopting MSCs as an option for regenerating tissues, regarding bone and cartilage, due to their ability to differentiate into multiple cytotypes, including chondrocytes and osteoblasts [91, 92]. Still, MSCs are also able to heal the damaged tendon [93]. Therefore, the "stromal vascular fraction" (SVF), which is mainly located around blood vessels, is a heterogeneous solution stemming from adipose tissue and composed of adipose stem cells (ASCs), endothelial cells, and stromal cells [94]. According to the literature, ASCs are genetically and morphologically stable in long-term cultures and characterised by slow senescence and a high [95-97]. Cell therapies and "minimally manipulated" tissue micrografts mainly differ because the adipose tissue is not enzymatically digested but only processed mechanically. Autologous adipose micrografts consequently contain MSCs and an extracellular matrix (ECM) [98, 99]. Compared to enzymatic digestion treatments, mechanically obtained micrograft approaches are considered advantageous due to preserving the stromal vascular niche, permitting adequate growth factor release, and discharge bioactive molecules by exosome-rich mechanically processed fat.

Furthermore, mechanically obtained-Adipose SVF techniques can retain the structure and morphology of the micro-environment where micrografts reside. Previous studies regarding "minimally manipulated" adipose tissue administration have confirmed its safety [100, 101], but specific issues are not as clear-cut. The benefits, for instance, of SVF in repairing tissue and its bridging potential of new and old tissue is well-known. Still, these advantages are not as appropriate concerning intra-articular fat injections due to the lack of tissue fragments to connect [102]. Interestingly, SVF possesses fundamental trophic, anti-apoptotic, anti-scarring, mitogenic and immunomodulatory properties [103, 104], which aid in generating numerous bioactive elements, growth factors and cytokines. Such cells can perceive and mark modifications within the specific microenvironment [105]. The field of research has also addressed the use of purified adipose tissue and revealed positive anti-inflammatory and reconstructive outcomes related to cartilage regeneration [106] within *in vitro* and *in vivo* studies. Good manufacturing practice regulations [107] exert restrictions on enzymatic therapy, and therefore minimally manipulated autologous adipose tissue is a favourable treatment alternative. In this context, micro-fragmented adipose tissue has been promptly used and commercialized to offer minimally manipulated [108] options, avoiding cell expansion and enzymatic treatments. However, it is worth recalling that optimal acquirement of the SVF is not always possible [99]. However, some authors have recently demonstrated [109-115] the efficacy of a medical device named Rigenera® (CE certification, Class II, Human Brain Wave, Turin, Italy), which can obtain adipose micrograft enriched by cellular progenitors which are immediately available for everyday clinical practice. Adipose micrograft is characterised by high cell viability and is obtainable through mechanical disruption [98, 116]. This work describes the SVF obtained by a well-known commercial system (Rigenera®) through mechanical disruption of canine adipose tissue without substantial manipulations.

ix) What we did and what we found

Isolation and Expansion of ASC

Adipose tissue samples (8 ml) were harvested from two different anatomical regions (lumbar and thigh) of n = 6 dogs, donated by the owners and with appropriate informed consent to the University of Camerino, using a standard surgical procedure previously described [116]. The study was conducted according to the guidelines of the Declaration of Helsinki and approved by the Animal Welfare Organization (or OPBA) of Camerino University (protocol code 1D580.18A).

Each adipose sample was divided into two portions. The first portion was processed in the Rigenera®, and the experiment was performed as stated before (page 19)

Cells Yield

Cells obtained from the Rigenera® and the ED process were counted through the Trypan Blue exclusion method by dividing the number of viable cells per ml of processed fat. Data are expressed as several likely cells/ml fat ± standard errors of the mean (SEM).

Cell Colony Forming Unit Assay

Colony-forming unit-fibroblast (CFU-F) assay was performed for tissue processed with Rigenera® and ED. Briefly, isolated cells were plated into six-well culture plates at a density of 1000 cells/cm^2 and cultured in the complete media. On the 15th day after plating, the total number of cell colonies (CFU-F, a cluster of at least 50 adhered and fibroblast-like cells) was rinsed with phosphate-buffered saline twice, fixed with 10% neutral buffered formalin for 30 min and then stained with toluidine blue (Sigma Aldrich, Milan, Italy) and counted. Colony-forming efficiency (CFE) was calculated by dividing the number of colonies counted by the number of cells seeded × 100. Data are expressed as CFE ± SEM.

Proliferation Capacity

On day four from ASC isolation, cells were detached using Trypsin-EDTA 1% (GIBCO Life Technology, Monza, Italy) and replated at a density of 10,000 cell/cm^2 plated into six-well culture (in triplicates). Cells were detached and counted with CytoSMART counter (Automated Image-Based Cell Counter, version 1.5.0.16380, CytoSMART technologies B.V, Eindhoven, The Netherlands) after 24, 72, and 96h. The population doubling time (PDT) was calculated using the following equation: $pdt = [t\ (h) \times \log 2]/\log (N_f/N_i)$ (as reported in Martinello T. et al. 2010) [115], where N_i and N_f are initial and final cell numbers, respectively.

Cellular Yield CFE and Proliferation Capacity: our findings

The cell yield of freshly isolated micrograft from Rigenera device was $2.23 \times 10^4 \pm 6.94 \times 10^3$ cells/ml fat $2.29 \times 10^5 \pm 4.54 \times 10^4$ cells/ml Fat (Figure 1a), for lumbar and thigh, respectively. Compared to ED, the cell yield of Rigenera results were 23.9 ± 3.2% and 41.6 ± 4.5% for lumbar and thigh, respectively. Moreover, the cell yield obtained from the thigh region was 10 and 6 times higher than the lumbar region for Rigenera and ED, respectively. To analyse the clonogenic potential of Rigenera cells, a CFU-F assay was performed, and CFE was evaluated (Figure 1b). The ED method allowed cell isolation with 2.58 ± 0.55% and 2.77 ± 0.47% of CFE, for lumbar and thigh, respectively, while Rigenera cells presented a clonogenic efficiency of 1.17 ± 0.44% for the lumbar region and 1.2 ± 0.29% for the thigh. The

difference between the lumbar and thigh region was not statistically significant. Figure 1c represents a clone for the CFU-F assay. To better characterise the cellular products, the proliferation capacity and the time required by cells to duplicate in number were estimated. As shown in Figure 12.d, ED cells needed less time to duplicate when compared to Rigenera cells. As reported in Figure 12, the population doubling time mean value was 50.17 ± 7.8h and 47.02 ± 6.4h for Rigenera lumbar and thigh, respectively. ED cells have a population doubling time 1.4 times higher than Rigenera (34.46 ± 4.8 and 32.16 ± 2.58 h for ED lumbar and thigh, respectively). Statistically significant differences between the lumbar and thigh were not detected.

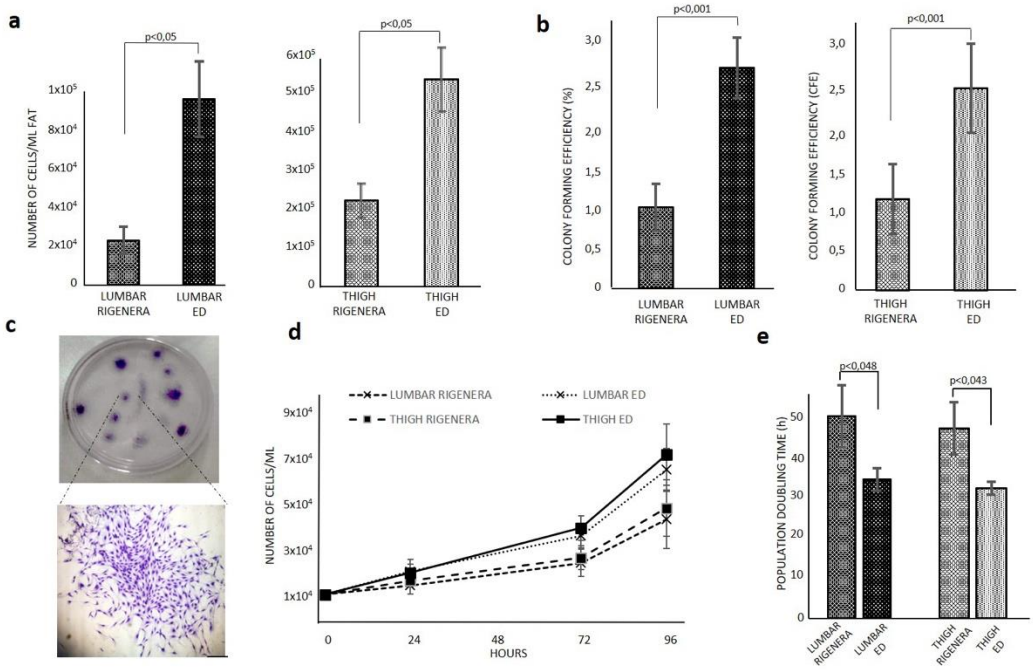

Figure 12. Cells yield, CFE and proliferation capacity of Rigenera® obtained from lumbar and thigh region. a) Cells yield of Rigenera® and ED product. b) CFE calculated based on CFU-F assay. c) Representative petri dish of CFU-F assay and an amplified image of a CFU-F observed with light microscope stained with Toluidine Blue (4x magnification). d) Proliferation capacity after 24, 72 and 96 hours (left) and population doubling time (right). Data are expressed as average ± SEM.

Immunophenotyping

After isolation, cells were counted, and 2×10^5 cells were placed in a tube for cytofluorimetric analysis. The pellet was washed with 1 ml of 1% FBS in PBS and then labelled with fluorescent-dyes conjugated antibodies in a final volume of 100

µl and incubated for 30 min in ice. This study examined specific antibodies: APC-conjugated CD90 (dilution 1:5), APC Alexa Fluo-conjugated CD73 (dilution 1:20), PE-conjugated CD34 (dilution 1:5), BV650-conjugated CD45 (dilution 1:20), and APC-conjugated MHC II (dilution 1:5). The antibodies were purchased from BD Biosciences (Becton Dickinson Italy S.p.A., Milan, Italy). After the incubation, the pellet was rinsed, resuspended in 300 µl of 1% FBS in PBS, and transferred to flow cytometry tubes. The immunophenotyping was performed through a FACS canto II (Becton Dickinson Italy S.p.A., Milan, Italy).

The relative expression percentages of surface markers of Rigenera micrograft analysed by flow cytometry are shown in Figure 13. a. The presence of surface molecules was analysed using specific monoclonal antibodies against MHC II, CD45, CD34, CD73, and CD90. MHC II was not expressed in the cell population examined, and CD45 was poorly expressed. In contrast, the hematopoietic marker CD34 (endothelial cells, pericytes and potential ASCs) was expressed, especially in cells extracted from the thigh region (6.5 ± 1.1%). Cells were positive for the mesenchymal stem cells marker CD 73 (23.2 ± 3.8% and 18.4 ± 7.1for lumbar and thigh, respectively) and CD 90 (24.9 ± 8.5% and 20.5 ± 5.3 for lumbar and thigh, respectively) (Figure 13. a). Comparing the surface marker expression profiles of cells obtained after Rigenera® and ED, no significant statistical differences were found (Figure 13.b).

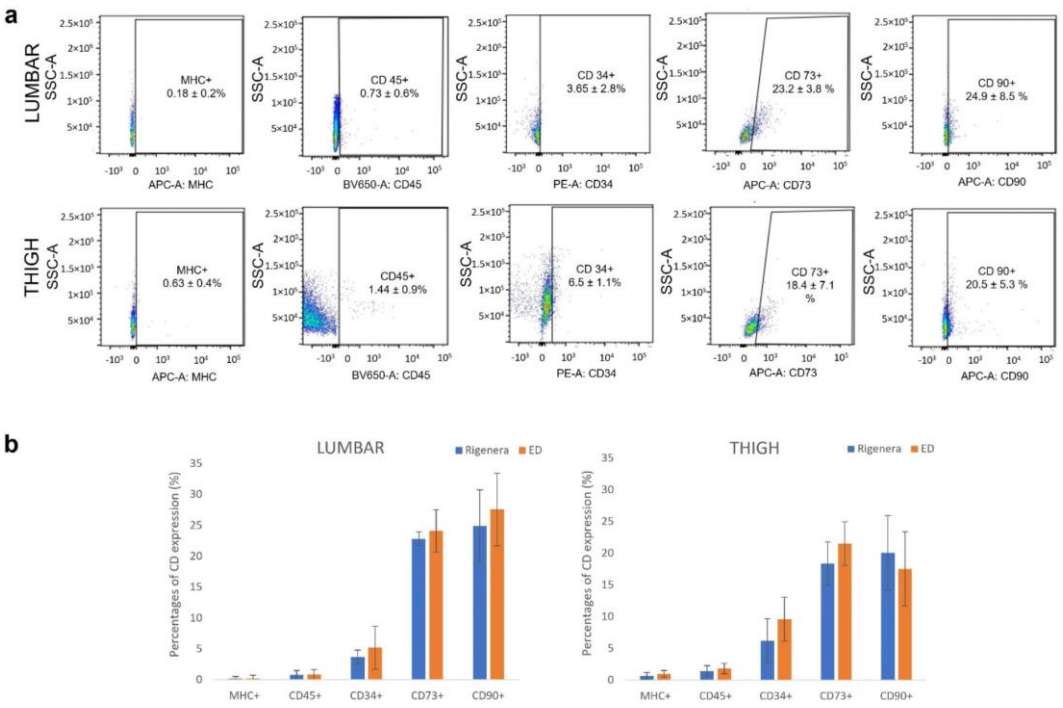

Figure 13. Immunophenotype of Rigenera® product. Representative results show that cultures were negative for MHC class II, low positive for CD45 and CD34, positive for CD73 and CD90. (Results are expressed as average ± SEM of n = 3 samples).

Qualitative Analysis of Multipotency

The potential of the ASCs, obtained after Rigenera® and ED, to differentiate into multilinear cell lineage (adipocytes, chondrocytes, and osteocytes) was evaluated by adding adipogenic, chondrogenic, and osteogenic media separately. ASCs were cultured until p3 to remove peripheral blood contaminants and other non-adherent stromal cells, detached using Trypsin-EDTA 1% (GIBCO Life Technology, Monza, Italy) and replated in triplicates in a multi-well plate with the above-mentioned different media.

Adipocyte differentiation was achieved after 16 days of culture of MSCs with adipogenic medium, containing 10^{-6} M dexamethasone, 10 μg/ml insulin, and 100 μg/ml 3-isobutyl-1-methylxanthine (Sigma Aldrich, Milan, Italy). Chondrocyte differentiation was achieved after 14 days of culture with the StemPro chondrogenesis differentiation kit (GIBCO Life Technology, Monza, Italy). Osteocyte differentiation was achieved after 21 days of culture with the StemPro osteogenesis differentiation kit (GIBCO Life Technology, Monza, Italy). The non-induced cells of the control group were cultured with the ASC complete medium (Dulbecco's Modified Eagle Medium (DMEM), 10% FBS, and 1% p/s).

Oil Red O, Alcian blue, and Alizarin Red Stain were employed to identify adipocytes, chondrocytes, and osteocytes.

Adipogenic Differentiation

Around 5000 cells were seeded, and the same procedure was followed as described on page 21. Images were obtained using optical microscopy (Olympus BX-51 microscope, equipped with a KY-F58 CCD camera, magnification 20×).

Chondrogenic Differentiation

The cells were cultured as described on page 22. The cells were then washed with normal water and fixed with aqueous mounting media. Images were obtained using an Olympus BX-51 microscope, equipped with a KY-F58 CCD camera (Magnification 10×).

Osteogenic Differentiation

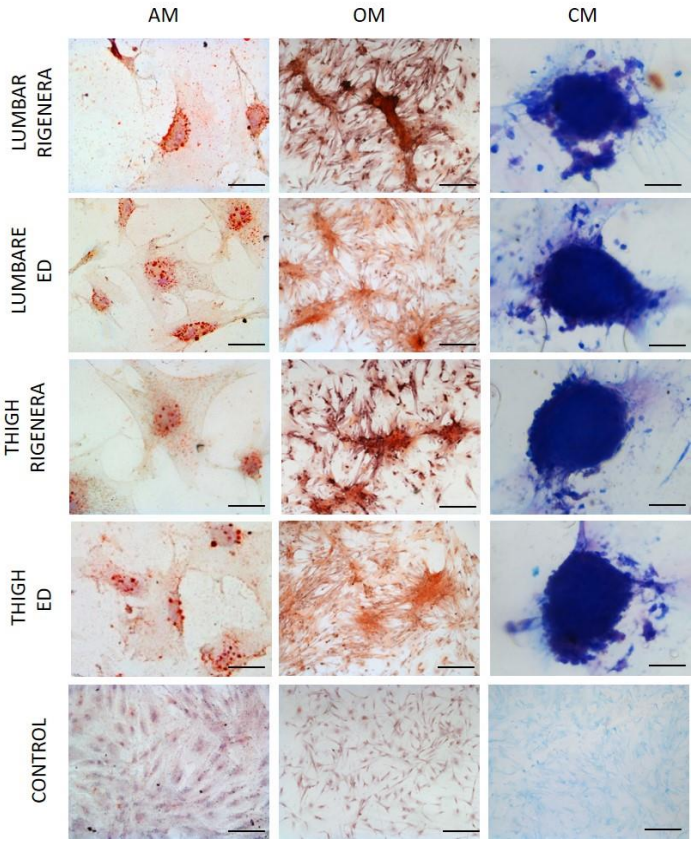

Figure 14. Representative photographs of differentiation capacity of ASCs obtained with Rigenera device. AM, adipogenic medium; CM, chondrogenic medium; OM, osteogenic medium. Control cultures were maintained in a normal medium. The samples were stained with Oil Red O, Alizarin Red, and Alcian Blue for adipo-, osteo- and chondrogenic differentiation. Scale bar: AM, 5 µm; OM, 20 µm; CM, 50 µm; Control, 20 µm.

The same procedure was performed as stated for the previous differentiation assay. Images were obtained using optical microscopy (Olympus BX-51 microscope, equipped with a KY-F58 CCD camera, magnification 4×).

To evaluate the multi-potency of Rigenera® micrograft, ASCs were exposed to the adipogenic, osteogenic, and chondrogenic medium. As shown in Figure 14, all samples could differentiate into mesodermal lineages. Oil Red O staining confirmed the adipogenic differentiation and red lipid droplets were visible in the cytoplasm of cells; Alizarin Red staining highlighted the extracellular matrix calcification typical of osteogenic differentiation, while chondrogenesis was observed by deposing sulfated proteoglycan-rich matrix stained with Alcian blue. No significant differences were observed between Rigenera® and ED and between the lumbar and thigh regions.

Hy-Tissue SVF® (Fidia pharmaceuticals, Italy)

x) Overview of the device

Biological therapies have become popular in the last few decades since they represent an alternative to the classical pharmacologic or surgical approaches to treat acute and degenerative chronic injuries. In this sense, adipose tissue has been an essential biological product for treating chronic and acute degenerative conditions since it is a source rich in adult multipotent stem cells [126].

This work aims to characterise a novel commercial system (Hy-Tissue SVF) for obtaining SVF by mechanical disruption of adipose tissue without substantial manipulations. As we stated, SVF represents a freshly isolated heterogeneous cell mixture present in the adipose tissue. It comprises smooth muscle cells, preadipocytes, endothelial cells (ECs), and multipotent adult stem cells, such as endothelial and hematopoietic progenitor cells (EPC), pericytes, and ADSCs, among others [127, 128]. The higher mesenchymal stem cell concentration in the native adipose tissue has led researchers and clinicians to focus on the bone marrow to the adipose tissue. For example, the frequency of MSC in bone marrow is 0.01–0.001% cells [129], while adipose tissue contains 500 times more MSC per volume of fat than the volume of bone marrow [127].

Moreover, ADSC has been proven helpful in modifying inadequate healing responses that lead to the degeneration of a tissue and its improper remodelling, such as chronic inflammation [130], fibrosis [131], and hypermetabolic responses [132]. Thus, SVF is considered important due to its potential in regenerative medicine, particularly for osteoarthritis treatment [133-135]. SVF can be obtained from adipose tissue by enzymatic or non-enzymatic processes [136]. Enzymatic digestion of adipose tissue is the most common isolation technique based on proteases, such as collagenases, which digest the tissue matrix [137]. This procedure results in an SVF cell product with a high cellular yield with a high frequency of progenitor cells. However, it is time-consuming (requires a 30–45 min incubation step with a controlled temperature of 37 °C), and the cells obtained are considered substantially manipulated, which makes the product to be classified as an advanced-therapy medicinal product (ATMP) by regulatory authorities in Europe and USA (Regulation (EC) No 1394/2007; 21 CFR 1271.10, respectively). Alternatively, non-enzymatic (mechanical) methods use physical forces to disrupt the tissue and obtain adipose stroma [138]. This procedure has the advantage that it is not considered a substantial manipulation, and, on the other hand, it is faster and more straightforward than the enzymatic method.

xi) Characterizing and analysing the product

Adipose Tissue Collection

The adipose tissue was collected from 27 women undergoing liposuction for aesthetic purposes, aged between 41 and 69 years. Informed consent was taken before the collection of adipose tissue by the ethical guidelines established as written before.

Procedure for SVF Production

Each sample of adipose tissue (about 30 ml) was decanted to remove excess oil and divided into 2 portions. The first portion of the lipoaspirate sample was processed by different trained technicians with the Hy-Tissue SVF kit (Fidia Farmaceutici, Abano Terme, Italy) through a mechanic disaggregation process. The kit provided a sterile, single-use, tissue collection double bag with an inner filter bag of 120 μm mesh. A volume of lipoaspirate (25–30 ml) was transferred into the inner bag by the upper port. Placing the bag vertically, the Klein solution containing part of blood cells was recovered in the lower part of the processing bag and removed. At the same time, the adipose tissue remained in the inner filter bag. An equal volume of PBS solution equal to Klein solution removed was introduced into the processing bag through the upper port. The fat was processed according to the instruction for use. Briefly, fat tissue was massaged for 5 min and disaggregated using a small plastic rod and enforced to pass through the filter bag by manual massaging. The disaggregated tissue was collected with a syringe using the lower valve port of the outer bag and centrifuged at 400 G for 10 min at room temperature, followed by resuspension in 1 ml of complete culture medium to count the number of cells inside. The product obtained by this method was named “SVF”.

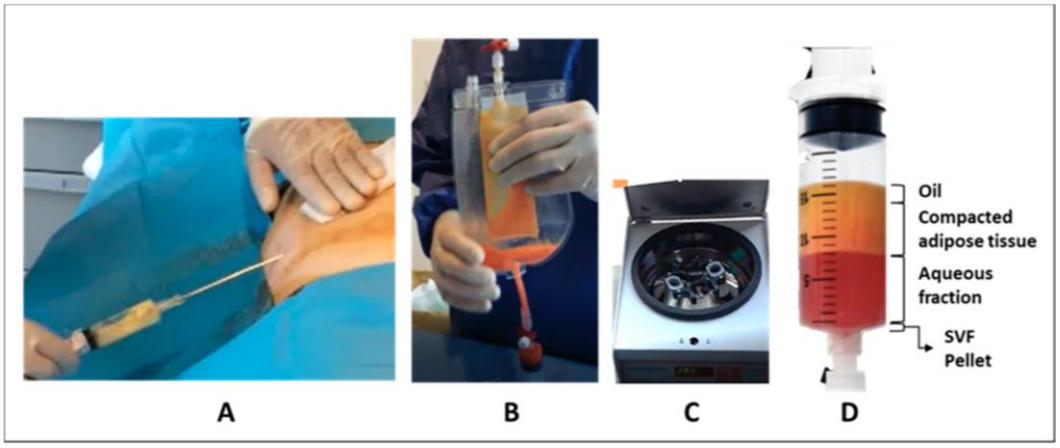

Figure 15. Diagram of the Hy-Tissue Stromal Vascular Fraction (SVF) process; (A) Lipoaspiration; (B) mechanical disaggregation of adipose tissue using the double bag; (C) centrifugation, (D) phase separation: From up to down, it is possible to distinguish the following layers: Oil, condensed fat, aqueous fraction, and a bottom pellet with the SVF product.

We have investigated the composition of the SVF obtained with the Hy-Tissue SVF kit. For this purpose, 22 lipoaspirates were processed following the protocol recommended by the manufacturer. Once the adipose tissue was filtered (and disrupted) by the nylon membrane of 120 µm, the centrifugation step separated the disrupted tissue into three different layers, based on the water or lipid content. The upper phase consisted of a liquid oily phase resulting from the release of stored oil from mature adipocytes. Then, there is a phase of condensed adipose tissue (Coleman-like), which still have adipocytes allowing it to float in an aqueous solution, and finally, a non-floating pellet that contains the SVF (Figure 15)

Enzymatic Digestion of the Fat

The 2nd portion of lipoaspirate (5 ml) was processed using an enzymatic method, as reported in Dai Pre et al., 2020. Briefly, fat samples were digested with collagenase type I at the concertation of 1 mg/ml (GIBCO Life Technology, Monza, Italy) resuspended in Balanced Salt Solution of Hank (HBSS, GIBCO Life Technology, Monza, Italy) and bovine serum albumin (BSA, 2%, GIBCO Life Technology, Monza, Italy) at 37 °C for 45 min. Complete culture medium was added to neutralise the enzyme action, and the sample was centrifuged at 400 G for 10 min. After centrifugation, the pellet was incubated with 2 ml of lysis buffer for 10 min. The cell suspension was centrifuged and resuspended with 2 ml of complete culture medium. The product obtained by this method was named “FAT-ED”.

Enzymatic Digestion of the SVF

Adipose tissue (25 ml) of N = 5 patients was subjected to Hy-Tissue SVF treatment using the described protocol. An aliquot of each SVF product was stored for proliferation capacity and CFU-F analysis of the portion of the free cell while the rest was centrifuged at 400 G for 10 min. The pellet obtained was resuspended in 1 ml of 1 mg/ml of collagenase type I (GIBCO Life Technology, Monza, Italy) solution in the HBSS (GIBCO Life Technology, Monza, Italy) and 2% of BSA (GIBCO Life Technology, Monza, Italy) for 20 min at 37 °C inside a shaking incubator, then the complete medium was added (1:1 v/v) to block enzymatic digestion. The digested material was centrifuged (400 G, 10 min). The product obtained by this method was named "SVF-ED".

Cell Counting and Yield

Free cells were counted using Trypan Blue exclusion assay using a Burker chamber manually and with CytoSMART counter (Automated Image-Based Cell Counter, version 1.5.0.16380, CytoSMART Technologies B.V, Eindhoven, The Netherlands). Cell or CFU-F yield was calculated considering the total amount of free cells of SVF, SVF-ED, or FAT-ED divided by the volume of fat processed after discarding the Klein solution.

Cell Proliferation Capacity

To determine the cell proliferation capacity of the free cells in either SVF, SVF-ED, or FAT-ED, 2×10^5 cells of each product were plated on a 25 cm^2 T-flask and incubated at 37 °C with 5% CO_2. Three days after the cell extraction, the complete medium was changed every 48 h until 80% confluence. The days the culture required to reach confluence (passage 1) determined the proliferation capacity. Moreover, to estimate the time required by cells to duplicate their number, population doubling time assays were performed. Four days after the seeding, 5×10^4 cells from

"SVF," "SVF-ED," and "FAT-ED" were plated in T-25 Flasks (in triplicates) and cultured with 5 ml of complete media and incubated at 37 °C, 5% CO_2, for 24, 72, and 96h. At each time point, cells were washed with PBS 1x, detached with trypsin/EDTA, resuspended in 1 ml of media, and counted using a CytoSMART counter (Automated Image-Based Cell Counter, version 1.5.0.16380, CytoSMART Technologies B.V, Eindhoven, The Nether- lands). The population doubling time (pdt) was calculated using the following equation: pdt = [t(h)*log2]/log (Nf/Ni) (as reported in Martinello T. et al., 2010), where Ni and Nf are initial and final cell numbers, respectively.

Colony Forming Unit Assay

In triplicate, free cells from SVF, SVF-ED, or FAT-ED were seeded in a 6-well plate at 1000 and 5000 cells/well. Cells were cultured for 14 days. Toluidine blue (Sigma- Aldrich, Milan, Italy) staining was performed to count the colony, and only clusters of at least 50 fibroblast-like cells were considered. The frequency of CFU-F within SVF, SVF-ED, or FAT-ED was expressed as a percentage of seeded cells.

Optical Microscopy

SVF pellets (N = 8) obtained after Hy-Tissue SVF treatment were analysed by the whole-mount method (Larsen PL 1989) and paraffin included. Briefly, N = 4 pellets were washed with saline, stained with Hematoxylin and Eosin (Bio-Optica, Milan, Italy), and placed on the slide without dissection with the whole-mount method. Other pellets (N = 4) were washed with PBS and fixed with 10% formalin (Sigma-Aldrich, Milan, Italy) for 4h, dehydrated until xylene, and included in paraffin. Sections of 5 μm were cut with a microtome into sections. The sections were then dried at 37 °C for 24h and stained with Hematoxylin and Eosin (Bio-Optica, Milan, Italy). All slides were examined under an Olympus BX51 microscope (Olympus, Tokyo, Japan) equipped with a digital camera (DKY- F58 CCD JVC, Yokohama, Japan). The digital images were analysed with Image-ProPlus 7.0 software (Media Cybernetics, Silver Spring, MD, USA).

SEM Analysis

For scanning electron microscopy analysis (SEM), SVF pellets (N = 4) were fixed in 2% glutaraldehyde (Sigma-Aldrich, Milan, Italy for 4h, postfixed in 1% osmium tetroxide (Sigma-Aldrich, Milan, Italy) for 1 h, and dehydrated in graduated acetone concentrations (Sigma-Aldrich, Milan, Italy). The samples were treated with a critical-point dryer (CPD 030, Balzers Vaduz, Liechtenstein), mounted on metal samples, and coated with gold (MED 010 Balzers). SEM images were acquired with XL30 ESEM (FEI-Philips, Eindhoven, The Netherlands).

Immunophenotyping

Free cells from SVF and SVF-ED products and the subsequent subculture cells (named as passage 1–P1) were characterised by flow cytometry. For this purpose, SVF and FAT-ED products were passed through a 45 μm cell-strainer to remove micro-fragments and cell clumps. Then, 0.2×10^5 cells were washed with 1 ml in PBS (1X). Cells were incubated with conjugated antibodies for 30 min. After incubation, the pellets were centrifuged (7000 rpm, 5 min) and resuspended in 300 μl of PBS (1X). The antibodies used were: CD90 APC conjugate (1:5 dilution), CD105.5 PerCP-Cyt5.5 conjugate (1:20 dilution), CD73 BV421 conjugate (1:20

dilution); CD44 BV785 conjugate (1:20 dilution), CD34 PE conjugate (1:5 dilution), CD29 FITC conjugate (1:20 dilution), CD45 FITC conjugate (1:20 dilution), CD146 APC conjugate (1:20 dilution), CD68 FITC conjugate (1:20 dilution), CD116 FITC conjugate (1:20 dilution). For cell viability, Propidium Iodide was used. All antibodies were purchased from BD Biosciences (Becton Dickinson Italy S.P.A., Milano, Italy). Immunophenotyping was performed through a chant II FACS (BD, Becton Dickinson, Milano, Italy). Moreover, we performed a white blood cell differential (WBC diff) count on the Advia 120 automated haematology analyser (Bayer Diagnostics, Berkshire, Newbury, UK). The WBC was divided into four main cell subpopulations, corresponding to neutrophils (NEUT), lymphocytes (LYMPH), monocytes (MONO), eosinophils (EO). Basophils (BASO) were counted in a separate channel.

In Vitro Differentiation Assays

The differentiation potential was evaluated in vitro for SVF and SVF-ED (control). Differentiation was carried out employing expanded cultured cells from passage 4. For adipogenic differentiation, 7000 cells were seeded on a 6-well plate, incubated, and after 24h, the media was replaced with adipogenic media (Sigma-Aldrich, Milan, Italy) and incubated for 16 days. Then, cells were fixed with 4% paraformaldehyde (PFA) for 30 min at 4 °C, washed twice with PBS, and stained with Oil Red O (Bio-Optica, Milan, Italy) for 20 min and Hematoxylin (Bio-Optica, Milan, Italy) for 1 min. For chondrogenic differentiation, 1×10^6 cells resuspended in 5 µl of complete media were seeded in a 24-well plate. After 2h, the chondrogenic media was added (StemPro chondrogenic differentiation Kit -GIBCO Life Technology, Monza, Italy). After 14 days of incubation, changing the media every 3 days, cells were fixed with 4% PFA for 30 min at 4 °C, washed twice with PBS, and stained with Alcian Blue 8GX (Sigma-Aldrich, Milan, Italy) to detect mucopolysaccharide extracellular matrix. Five thousand cells were seeded on a 12-well plate with complete media for osteogenic differentiation. After 24h, the media was changed with osteogenic media (StemPro osteogenesis differentiation Kit– GIBCO Life Technology, Monza, Italy). After 21 days, cells were fixed with 4% PFA for 30 min at 4 °C, washed twice with PBS, and incubated with 0.2% Alizarin Red (Sigma-Aldrich) for 5 min and Hematoxylin (Bio-Optica, Milan, Italy) for 1 min. Images were obtained using optical microscopy.

xii) Result

We have investigated the composition of the SVF obtained with the Hy-Tissue SVF kit. For this purpose, 22 lipoaspirates were processed following the protocol recommended by the manufacturer. Once the adipose tissue was filtered (and disrupted) by the nylon membrane of 120 µm, the centrifugation step separated the disrupted tissue into three different layers, based on the water or lipid content. The upper phase consisted of a liquid oily phase resulting from the release of stored oil from mature adipocytes. Then, there is a phase of condensed adipose tissue (Coleman-like), which still have adipocytes allowing it to float in an aqueous solution, and finally, a non-floating pellet that contains the SVF (Figure 15)

Microscopical Analysis of the SVF

Microscopical analysis of the sediment obtained with the mechanical dissociation process of the fat (SVF) revealed the presence of a cells pellet (Figure 16. A) composed of free cells (Figure 16. B) and micro-fragments (Figure 16. C) of stromal connective tissue.

A heterogeneous cell population was observed) and stars in Figure 16. B highlights the nuclei and cytoplasm (see stars in Figure 16. B). The micro-fragments appeared as elongated cylinders with an average diameter of about 30 - 70 µm of variable length with a fibrinoid assembly with tubular structures (stained in deep purple), which represents microvascular elements consistent in capillaries of variable length containing endothelial and perivascular cells (Figure 16.D, E). The evidence of optical microscopy was supported by SEM images (Figure 16. F, H). The micro-fragments were composed of dense connective tissue with the presence of collagen structured as isolated fibrils (Figure 16. F arrow) or coarse bands (Figure 16G arrow) containing adherent cells (Figure 16. F, G*). Moreover, SEM images show the presence of adipocytes (Figure 16. H) that appear of small size (10^{-2} µm), attributable to adipocytes that have lost their lipid content or are not completely differentiated.

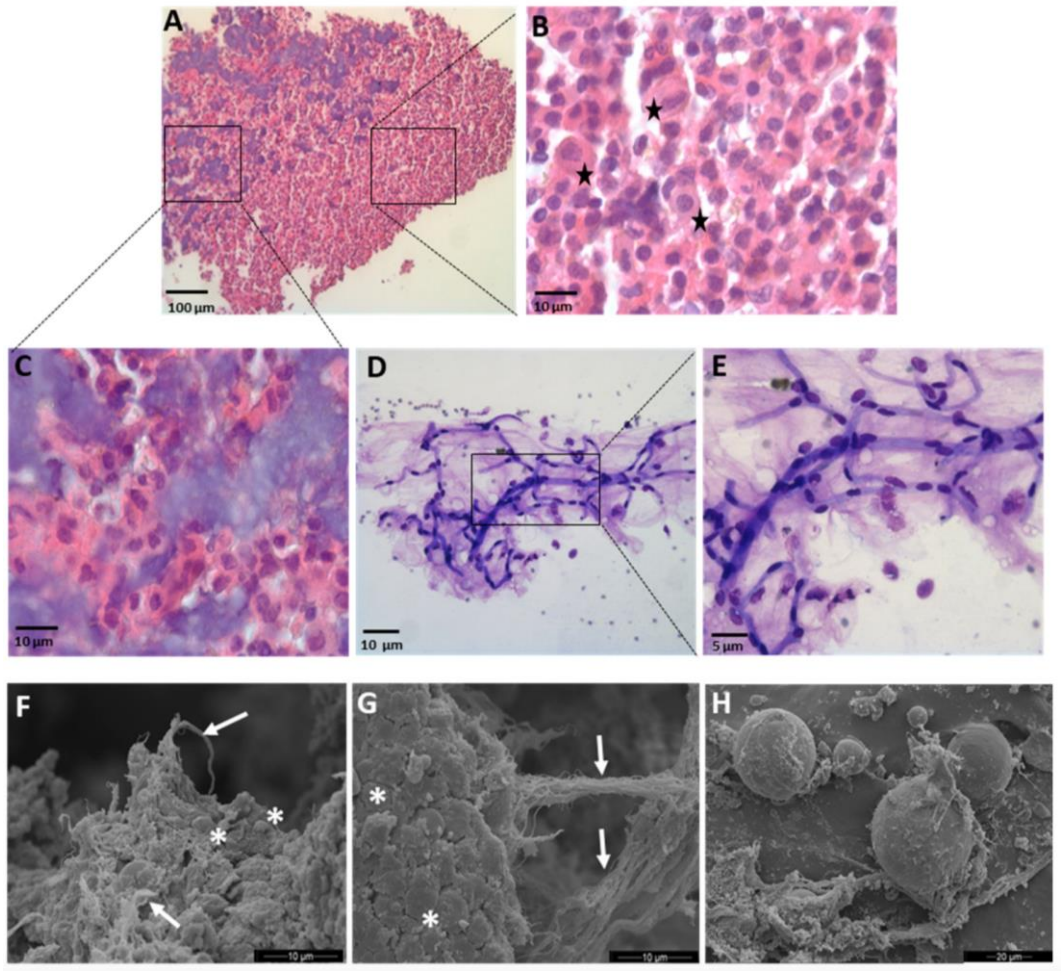

Figure 16. Morphological and ultrastructural analysis of Hy-Tissue SVF product. (A–C) Light microscopy of a single-layer section of pellet stained with Hematoxylin and Eosin. Black stars in (B) highlight cell heterogeneity. The squares indicate the location of the higher magnification image in (B, C). (Scale bar: (A) 100 µm, (B, C) 10 µm). (D, E) Hematoxylin and Eosin Staining location of the higher magnification image in (E) (scale bar: (D): 10 µm; (E): 5 µm). (F–H) SEM images of connective as tubular structures (stained in deep purple) containing endothelial and perivascular cells. The rectangle indicates the tissue micro-fragments. Arrows: collagen fibres; asterisks: adherent cells. SEM allows identifying also small adipocytes in Hy-Tissue SVF product (H) (Scale bar: (F, G): 10 µm; (H) 20 µm).

In Vitro Characterization of the SVF

The SVF products obtained by the mechanical disaggregation process of the Hy-Tissue SVF kit were analysed in terms of cell yield, product quality, viability, proliferation capacity, immunophenotyping, and differentiation potential.

The cell yield of free nucleated cells of the SVF product was $4.1 \times 10^4 \pm 2.0 \times 10^4$ cells/ml Fat (Figure 17. a). When the SVF pellet (containing free cells and adipose tissue micro-fragments) was submitted to enzymatic digestion, the product obtained (SVF-ED) increased 3.2 times the yield of free nucleated cells ($1.3 \times 10^5 \pm 4.7 \times$

10^4 cells/ml Fat: Figure 17. a). To evaluate the ability to form colonies of Hy-Tissue SVF product, colony-forming unit-fibroblast (CFU-F) assays were performed. CFU-F assay revealed that CFU-F yield of SVF was 178 ± 49 CFU-F/ml fat and after enzymatic digestion of the micro- fragments of the SVF increased over 2.4 times (424 ± 181 CFU/ml fat, Figure 17. c). The relative proportion of CFU-F in the SVF (0.3 ± 0.2%) did not increase significantly after the enzyme digestion of the micro-fragments (Figure 17.d), suggesting that the micro-fragments were composed not only of cells with adhesion potential but also of other non-adherent cell types. Free-cells yield and CFU-F of SVF were compared to fat tissue digested enzymatically (FAT-ED), used as a control. FAT-ED yielded 12-times more nucleated cells ($5 \times 10^5 \pm 2 \times 10^5$ cells/ml FAT) and 27-times more CFU-F (4877 ± 2477 CFU-F/ml Fat) compared to the SVF component based on the fraction of the free cells obtained by mechanical procedures. Additionally, the frequency of CFU-F of the fat tissue treated with enzymes (FAT-ED) was 5.6 times higher than the SVF product (FAT-ED: 1.7 ± 1.9%; SVF: 0.3 ± 0.2%; SVF-ED: 0.3% ± 0.1). Finally, to analyse the proliferation capacity of adherent cells in the SVF product, cells from SVF, SVF-ED, or FAT-ED (control) were seeded in T-flasks until confluence (Figure 17. e). SVF and SVF-ED cells did not show statistically significant differences to reach confluence (8 ± 2 days; 8 ± 1 day, respectively; $p > 0.05$). FAT-ED (control) required less time to reach confluence (5 ± 2 days), probably due to the higher frequency of adherent cell content. Proliferation capacity results were confirmed with a population doubling time assay (Figure 17. f). Histograms show that the doubling time of SVF and SVF-ED cells was comparable (59.35 ± 2.8 and 57.38 ± 3.9 h, respectively), while cells from FAT-ED required less time to duplicate their number (45.31 ± 3.95h).

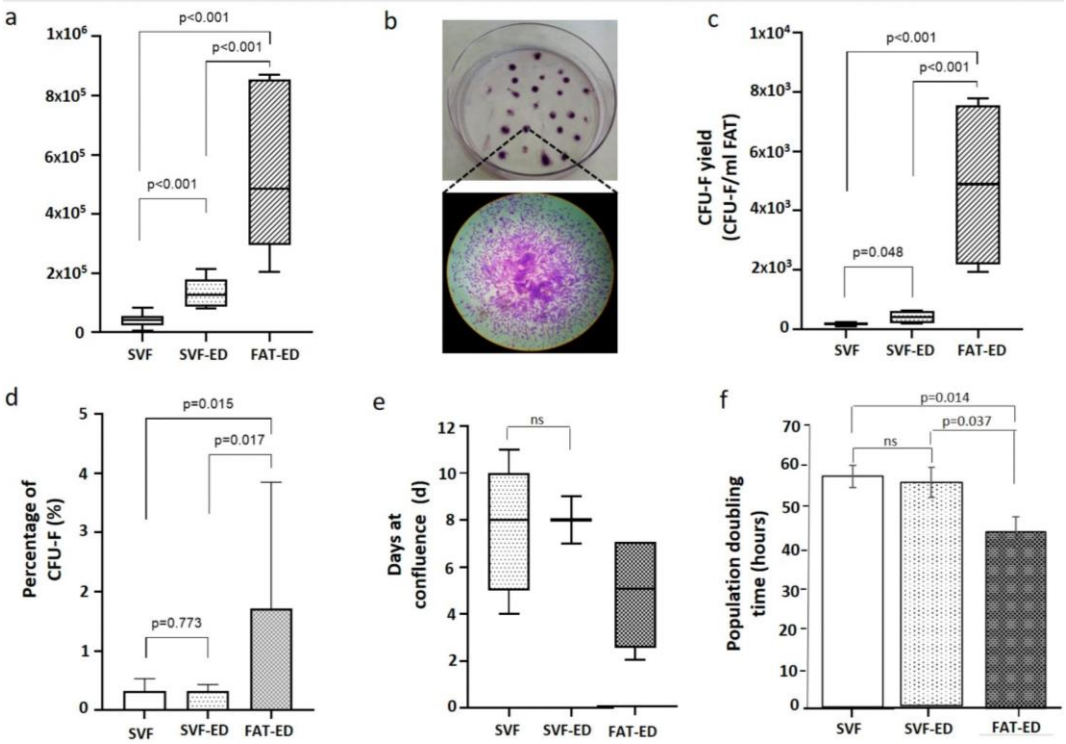

Figure 17. (a) Nucleated cells of the SVF obtained after treatment with Hy-Tissue SVF and the SVF after enzyme digestion Figure 3. (a) Nucleated cells of the SVF obtained after treatment with Hy-Tissue SVF and the SVF after enzyme digestion of the micro-fragments (SVF-ED). Fat tissue enzymatically digested (FAT-ED) was used as a control.; (b) representative T-flask flask of the CFU-F assay and an amplified image of a CFU-F observed with a light microscope after Toluidine Blue staining (4× magnification). (c) CFU-F yields of the SVF were obtained after treatment with Hy-Tissue SVF and the SVF after enzyme digestion of the micro-fragments (SVF-ED). Fat tissue enzymatically digested (FAT-ED) was used as control; (d) percentage of CFU-F contained in SVF, SVF-ED and FAT-ED. The results are shown as the mean and error bars represents standard deviation; (e) proliferation capacity of cells contained in SVF, SVF-ED and FAT-ED in t-25 flasks. Box and whisker plots represent the median, the lower and upper quartile, and the minimum and maximum; (f) Population doubling time of SVF, SVF-ED and FAT-ED. The results are shown in the mean, and the error bars represent the standard deviation.

Immunophenotypic Analysis

To determine the stromal vascular fraction composition obtained with Hy-Tissue SVF, we used flow cytometry to evaluate the proportions of $CD34^+$ (endothelial cells, pericytes, and potential ADSC) in the free cell fraction. Cells from a scatter plot (FSC/SSC) were analysed for viability, and dead cells were excluded. The proportion of $CD34^+$ cells in the SVF fraction was 9.9 ± 1.5% (Figure18.a) compared to the cells obtained after enzyme digestion of the fat (3.7 ± 1.3%). Moreover, the frequency of CD73 and C105 positive cells (mesenchymal stem cells marker) were analysed (Figure 18. a). The percentage of expression was 7.61 ±

2.59% and 6.28 ± 2.40% for CD73 and CD105, respectively (Figure 18. a), not thus far from the percentage of expression obtained for the same antibody with ED (control). Flow cytometry was performed to characterise the cellular composition of SVF obtained with Hy-Tissue SVF kit, labelling SVF cells with CD146, CD 116, CD68 and CD45. Figure 18. b (left) reported the percentage of maker expression. The proportion of CD146, CD116, CD68, and CD45 cells in SVF fraction was 2.6 ± 0.2%, 0.7 ± 0.1%, 3.5 ± 1.5%, and 5.5 ± 1.34%, respectively. Among the WBC fraction, four main cell subpopulations were determined, and the percentage of expression for neutrophils, lymphocytes, monocytes, eosinophils, and basophils was reported in Figure 18. b (right).

Figure 18. c shows the immunophenotypic analysis of surface marker expression profiles of MSC obtained after the cellular expansion of the adherent cells obtained from SVF or enzymatic digestion of the FAT (FAT-ED) were similar. Most cells have expression low for CD45 and CD34 and positive for MSC-associated markers such as CD105, CD90, CD73, CD29, and CD44 (Figure 18c).

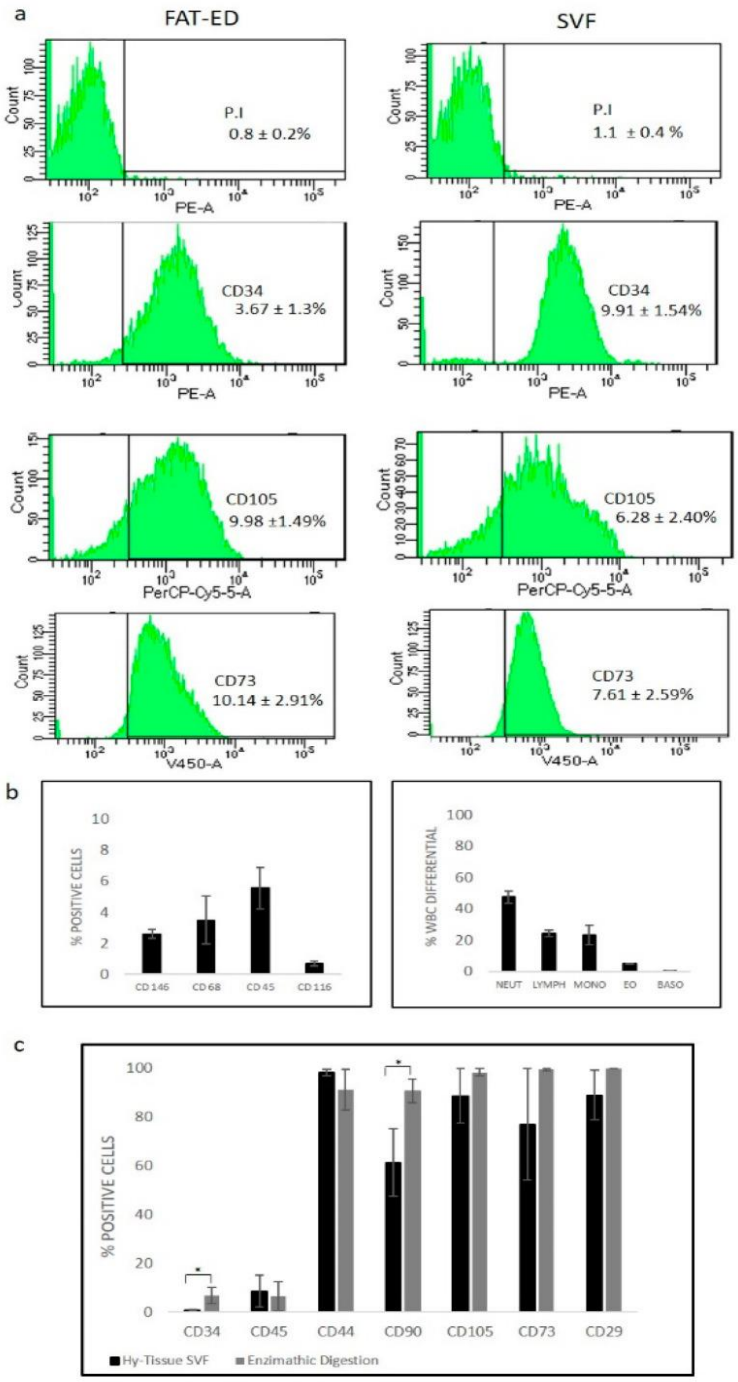

Figure 18. Expression of surface markers detected by flow cytometric analysis of free cells from SVF or FAT-ED (a). The percentage of positive cells for each marker was calculated after subtracting the non-specific fluorescence obtained with the control (unmarked). Data show a representative set of dot-plot from one individual in each isolation protocol. (b) Percentage of positive cells to CD markers to characterise cell subpopulations in SVF (left), White Blood Cells differential (WBC diff) to characterise the Neutrophils (NEUT), Lymphocytes (LYMPH), Monocytes (MONO), Eosinophils (EO) and basophils (BASO) subpopulation in SVF (percentage of positive cells). (c) Percentage of positive cells to CD markers (as an average of the samples) after in vitro cell expansion for SVF or FAT-ED (control). Results are presented as the mean and error bars one standard deviation; significant statistical differences are indicated with "*", p-value < 0.05

Analysis of Multipotency of SVF Product

The multilineage differentiation potential of the SVF obtained with Hy-Tissue SVF was evaluated by testing the ability of adherent cells obtained in the SVF to differentiate toward adipocytes, chondrocytes, and osteocytes using the expanded cells from FAT-ED as a control. Peripheral blood contaminants and other non-adherent stromal cells of the SVF were removed by replating until passage 4, and only adherent cells with fibroblastic morphology remained in the flask. The results of the multipotency of the SVF product are shown in Figure 19. Adherent cells obtained with Hy-Tissue SVF can differentiate into the three mesodermal lineages as enzymatically extracted (FAT-ED) cells. Oil Red O, Alizarin Red, and Alcian Blue staining were positive compared to the control for adipogenic, osteogenic, and chondrogenic differentiation.

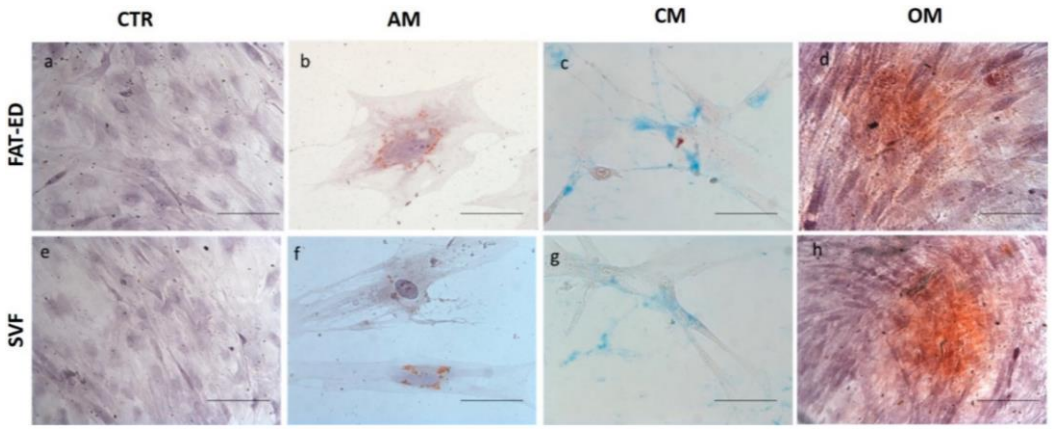

Figure 19. Multilineage differentiation of passage 4 of SVF or FAT-ED adipose-derived stromal cells isolated by each method. AM: Adipogenic medium; CM: Chondrogenic medium; OM: Osteogenic medium. (a–h): Optical microscopy images of cells induced or not (control; a, e) with differentiation medium (scale bar 100 μm); (b, f) adipogenesis was indicated by the accumulation of neutral lipid vacuoles that stained with Oil Red O; (c, g) chondrogenesis was indicated by the deposition of the sulfated proteoglycan-rich matrix that stained with Alcian Blue; (d, e) osteogenesis was indicated by Alizarin red S staining of extracellular matrix calcification.

The technique evaluated was simple and provided SVF in free cells and micro-fragments within a short time (15–20 min), without expansion and enzymatic treatment.

The technique reduced the size of the cluster inside the adipose tissue (previously fragmented by the lipoaspiration procedure) by gently forcing the tissue to pass through a sieve of 120 μm (filtered microfat) and a subsequent centrifugation step that allowed to break most of the mature adipocytes for finally obtaining a pellet with free cells (blood and stroma origin) and micro-fragments of adipose tissue

without mature adipocytes, which were broken by the mechanical disaggregation and the centrifugal forces.

Application of the HY-Tissue SVF® product with HA

xiv) Introduction

In plastic surgery, soft tissue reconstruction is a challenge when replacing lost materials and correcting contour defects. Many permanent and temporary fillers have been used to restore the volume of these lesions, but often with poor results and even complications. ASCs and adipose tissue engineering have been suggested as valuable alternatives. It was essential to find a suitable vehicle to inject these cultured cells. This study aimed to evaluate the induction of adipogenesis via SVF in contact with HA, an injectable biomaterial. HA, an extracellular matrix glycosaminoglycan, may play a role in mesenchymal stem cell differentiation to fat but results using murine models and cell lines are conflicting. Adipogenesis was evaluated using Oil Red O (ORO), counting adipogenic foci, and a terminal differentiation marker. MTT was performed to test the toxicity of the HA. For *in vivo* experiment, MRI was done of the mice injected with HA and SVF to check for adipogenesis. HA1 is ACP, and the other two HA were termed HA2 and HA3 (Fidia pharmaceuticals, Italy)

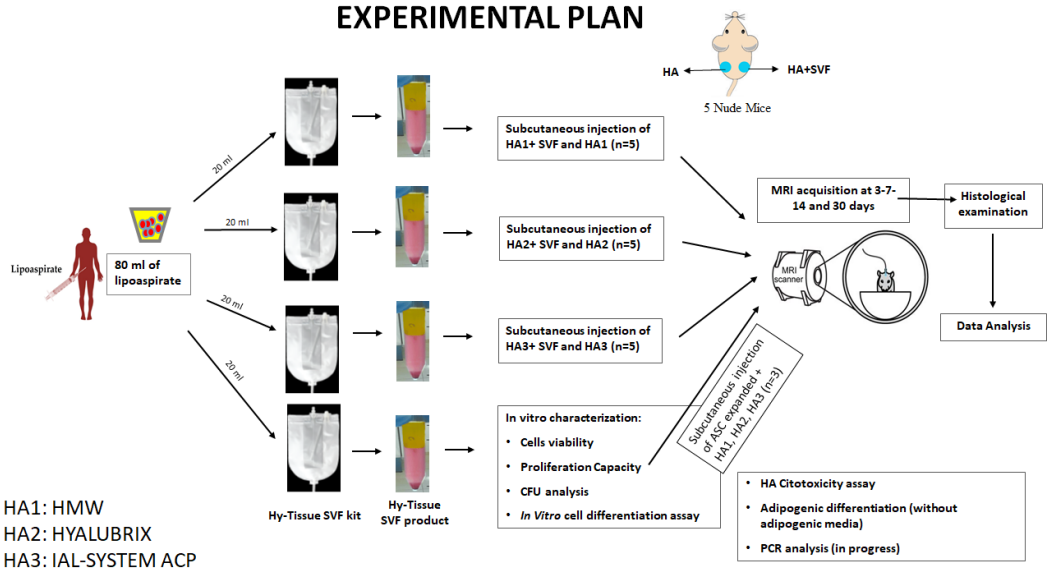

Figure 20. The lipoaspirate was divided into parts and the product SVF was injected with three different HA provided by Fidia Pharmaceuticals, Italy.

xv) Materials and Method

Collection of adipose tissue

The adipose tissue was collected from 10 patients undergoing liposuction.

Sample processing

The patients' adipose samples (around 80 ml) were divided into four groups. The first three collected SVF were mixed with three different HA (ACP named as HA1, and the other two HA2, HA3).

In vitro experiments

Cell seeding

The extracted SVF was diluted in 1 ml of complete culture media (Sigma-Aldrich, Italy) containing 10% FBS, 1% of a mixture of penicillin/streptomycin 1:1 (GIBCO Life Technology, Italy), and 0.5% of amphotericin B (GIBCO Life Technology, Italy). The mixture was then filtered through a 0.45 mm cell strainer followed by plating into a T25 flask with the other 4 ml of complete media. After three days, the media was changed every two days until confluency.

Cell proliferation capacity test

To determine the cell proliferation capacity of the cells inside the SVF, the media was changed every three days and then every two days until confluency, which was incubated at 37 °C 5% CO2. The cells were grown until passage four, and every time detaching, the number of cells and viability was counted using trypan blue.

CFU assay

Around 5000 cells from SVF were seeded in a 6-well plate in triplicate. Cells were cultured in complete culture media for 14 days. For colony counting, wells were stained with Toluidine Blue (Sigma). The only cluster of at least 50 fibroblasts-like cells was counted.

Cell cytotoxicity test (MTT assay)

To test the metabolic activity of cells and the toxicity of the Hyaluronic Acids, an MTT assay was performed at two different time points, i.e., 24h and 72h. Five thousand and two thousand five hundred cells (for 24h and 72h, respectively) were mixed with 100 µl of complete media and plated in the wells of 96-multiwell (6 micro-wells for each HAs). After 24h, the media was removed, and 100 µl of three different concentrations of HAs were plated (i.e., 25%, 15%, 7%) in contact with cells and without cells. Next, 100 µl of MTT solution (0.5 gm/ml, i.e., 10% of MTT solution in 90% of complete media) was added to each well and incubated in the dark at 37 °C for 4h. After the incubation, the MTT solution was removed, and 100 µl of DMSO (solubilising solution) was added to each well and incubated on a rotating mixer slowly for 20 min. Then the absorbance was measured with a spectrophotometer at 570 and 630 nm. The same procedure was performed for the 72h incubated plate as well.

Optical microscopy of SVF

The SVF pellets (N=10) obtained after Hy-Tissue SVF treatment were analysed by the whole-mount method (Larsen PL 1989) and paraffin inclusion. Briefly, pellets were washed with saline, stained with hematoxylin and eosin, and placed in the slide without dissection with the whole mount method. Other pellets (N=4) were washed with 0.1 M PBS and fixed with 10% formalin for 4h. Subsequently, the samples were dehydrated with a gradient of increasing alcohol concentration from 70% to 100% and then xylene for final processing. Finally, the pellets were included in paraffin and cut with the microtome into 5 µm sections. The sections are then dried at 37 °C for 24h and stained with hematoxylin and eosin. All slides were examined under an Olympus BX51 microscope (Olympus, Tokyo, Japan) equipped with a digital camera (DKY-F58 CCD JVC, Yokohama, Japan). The digital images were analysed and processed with Image-ProPlus 7.0 software (Media Cybernetics, Silver Spring, MD, USA).

In Vitro Cell differentiation assay

The differentiation potential of the SVF into three different cell lines (adipocytes, osteocytes & chondrocytes) were evaluated in *vitro* and was compared to control. Differentiation was done using expanded cultured cells from passage 4. For adipogenic differentiation, 7000 cells were seeded on a 6-well plate incubated. After 24h, the media was changed to adipogenic media (Sigma SCM122-1KT) and set for 16 days while the media was changed every 72. Then, cells were fixed with 4% paraformaldehyde (PFA) for 30 min, washed, and stained with a solution of oil red O (Bioptica) for 20 min and hematoxylin (Bioptica) for 2 min. For chondrogenic differentiation, $1x10^6$ cells were seeded in a 24-well plate, and after two h, the media was changed to chondrogenic medium (StemPro chondrogenic

differentiation Kit (GIBCO Life Technology, Italy). After 14 days of incubation, cells were fixed with 4% PFA for 30 min and stained with Alcian Blue 8GX (Sigma-Aldrich) to detect the mucopolysaccharide extracellular matrix. For osteogenic differentiation, 5000 cells were seeded on 12 well plates, and after two h, the medium was changed to osteogenic medium (StemPro osteogenesis differentiation Kit - GIBCO Life Technology, Italy). After 21 days, cells were fixed with 4% PFA for 30 min and incubated in 0.2% Alizarin Red S (Sigma-Aldrich) for 5 min and hematoxylin (Bioptica) for 2 min. Images were obtained using optical microscopy.

In Vivo experiment

Injection of Hyaluronic acid

Only HA (300 µl) was injected subcutaneously on the left side of the mouse, and 250 µl of HA plus 40 µl saline solution mixed with the SVF was injected on the right side. Fifteen nude mice were taken for this injection, five each for three different HA. At several time points for one month, MRI was performed to observe the behavioural growth of adipose tissue. Proliferated cells from SVF obtained after Hy-Tissue manipulation were expanded, termed 'ASCs.'

Magnetic resonance imaging (MRI) acquisition

MRI was performed at different time points (1, 7, 15, and 30 days after subcutaneous implants and injection) to evaluate any possible growth of newly formed tissue. MRI images were acquired using a 7Tesla using the following parameters: TE = 7 ms, TR= 2800 ms, a field of view = 22 x 8 mm, number of averages = 16, flip angle 180 degrees, slice thickness 0.350 mm, and matrix size 256 x 128 pixels. During the procedure, mice were anaesthetised by inhaling isoflurane at 2% and placed in a prone position in the heated bed positioned in the birdcage coil. The acquisition parameters were maintained during observation for all the animals. Moreover, the volume of each subcutaneous implant was determined on MRI slices to quantify the reabsorption degree at different time points. On each piece, the area occupied by the subcutaneous implant of the 3D scaffold and injection of HA was manually tracked and measured by fat suppression technique, and 1H Magnetic Resonance Spectroscopy was performed.

Ex Vivo analysis

Histological analysis

At the end of *in vivo* experiment, after 30 days, all the mice were sacrificed, and the skin was cut near the injection area (for HA injection). The tissue was immediately transferred to buffered formalin 4% for 4 hours, dehydrated in a gradient of ethanol (from 70% to 100%), and two passages of xylene (100%) followed by paraffin embedding cut with the microtome to 5 µm sections. The sections were then dried at 37 °C for 24 hours and stained with Hematoxylin and Eosin. Alcian Blue staining was also performed in the sample in another slide to confirm the new collagen formation. All slides were examined under an Olympus BX51 microscope (Olympus, Tokyo, Japan) equipped with a digital camera (DKY-F58 CCD JVC, Yokohama, Japan). The slices were stained with Hematoxylin and Eosin staining for histological evaluation and were studied with Image-ProPlus 7.0 software (Media Cybernetics, Silver Spring, MD, USA).

xvi) Results

CFU, *in vitro* Differentiation assay & cells yield:

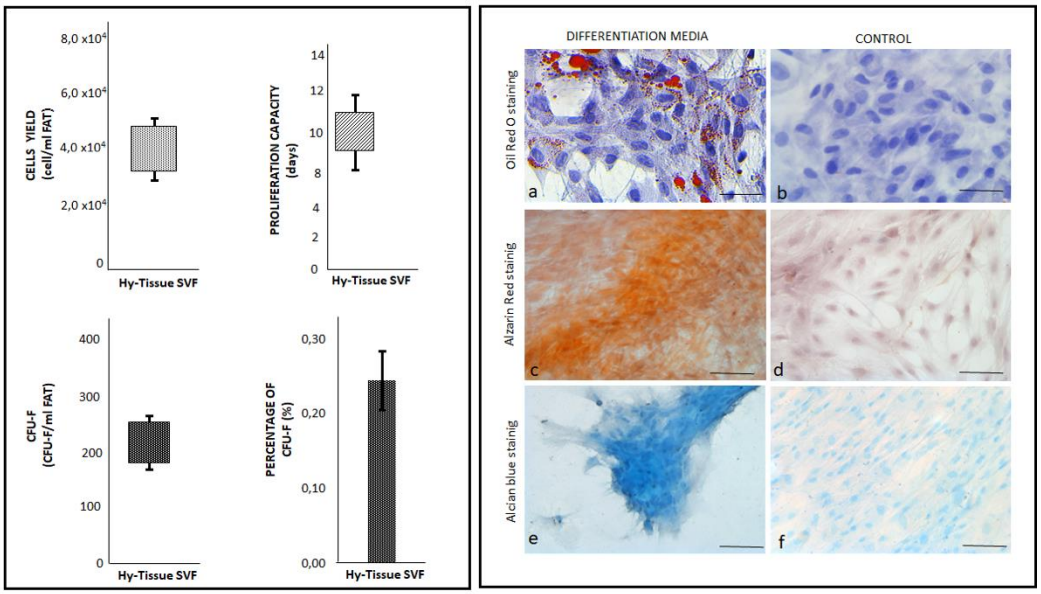

Figure 21. The Figure on the left side shows that cell yield, CFU-F rate, and proliferation capacity are comparable to previously obtained results. Figure a-f (right side) shows the cells stained with ORO, Alcian Blue, Alizarin Red and after putting them into three differential media.

The obtained ASCs were then incubated with HA1, HA2, and HA3 to test a possible cytotoxic effect of hyaluronic acids. The MTT test was performed at three different

concentrations of hyaluronic acids (7, 15 and 25% of HA concerning the culture medium) after 72h of incubation. The results obtained are shown in the graphs in figure 23. None of the concentrations tested altered the cell viability of the ASCs after 72h. Subsequently, the ASC cells were cultured with the three different HAs (25% of HA to the culture medium) for ten days to evaluate a possible adipogenic stimulation induced by HA 1, HA2, HA3. The images in figure 21 show how after ten days, the three HAs can induce adipogenic differentiation *in vitro*

Viability	25%	15%	7%
ASC	100,00	100,00	100,00
HA1	100,89	98,02	98,42
HA2	96,21	103,59	99,67
HA3	94,07	96,25	96,85

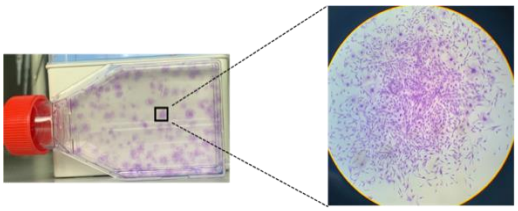

Figure 22. The table shows the viability of ASCs cells with and without contact with the HAs. The right picture proves that these cells can form CFU cultured in T25 flasks. The rightmost image is a magnified form of one of those colonies.

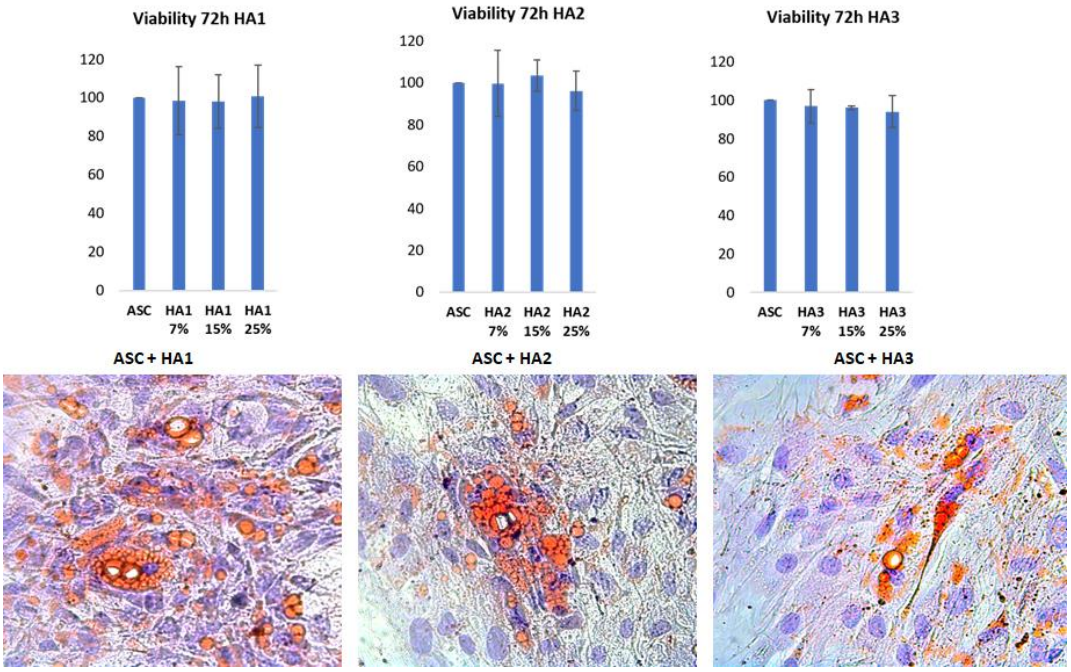

Figure 23. MTT assay to evaluate the cell viability of ASCs incubated with three different concentrations of HA1, HA2, HA3 for 72h (top); ASC cells after ten days of incubation with HA1, HA2, HA3 show lipid droplets, adipogenic differentiation characteristics (staining: Oil Red O, Magnification 10x).

The images revealed that SVF-HA1 induces adipogenesis *in vivo* about 14 days after injection and is maintained for up to 30 days (Figure 23). MRI analyses also showed that HA1 is reabsorbed seven days after the subcutaneous injection.
The results obtained *in vivo* were confirmed by subsequent histological analyses (Figure 23). The tissue extracted at the injection of only HA1 shows an unaltered morphology. In contrast, in the tissue extracted at the injection of SVF-HA1, the formation can be observed of newly formed adipose tissue underlying the furrier's muscle. Furthermore, the presence of micro-vessels is noted in the newly formed tissue. Micro-vessels.

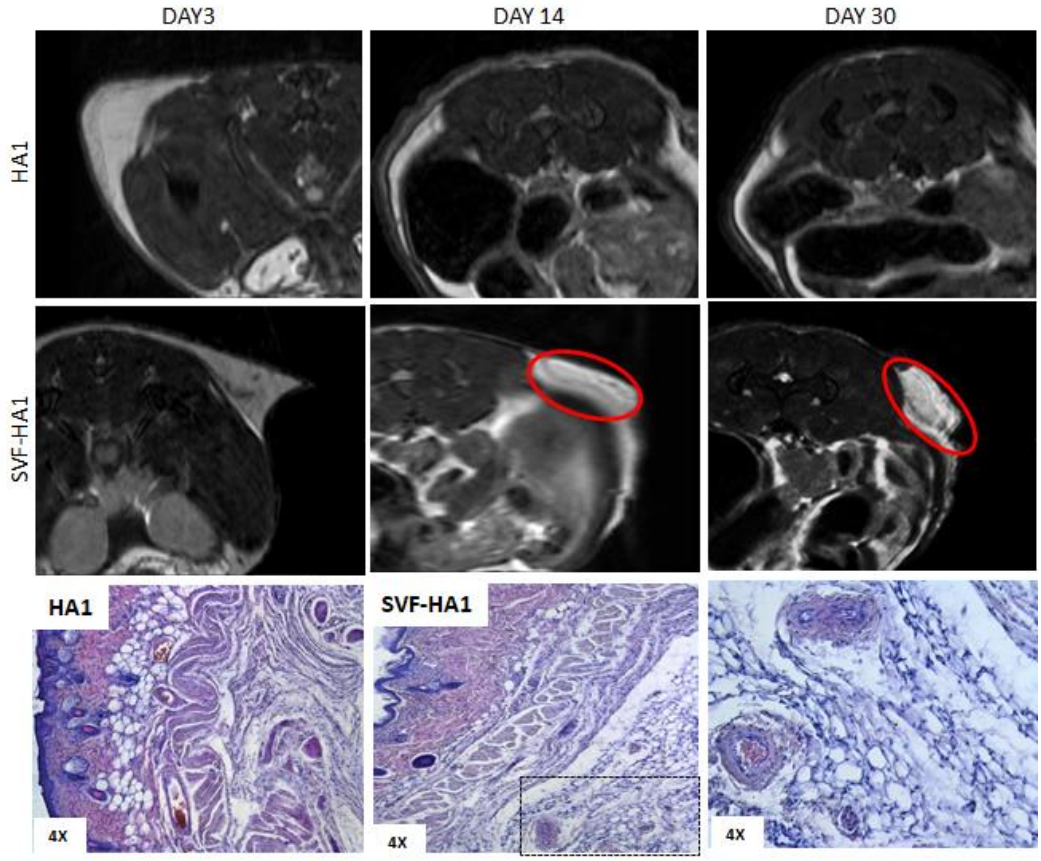

Figure 23. Magnetic resonance images at 3, 14, 30 days after the injection of HA and SVF-HA. Fourteen days after the SVF-HA injection, the newly formed adipose tissue is circled (red) in the image. The histological images of the area where the injection took place (after 30 days) confirm the results obtained (staining with hematoxylin and eosin) (magnification 4x and 20x).

The analysis of images obtained with magnetic resonance (Figure 24) revealed that SVF-HA2 shows an adipogenic power after 14 and 30 days after injection, while HA2 is reabsorbed within seven days. The subsequent histological and ultrastructural analysis confirmed this observation. The formation of newly formed adipose tissue interposed by collagen matrix and micro-vessels can be observed in

the underlying part of the furrier's muscle. The newly formed tissue appears more like fibrogenic tissue with accumulations of lipid drops inside. Histological analyses of tissue injected with HA2 alone show an unaltered morphology.

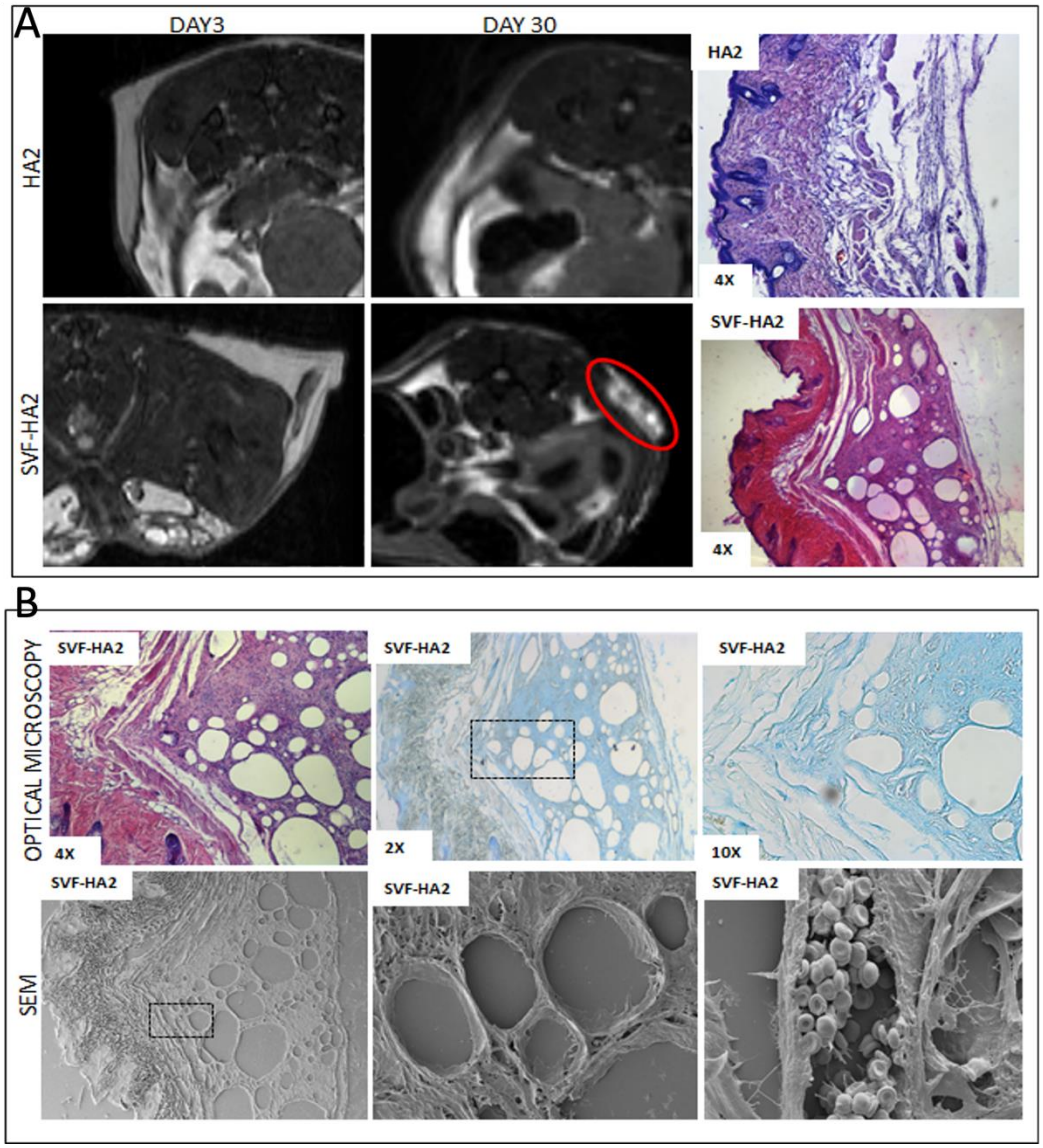

Figure 24. A. MRI images of mic injected with HA2 only and with SVF. The histological images show adipogenesis (bottom right) and no adipogenesis induction with only HA2 (top right) Magnetic resonance images at 3 and 30 days after the injection of HA2 and SVF-HA2 The newly formed adipose tissue 14-30 days after the injection of SVF-HA is circled (red) in the image. The histological and ultrastructural images of the area where the injection took place (after 30 days) confirm the results obtained, stained with hematoxylin (B, top left) and eosin and Alcian blue (B, top middle and tight), Magnification 4x and 20x

Analysis of images obtained with magnetic resonance revealed that SVF-HA3 mediates adipogenic stimulation seven days after injection (Figure 25). The MR analyses also showed that HA3 tends to be reabsorbed seven days after the subcutaneous injection. The subsequent histological analysis confirms the *in vivo* results (Figure 25). In the tissue extracted from the right side of the animals, the formation of newly formed adipose tissue organised in lobules and the presence of micro-vessels can be noted. In contrast, the tissue in which only HA3 was injected (left side) shows an unaltered morphology.

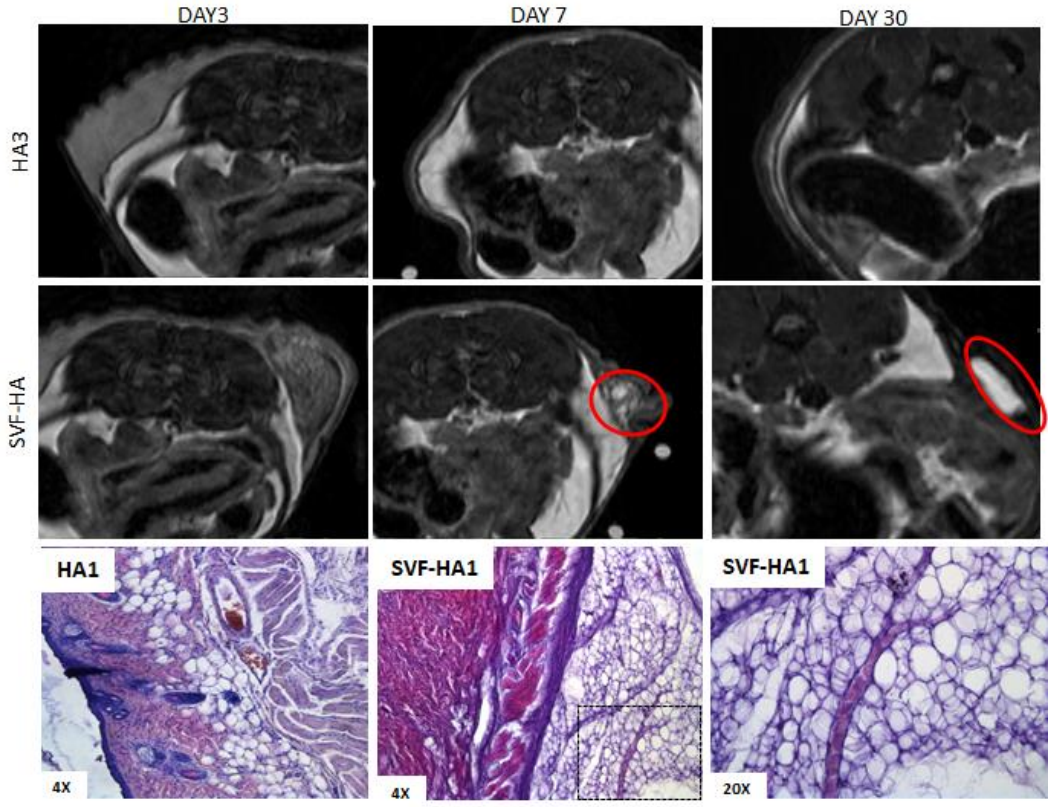

Figure 25. Magnetic resonance images at 3, 7, and 30 days after the injection of HA3 and SVF-HA3. The red circles in the resonance images highlight the newly formed adipose tissue 7 and 30 days after the injection of HA3. Histological images of the area where the injection took place (after 30 days) stained with hematoxylin and eosin with magnification on the formation of new adipogenic tissue (magnification 4x and 20x).

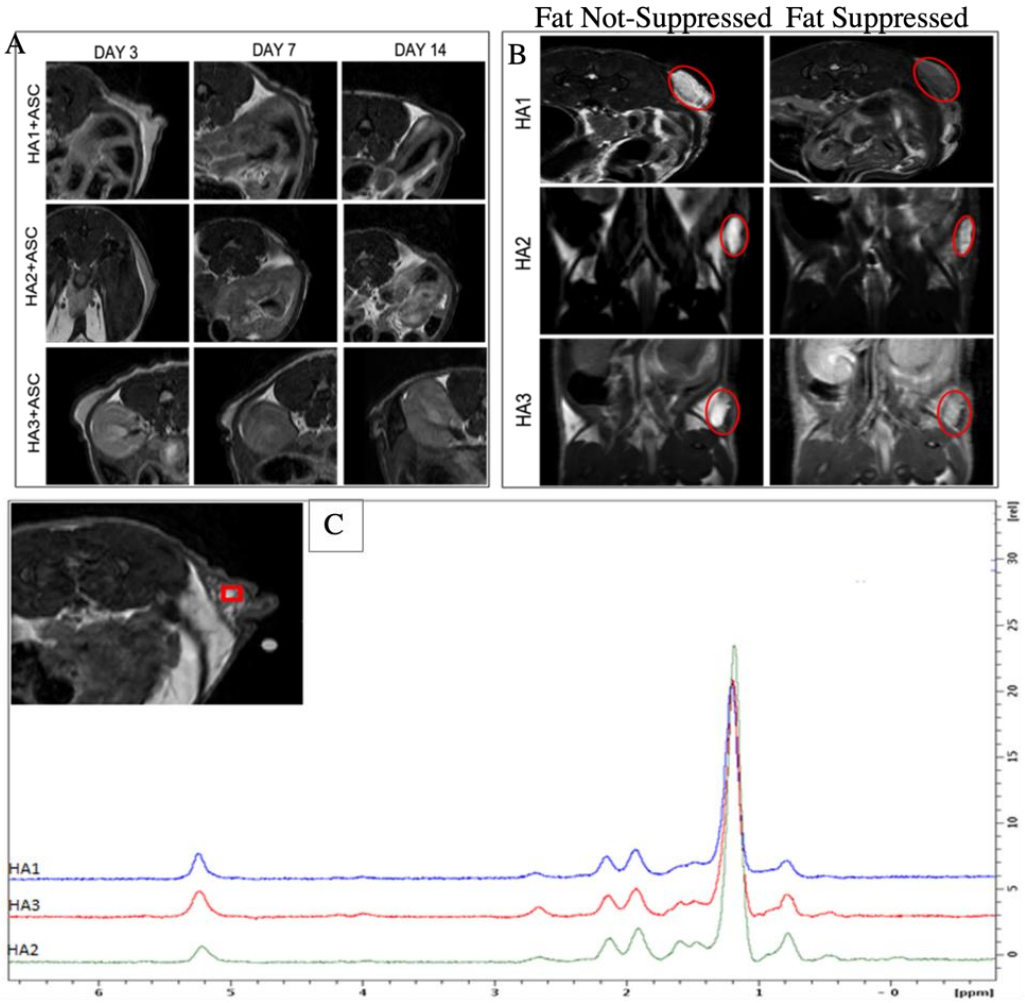

Figure 26. The top left figure (a) shows the images of MRI at days 3, 7, and 14 of the mice injected with ASC and the hyaluronic acids, whereas the top right picture (b, fat-suppressed, and fat not suppressed) shows the mice injected with only three different HAs. The last figure (c) is the MRI image is T2 weighted FAT-SUPPRESSED sequence and 1H-MRS Image.

No evident formation of adipose tissue was found *in vivo* after 14 days of injection (Figure 26). The MRI images show how at seven days after injection, ASC-HA is still visible (red circle), while it is wholly reabsorbed on day 14. The histological pictures confirm the result obtained *in vivo*, showing an unaltered tissue morphology.

Hy-Tissue Nanofat® (Fidia pharmaceuticals, Italy)

xvii) Overview

Fat graft is widely used in plastic and reconstructive surgery. However, the size of the injectable product, the unpredictable fat resorption rates and subsequent adverse effects make it tricky to inject untreated fat into the dermal layer. Mechanical emulsification of fat tissue, which Tonnard introduced, solves these problems, and the product obtained was called "nanofat". Nanofat is widely used in clinical, such as to treat facial compartments, hypertrophic and atrophic scars, wrinkle attenuation, skin rejuvenation and alopecia. Several studies demonstrate that the tissue regeneration effects of nanofat are attributable to its rich content of adipose-derived stem cells. This study aimed to characterise Hy-Tissue Nanofat product at the macrostructural and cellular level, investigating the morphology, cellular yield and viability, ASC proliferation rate and clonogenic capability, and immunophenotyping and differential potential. The percentage of SEEA3-CD105 expression was also analysed to establish the presence of multi-lineage differentiating Stress Enduring cell (MUSE). NANOFAT-derived Adipose Stem Cells were compared to ASC obtained with enzymatic digestion. Our results showed that the Hy-Tissue Nanofat system could isolate $3.75\times10^4 \pm 1.55\times10^4$ proliferative nucleated cells for each ml of the treated fat. NANOFAT-derived ASC can grow in colonies and show high differentiation capacity into adipocyte, osteocyte, and chondrocytes. Finally, immunophenotyping analysis revealed the expression of typical mesenchymal stem cells marker, including SEEA3-CD105 specific for MUSE cells, making this product of potential interest in regenerative medicine.

The autologous fat graft is primarily used in aesthetic medicine for face rejuvenation and volume restoration, thanks to its simple harvesting through liposuction and its autogenous and biocompatible nature [171]. Nevertheless, fat graft presents some limitations, such as the size of the injectable product, the unpredictable fat resorption rates [172] and subsequent adverse events [173]. Moreover, injecting the fat graft into the dermal layer to treat superficial rhytides, wrinkles, and atrophic scars is still challenging [174]. Therefore, surgeons and researchers tested different protocols to manipulate fat to inject it rapidly and without inflammatory reactions during the last years. One of these protocols were generally named nanofat [175].

Nanofat is defined as an autologous liquid obtained through the mechanical manipulation of lipoaspirates. During this process, the harvested fat is filtered and shuffled between two 10-cc syringes with a 30 passes connector, which destroys

nearly all adipocytes, resulting in a purified emulsion product [175]. The final product can be directly injected into the target site with high precision, even in difficult areas, working superficially with still more delicate, sharp needles (27 gauge) [176, 177]. Nanofat is widely used in the clinical field to treat facial compartments, hypertrophic and atrophic scars, wrinkle attenuation, skin rejuvenation, and alopecia [178-181]. Moreover, it has been under investigation for broader applications, such as wound healing and vascularisation [171].
Previous clinical studies of nanofat injection evaluated the long-term survival in transplant areas in volume maintenance [182]. Recently, several studies demonstrated that the tissue regeneration effect of Nanofat is attributable to its rich content of adipose-derived stem cells (ASC) and different growth factors [171, 182, 183].

ASCs are adult plastic-adherent mesenchymal stem cells easily isolable from adipose tissue allowing autologous cells transplantation [184, 185]. According to the literature, ASC module the inadequate healing responses lead to tissue degeneration, such as chronic inflammation [186], hypermetabolic answers [187] and fibrosis [188]. Moreover, ASC stimulates extracellular matrix production, new collagen deposition and early revascularisation [189, 200]. Their biological effect is due to the self-renewal property, immunosuppressive potential, and ability to differentiate into different mesodermal cell lineages, such as adipocytes, osteocytes and chondrocytes [201-203]. For these reasons, in vitro characterisation of nanofat in terms of ASC content could reflect the regenerative potential of the product, indicating how many cells are capable of duplicating and differentiating to guarantee a replicable result on patients.

Recent studies have been focused on a subpopulation of mesenchymal stem cells defined as multi-lineage differentiating stress enduring cells (MUSE). MUSE are non-tumorigenic stress-tolerant and pluripotent cells, with high regenerative potential [204-207] and migration capacity into the damaged tissue [208]. MUSE cells can regenerate skin, muscle, liver, and kidney tissues [207], exhibiting high integration capacity able to restore the function of the tissues, as evidenced in preclinical studies [207]. MUSE cells result in a promising candidate for tissue regeneration and stem cell therapy, thanks to their unique features.

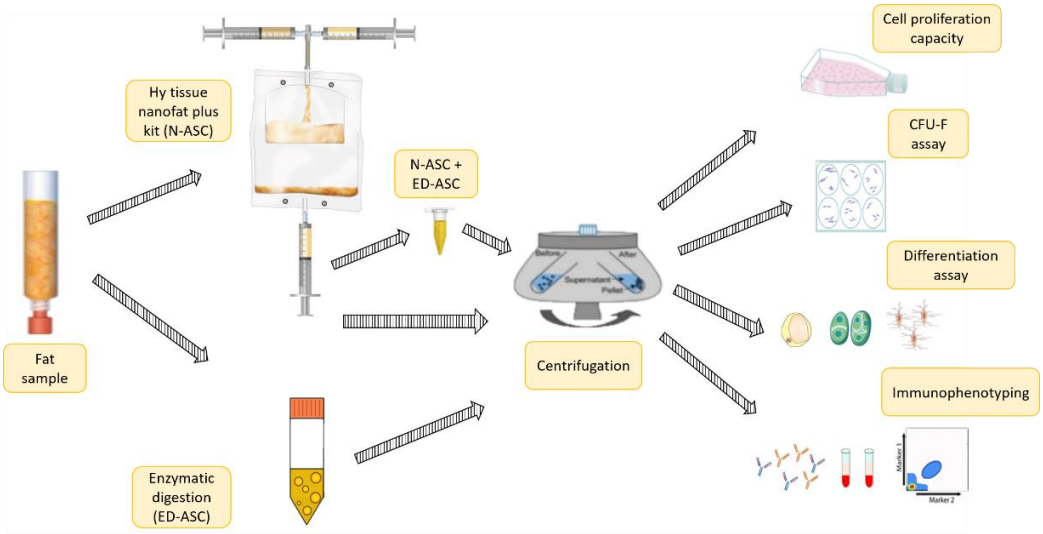

Figure 27. Experimental methodology. The fat sample was divided into three portions to be processed in N-ASC, N-ED-ASC and ED-ASC and evaluated for cell proliferation capacity, CFU-F assay, immunophenotyping and differentiation potential.

xviii) Method of Experiment

The adipose tissue was collected from 10 women undergoing liposuction for aesthetic purposes, aged between 41 and 69 years. Informed consent was taken before collecting adipose tissue following the ethical guidelines established by the review committee for human studies of AOU "Ospedali Riuniti", Ancona, Italy (Micro-adipose graft_01, 18 May 2017). In brief, Klein tumescence solution (2% Lidocaine solution: 0.08% w/v; Adrenaline 1mg/ml solution: 0.1% v/v in 0.9% saline) was injected 10 min after the liposuction. A cannula of 11 G, six holes, and 20 ml Vac-Lock syringe provided with the kit was employed to lipoaspirate between 30 ml of fat from each donor's abdominal area. The fat was transported in an adiabatic container to the laboratory and processed within 18h from harvest.

Procedure for NANOFAT-derived ASC production

Each adipose tissue sample (about 30 ml) was divided into three portions. The first portion (about 10 ml) was processed with the Hy-Tissue Nanofat system (Fidia Farmaceutici, Abano Terme, Italy). The lipoaspirate was shuffled and emulsified through two 10 cc coupled syringes via a 30 passes connector. Next, the emulsified lipoaspirate was filtered into the inner bag with a pore size of 120 µm and was collected into a lower syringe. To characterise the product at a cellular level, it was centrifuged at 3000 rpm for 6 min and filtered through a 70 µm nylon mesh. The product obtained by this method was named "NANOFAT-derived ASC (N-ASC)".

Enzymatic Digestion of Fat

The second portion of lipoaspirate (about 10 ml) was processed using an enzymatic method, as reported by Busato et al., 2020 [193]. The samples were digested with collagenase type I at the concertation of 1 mg/ml (GIBCO Life Technology, Monza, Italy) dissolved in Hank's Balanced Salt Solution (HBSS, GIBCO Life Technology, Monza, Italy) with 2% of Bovine Serum Albumin (BSA, GIBCO Life Technology, Monza, Italy) for 45 min at 37°C. Complete culture medium (Dulbecco's Modified Eagle's Medium (DMEM), Sigma-Aldrich, Italy), supplemented with 10% of Fetal Bovine Serum (FBS, GIBCO Life Technologies, USA), 1% of 1:1 penicillin/streptomycin (P/S solution, GIBCO Life Technologies, USA) and 0.6% of Amphotericin B (GIBCO Life Technologies, USA), was added to neutralise the enzyme action. After the neutralisation process, the sample was centrifuged at 3000 rpm for 5 min. The cell pellet was incubated with 1 ml of erythrocyte lysis buffer 1X (Macs Miltenyi Biotec, Milan, Italy) for 10 min at room temperature. The cell suspension was again centrifuged and resuspended with 1 ml of complete culture medium. Finally, the cells were filtered through a 70 µm nylon mesh. The product obtained by this method was named "ED-ASC".

Enzymatic Digestion of Hy-Tissue Nanofat product

The remaining portion of lipoaspirate (10 ml) was first processed with the Hy-Tissue Nanofat kit, followed by the treatment with collagenase type I. The product was incubated with collagenase type I at the concertation of 1 mg/ml (GIBCO Life Technology, Monza, Italy) dissolved in Hank's Balanced Salt Solution (HBSS, GIBCO Life Technology, Monza, Italy) with 2% of Bovine Serum Albumin (BSA, GIBCO Life Technology, Monza, Italy) for 45 min at 37 ◦C. Complete culture medium (Dulbecco's Modified Eagle's Medium (DMEM), Sigma-Aldrich, Italy), supplemented with 10% of Fetal Bovine Serum (FBS, GIBCO Life Technologies, USA), 1% of 1:1 penicillin/streptomycin (p/s solution, GIBCO Life Technologies, USA) and 0.6% of Amphotericin B (GIBCO Life Technologies, USA, was added to neutralise the enzyme action. After the neutralisation process, the sample was centrifuged at 3000 rpm for 5 min. Next, the cell pellet was incubated with 1 ml of erythrocyte lysis buffer 1X (Macs Miltenyi Biotec, Milan, Italy) for 10 min at room temperature. The cell suspension was again centrifuged and resuspended with 1 ml of complete culture medium. Finally, the cells were filtered through a 70 µm nylon mesh. The product obtained by this method was named "N-ED-ASC".

Optical microscopy

To evaluate the morphology of the Hy-Tissue Nanofat product whole-mount assay was performed, as reported in Busato et al. 2020 [193]. The emulsion was swiped in a

histological glass and stained with Toluidine Blue (Sigma-Aldrich, Milan, Italy). All slides were examined under an Olympus BX-51 microscope (Olympus, Tokyo, Japan) equipped with a digital camera (DKY-F58 CCD JVC, Yokohama, Japan).

Cellular Yield

Collected cells were counted using Trypan Blue exclusion assay using a CytoSMART counter (Automated Image-Based Cell Counter, version 1.5.0.16380, CytoSMART Technologies B.V., Eindhoven, Netherlands). Cell yield was calculated considering the total amount of free cells of N-ASC, ED-ASC, and N-ED-ASC divided by the fat volume.

Proliferation capacity

To evaluate the cell proliferation capacity of the cells collected with N-ASC, ED-ASC, and N-ED-ASC, 2×10^5 cells of each product were plated on a 25 cm^2 T-flask and incubated in a humidified atmosphere with 5% CO_2 at 37 °C. 72 h after the cell extraction, the complete culture medium was changed and, subsequently, every 48 h until 80% confluence. The days required at the cultured cells to reach confluence (cellular passage 1) were used for determining the proliferation capacity. Furthermore, the population doubling time (PDT) assay was performed to estimate the time request for cell replication. Four days after the seeding, five $\times 10^4$ cells from N-ASC, ED-ASC, and N-ED-ASC were plated in T-25 Flasks (in triplicates) with 4 ml of complete culture media. They were incubated in a humidified atmosphere with 5% CO_2 at 37 °C for different time points, 24, 72, and 96 h. At each time point, after a brief wash with PBS, the cells were incubated with 0.25% trypsin (GibcoBRL/Life Technologies) at 37 °C for 5 min, centrifugated, and the cell pellet was resuspended in 1 ml of complete culture media. CytoSMART counter (Automated Image-Based Cell Counter, version 1.5.0.16380, CytoSMART Technologies B.V., Eindhoven, Netherlands) was used to detect the number of cells in each time point.

Clonogenic capacity

N-ASC, ED-ASC, and N-ED-ASC were seeded in a 6-well plate l triplicate.
For N-ASC were plated 5×10^3, while N-ED-ASC and ED-ASC were used 1×10^3 cells, Cells were cultured for 14 days. Toluidine Blue (Sigma-Aldrich, Milan, Italy) staining was performed to count the colonies. The frequency of CFU-F within N-ASC, ED-ASC, and N-ED-ASC was expressed as a percentage of seeded cells.

Immunophenotyping

N-ASC, ED-ASC, and N-ED-ASC and the subsequent subculture cells (cellular p2) were characterised by flow cytometry. To perform cytofluorimetric analysis, the different cells product was centrifuged at 3000 rpm for 6 min. Next, the cell pellet obtained was resuspended with a complete culture medium, incubated with 1 ml of erythrocyte lysis buffer 1X (Macs Miltenyi Biotec, Milan, Italy) for 10 min at room temperature, and filtered through a 70 µm cell-strainer. Subsequently, cells were washed with 1 ml in PBS and incubated (1×10^5 for each tube) with conjugated antibodies on ice for 30 min. After incubation, the pellets were centrifuged (5000 rpm, 7 min) and resuspended in 100 µl of PBS.
The antibodies used were: CD105 APC conjugate (1:20 dilution), CD73 BV421 conjugate (1:20 dilution), CD34 PE conjugate (1:5 dilution), CD45 FITC conjugate (1:20 dilution), CD146 APC conjugate (1:20 dilution), SEEA3 FITC conjugate (1:20 dilution). All antibodies were purchased from B.D. Biosciences (Becton Dickinson Italy S.P.A., Milano, Italy). Immunophenotyping was performed through a chant II FACS (BD, Becton Dickinson, Milano, Italy).

Differentiation assay

The differentiation potential was evaluated in vitro for the N-ASC. ED-ASC was used as a control. Differentiation was carried out employing expanded cultured cells from p4.
For adipogenic differentiation, 5000 cells were seeded on a 12-well plate, incubated at 37°C, 5% CO_2, and after 24h, the complete culture medium was replaced with adipogenic media (Sigma-Aldrich, Milan, Italy). To evaluate the adipogenic differentiation capacity, after 5 and 10 days of incubation, the cells were fixed with Baker's fixative (Bio-Optica, Milan, Italy) for 10 min at 4 °C, washed with tap water for 10 min, and stained with Oil-Red-O solution (Bio-Optica, Milan, Italy) for 10 min and Mayer's hematoxylin (Bio-Optica, Milan, Italy) for 5 min. Finally, the glass coverslips were mounted with Mount Quick aqueous (Bio-Optica, Milan, Italy).
For chondrogenic differentiation, 1×10^6 cells resuspended in 5 µl of complete culture media were seeded in a 12-well plate. After 2h, the chondrogenic media was added (StemPro chondrogenic differentiation Kit -GIBCO Life Technology, Monza, Italy). After 5 and 10 days of incubation, changing of the media every 2 days, cells were fixed with 4% formaldehyde (Bioptica, Milan, Italy) in PBS 0.05M for 30 min at 4 °C, washed twice with distilled water, and stained with Alcian Blue solution (Merck KGaA, Darmstadt, Germany) for 40 min and with Nuclear Fast Red (Bioptica, Milan, Italy) for 20 min. Finally, after brief dehydration, the glass coverslips were mounted with Entellan (Merck KGaA, Darmstadt, Germany).

Five thousand cells were seeded on a 12-well plate with complete culture media for osteogenic differentiation. After 24h, the media was replaced with osteogenic media (StemPro osteogenesis differentiation Kit–GIBCO Life Technology, Monza, Italy). To evaluate the osteogenic differentiation capacity, after 5 and 10 days of incubation, the cells were fixed with 4% formaldehyde (Bioptica, Milan, Italy) in PBS 0.05M for 30 min at 4 °C, washed twice with distilled water, and incubated with Alizarin Red Solution (Merck KGaA, Darmstadt, Germany) for 2-3 min and Mayer's hematoxylin (Bio-Optica, Milan, Italy) for 30 sec. Finally, after brief dehydration, the glass coverslips were mounted with Entellan (Merck KGaA, Darmstadt, Germany).
Once the slides were dried under the cabinet, cells were observed with light microscopy using an Olympus BX-51 microscope (Olympus, Tokyo, Japan) equipped with a digital camera (DKY-F58 CCD JVC, Yokohama, Japan).

xix) Result

Microscopical Analysis of Hy-Tissue Nanofat product

The product obtained by the Hy-Tissue Nanofat system was examined at a morphological level to investigate its composition. For this purpose, lipoaspirates were processed following the protocol recommended by the manufacturer. The adipose tissue was shuffled 30 times between two connected syringes, filtered through a membrane of 120 µm, and collected with a syringe using the lower valve port of the outer bag, resulting in autologous whitish emulsion ready to inject.
The microscopical analysis revealed that the product was mainly composed of intact lipid droplets of different sizes (Figure 27. B). The size distribution of the lipid droplets (Figure 27. C) showed that nanofat was composed of droplets classified in four main clusters: with a diameter lower than 60 µm (42.42 ± 10.10), between 60-100 µm (76.59 ± 11.77), between 100-200 µm (143.43 ± 33.42) and over 200 µm (245.45 ± 38.07).

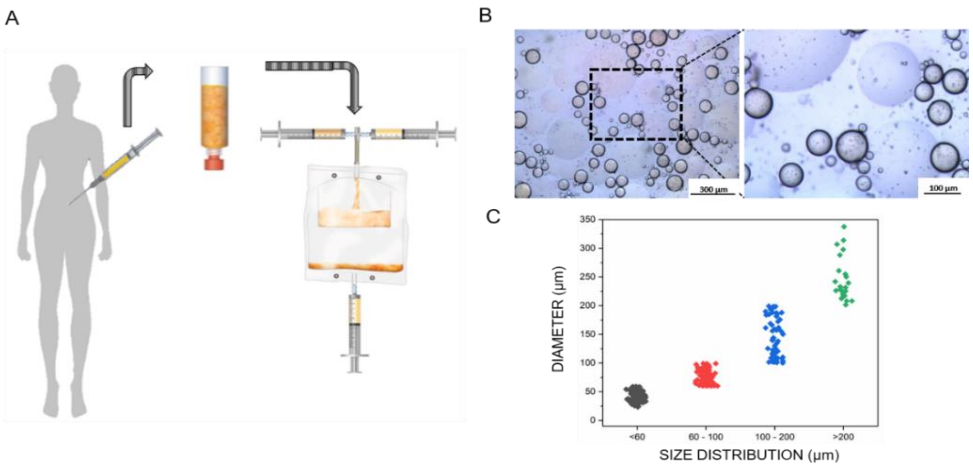

Figure 28. Morphological analysis of Hy-Tissue Nanofat product. (A) Scheme of the Hy-Tissue Nanofat procedure; (B) Light microscopy of Hy-Tissue Nanofat product obtained with the whole-mount method. The square (in Figure B, right) indicates the location of the higher magnification (Figure B left). (Scale bar: (right) 300 µm, (left) 100µm). (C) Size distribution of the lipid droplets.

The emulsion obtained was centrifuged to characterise the Hy-Tissue Nanofat product at a cellular level. The cellular pellet was analysed in terms of cells yield, cells proliferation capacity, and clonogenic potential. NANOFAT-derived ASC obtained with Hy-Tissue Nanofat system (N-ASC) were compared with ASC enzymatically extracted (ED-ASC). Moreover, to verify the regenerative unit's total amount and quality, the Hy-Tissue Nanofat product was subjected to enzymatic digestion (N-ED-ASC). Figure 28 shows the experimental procedure followed to characterise the cellular product.

Cellular yield, proliferation capacity, and clonogenic potential of N-ASC

The *N-ASC* products obtained by the mechanical disaggregation were analysed in terms of cell yield, product quality, viability, proliferation capacity, and clonogenic potential.

The number of nucleated cells per ml of fat obtained with Hy-Tissue Nanofat system was $3.75 \times 10^4 \pm 1.55 \times 10^4$ cells/ml fat (Figure 29. A), while the number of cells extracted after enzymatic digestion of the fat tissue and after the enzymatic digestion of the filtered emulsion was $1.25\times10^5 \pm 4.65\times10^4$ and $4.38\times10^5 \pm 9.41\times10^4$, respectively. Considering the enzymatic treatment as the gold standard protocol (cell yield 100%), the cellular yield for N-ASC resulted in 7.87 ± 3.15%, which increased to 28.53 ± 9.49% after the enzymatic digestion of the emulsion (N-ED-ASC), as reported in the table in Figure 29. A.

To analyse N-ASC's adhesion and proliferation capacity, cells were seeded in T-flasks until confluence (Figure 29. B). N-ASC and ED-ASC show statistically significant differences to reach confluence. Indeed, ED-ASC required less time to

reach confluence (4.80 ± 2.28 days) than N-ASC (10.8 ± 2.59 days). This result reflects the higher frequency of adherent cell content obtained with the enzymatic digestion of the fat. On the contrary, no significant statistical differences were shown between ED-ASC and N-ED-ASC (7.60 ± 3.29 days). Proliferation capacity results were confirmed with a PDT assay (Figure 29. C). PDT reveals that the replication rate of ED-ASC and N-ED-ASC was comparable (52.84 ± 6.40 and 57.06 ± 25.41h, respectively), while cells obtained from N-ASC required more time to duplicate their number (81.85 ± 18.87h). Figure 29D shows a representative image of N-ASC, N-ED-ASC, and ED-ASC morphology three days after extraction (first change of culture media). Hy-Tissue Nanofat treatment did not affect the cell morphology compared to cells obtained from enzymatic digestion, exhibiting a homogeneous fibroblast-like morphology. Moreover, cellular membranes and nuclei were well-preserved, indicating no signal of cell suffering.

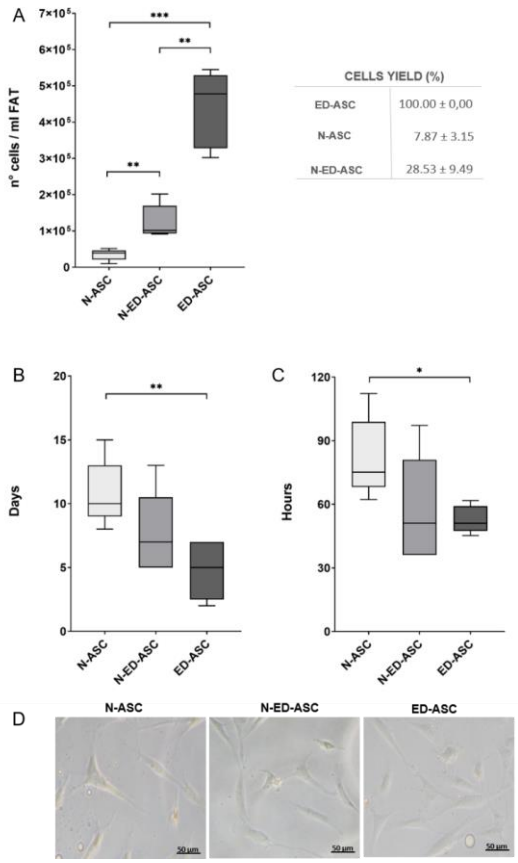

Figure 29. Cellular yield and proliferation capacity of N-ASC. (A) Nucleated cells were obtained after the three evaluated treatments. Cells yield (n° of cell/ml fat) was evaluated considering the enzymatic digestion as 100%; (B) Proliferation capacity N-ASC, N-ED-ASC, and ED-ASC in T25 flasks. The days required at the adherent cells to reach confluence (passage 1) were counted. (C) The population doubling time of N-ASC, N-ED-ASC and ED-ASC were analysed to evaluate the growth rate of adherent cells; (D) microscopic images of adherent cells three days after the extraction. The results are shown as the mean, and error bars represent the standard deviation. Box and whisker plots represent the median. Significant statistical differences are indicated (p-value <0.05=*, 0.005<p-value <0.001=** or p-value <0.001=***).

To evaluate the ability of N-ASC to form colonies, colony-forming unit-fibroblast (CFU-F) assays were performed. Figure 30. A shows a representative micrograph of CFU-F detected by Toluidine Blue staining after 14 days. On day 14, the morphology of CFU-F appeared comparable between the three treatments. CFU-F yield of N-ASC was 61.29 ± 45.10 CFU-F/ml fat, while CFU-F yield of N-ED-ASC increased over 11-times (702.29 ± 368.40 CFU/ml fat, Figure 30. B). Furthermore, the relative proportion of CFU-F in the N-ED-ASC (0.54 ± 0.09%) increases significantly after the enzyme digestion of the emulsion (Figure 30. C) compared to N-ASC (0.18 ± 0.05 %). CFU-F obtained with ED-ASC resulted in 29- and 3-times more (1830.59 ± 1190.82 CFU-F/ml fat) compared to the N-ASC and N-ASC-ED, respectively (Figure 30. B), with a relative proportion of CFU-F of 2.54 ± 0.69 % (Figure 30. C).

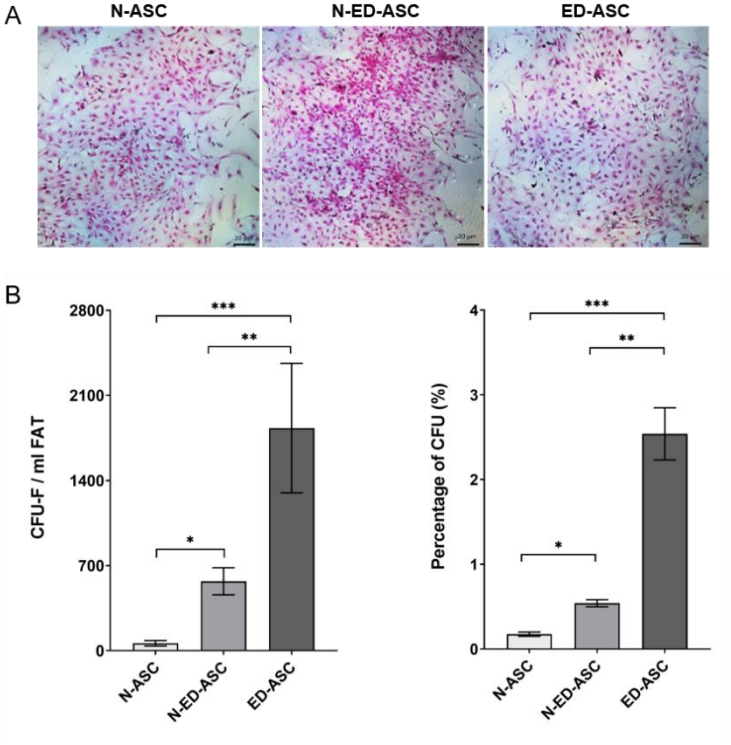

Figure 30. Clonogenic potential of Hy-Tissue Nanofat product. (A) The representative light microscope of CFU-F assay stained with Toluidine Blue (scale bar 20 µm); (B) CFU-F yields of N-ASC, N-ED-ASC, and ED-ASC. (C) Percentage of CFU-F contained N-ASC, N-ED-ASC, AND ED-ASC. Results are presented as the mean, and error bars represent the standard deviation. Significant statistical differences are indicated (p-value <0.05=*, 0.005<p-value <0.001=** or p-value <0.001=***).

Immunophenotyping

A cytofluorimetric analysis at p0 (immediately after the treatments) and after in vitro cellular expansion was performed to characterise N-ASC immunophenotypically.

Specific single antigens (such as CD43, CD45, CD105, CD29, CD73) were analysed on the previously selected cells. The proportion of CD34 cells in N-ASC was 3.37 ± 1.67% (Figure 31. A), not thus far from the percentage of CD34 expression obtained in N-ED-ASC and ED-ASC (7.99 ± 4.6 % and 4.91 ± 2.5 % for NANOFAT+ED and E.D., respectively). The hematopoietic surface marker CD45 was less expressed (1.27 ± 0.45%, 1.35 ± 0.71% and 1.53 ± 0.40 % for N-ASC, N-ED-ASC, and ED-ASC, respectively), as reported in Figure 31. B. Moreover, the frequency of CD105, C29, and CD 73 positive cells. (Mesenchymal Stem Cells marker) was evaluated. In N-ASC, the percentage of antibody expression was 15.9 ± 8.86 %, 3.59 ± 2.00% and 1.79 ± 0.23% for CD105, CD 29 and CD73, respectively (Figure 31. A), comparable with the results obtained for the same antibody in N-ED-ASC and ED-ASC (Figure 31. B). Finally, cultured cells (cellular passage 2) were also analysed to confirm the phenotype preservation over time (Figure 31. C). The immunophenotypic analysis after the cellular expansion showed that the surface marker expression profiles of N-ASC, N-ED-ASC and ED-ASC were comparable, revealing a low expression for CD45 and CD34 and a high expression for Mesenchymal Stem Cells associated markers such as CD105, CD73, and CD29 (Figure 31. C).

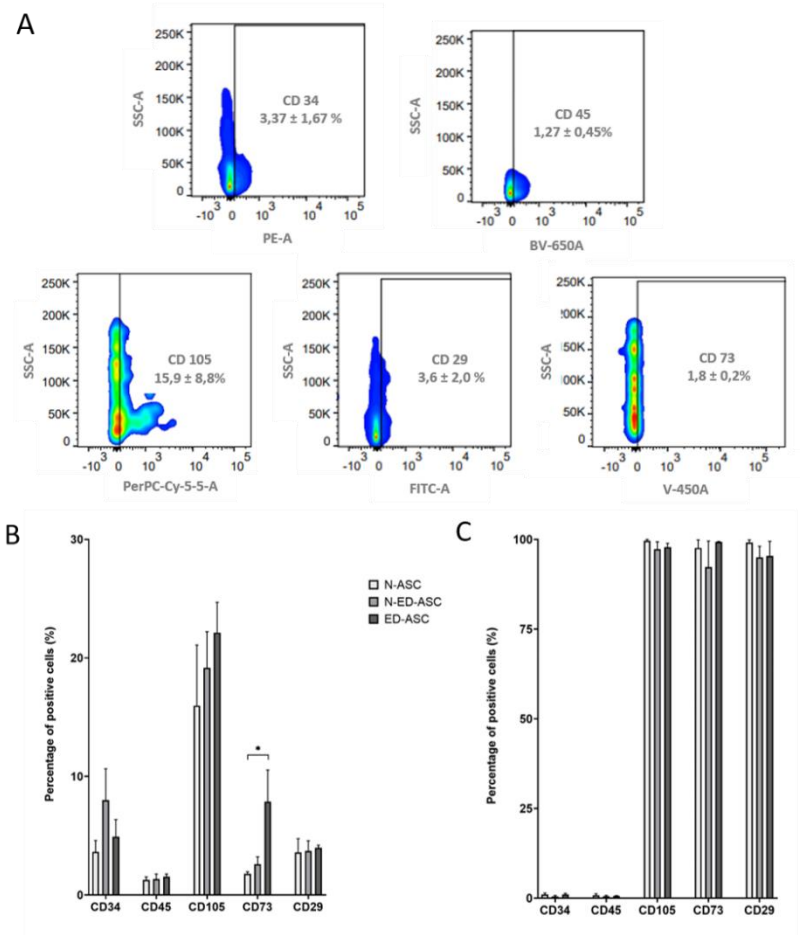

Figure 31. Surface markers expression was detected by flow cytometric analysis of N-ASC. The percentage of positive cells for each marker was calculated after subtracting the non-specific fluorescence obtained with the control (unmarked). (A) Representative set of flow cytometry analysis for CD34, CD45, CD105, CD29, CD73 markers performed on N-ASC. Percentage of positive cells to CD markers was indicated as an average of the samples; (B) Percentage of positive cells to CD markers (as an average of the samples) in N-ASC compared to N-ED-ASC and ED-ASC; (C) Percentage of positive cells to CD markers after in vitro cell expansion in N-ASC, N-ED-ASC and ED-ASC. Results are presented as the mean ± standard deviation (error bars represent the standard deviation); significant statistical differences are indicated (p-value <0.05=*).

Analysis of multipotency

The multilineage differentiation ability of N-ASC was determined by verifying the ability of adherent cells to differentiate toward adipocytes, chondrocytes, and osteocytes. Differentiation potential (Figure 32) was evaluated 5 and 10 days after the induction by a selective medium containing lineage-specific induction factor. Induced N-ASC were stained with Oil-Red-O, Alizarin Red, and Alcian Blue for adipogenic, osteogenic, and chondrogenic differentiation, respectively (Figure 32. A) and compared with ED-ASC (Figure 32. B). Figure 32. A shows that N-ASC

were able to differentiate into the three mesodermal lineages starting from day 5. Applying Oil-Red-O solution, red spots reveal the generation of lipid droplets at day 5, which increases during adipogenesis differentiation until day 10. Alizarin Red staining shows the formation of *in vitro* calcification 5 days after medium induction, resulting in a more intense extracellular matrix calcification at day 10. Chondrogenic differentiation assay reveals the generation of cartilage-like matrix started from the 5th day upon the specific culture media induction. On day 10, a well-organized cartilage-like matrix rich in collagen type II and sulfated proteoglycans was detectable, as shown with Alcian blue staining (Figure 32.A). All the positive staining were compared with the control not induced.

Likewise, the multipotency assay was performed on ED-ASC, showing positive staining compared with the not-induced control (CTR). However, the differentiation started ten days after the specific medium induction, indicating a slower differentiation capacity than N-ASC.

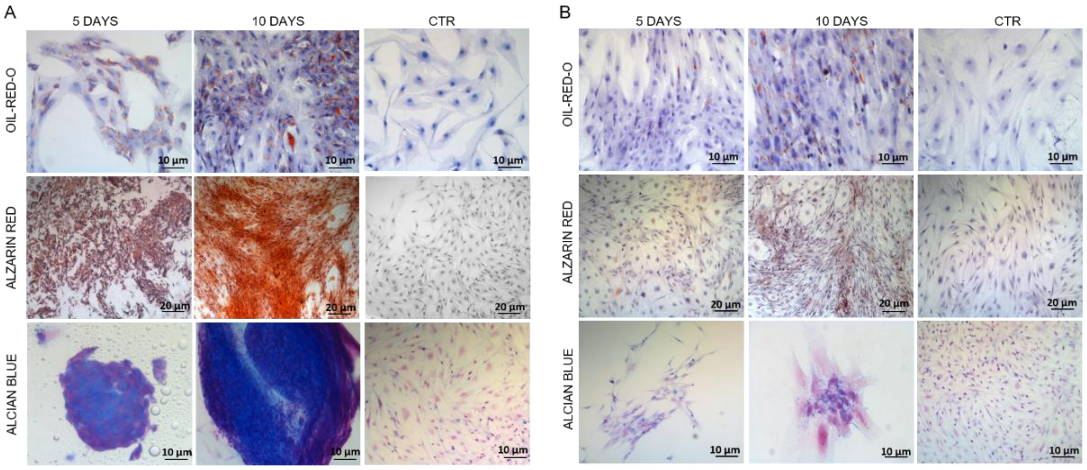

Figure 32. Multilineage differentiation assay. (A) Optical microscopy of N-ASC induced or not (CTR) with differentiation medium at day 5 and 10 (ORO staining bar m. Alizarin Red staining bar 20 µm. Alcian Blue staining bar 10 µm. (B) Optical microscopy images of ED-ASC induced or not (CTR) with differentiation medium at day 5 and 10 (ORO staining scale bar 10 µm. Alizarin Red 20 µm. Alcian blue 10 µm) Red spots indicated by the accumulation of neutral lipid vacuoles stained with ORO. Alizarin red staining reveals in red the extracellular matrix calcification, deposition of sulphated proteoglycans rich matrix was marked with Alcian Blue.

N-ASC and ED-ASC were then analysed by flow cytometry to verify the presence of the multi-lineage differentiating stress enduring cells (MUSE cells), investigating the SSEA-3 and CD105 antibodies expression. Figure 33 shows the percentage expression of the evaluated antibodies. N-ASC expressed 25.5 ± 6.5% of SSEA-3, while ED-ASC cells was 0.5 ± 0.2%. The expression of CD-105 antibody was 100% for both treatments as a typical percentage for cultured mesenchymal stem cells.

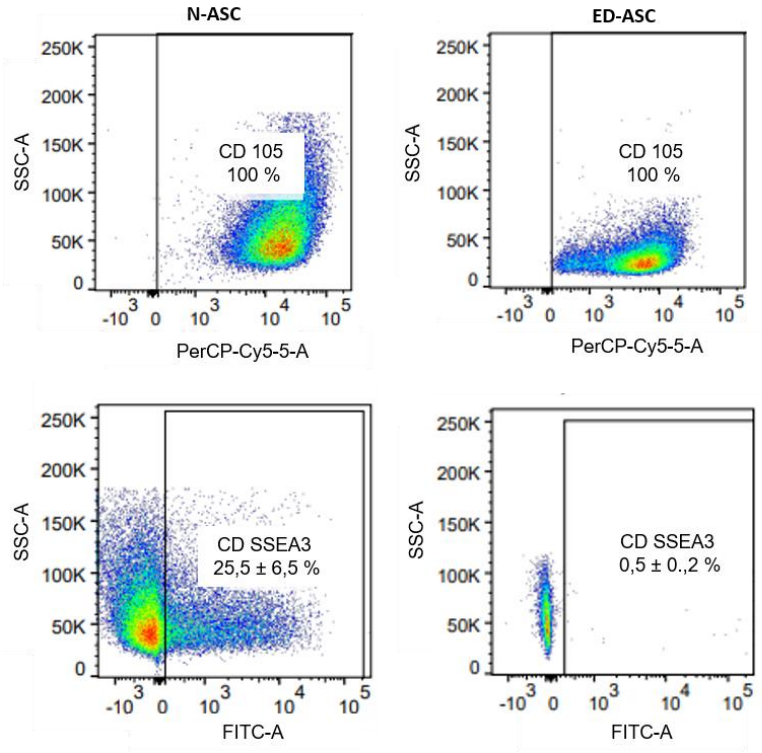

Figure 33. Multi-lineage differentiating stress enduring cells expression. Flow cytometry of N-ASC and ED-ASC to investigate the presence of MUSE cells. The percentage of positive cells to SEEA-3 and CD105 markers was indicated as an average of three samples. Results are presented as the mean ± standard deviation.

Existing mechanical devices for fat (adipose tissue) processing

Name of the device	Company
Adipopimer®	Korpo, Genoa, Italy, https://www.korpo.com/it/ adipofilling-adipopimer/
Arthrex ACP®	Arthrex, Inc., Naples, Florida, USA, https://www.arthrex.com/orthobiologics/bone-marrow- concentrate-bmc
GID700TM	GID Group, Inc., Louisville, Colorado, USA, https:// thegidgroup.com/gid-technology/
Goisis system	Microfat©, Milan, Italy, http://www.microfat. com
Hy Tissue SVF	Fidia Farmaceutici S.p.A., Abano Terme, Padua, Italy, https://pro.fidiapharma.com/it/
LipiVageTM	Genesis Biosystems, Inc., Lewisville, Texas, USA, https://www.genesisbiosystems.com/lipivage-system-autologous- fat-transfer/
Lipocell	Tiss'You srl, Domagnano RSM, https://www.tissyou. com/portfolio_page/lipocell/
Lipogems®	Lipogems International S.p.A., Milan, Italy, https:// www.lipogems.com/
LipoKitTM system	Medi-Khan International, Korea, http://www. medikanint.com/lipokit.html
Puregraft®	Cytori Therapeutics, Inc., San Diego, California, USA , http://www.puregraft.com/
RevolveTM system	LifeCell Corporation, Branchburg, New Jersey, USA, http://hcp.revolvefatgrafting.com/en
Rigenera	Rigenera-HBW, Turin, Italy, https://rigenerahbw.com/ All these devices perform purely mechanical treatments. Hy Tissue SVF (Fidia Farmaceutici S.p.A., Abano Terme, Padua, Italy
Hy-Tissue nanofat	Fidia Farmaceutici S.p.A., Abano Terme, Padua, Italy, https://pro.fidiapharma.com/it/

Table 2: Currently patented, published, or commercially available non-enzymatic adipose tissue defragmentation devices/ systems and their company

Method	Description
Centrifugation	Tissue is inserted into a canister, and a centrifugal force is applied to separate fat cells from contaminants that can degrade the adipocytes such as blood cells, lipids, and anaesthetics. Centrifugation speed (expressed in revolutions per minute, rpm, or in acceleration—gravitational force, g) is correlated with the final density of the adipose tissue, number of progenitors, cell viability, and contaminants removal.
Emulsification	This method can be performed manually or mechanically. In manual mode, tissue is inserted into a bag and manually massaged. In mechanical mode, tissue is slowly shifted several times (from 2 to 30 steps) between two syringes connected to each other by a Lock connector.
Filtration	Tissue is filtered under sterile conditions using different strainers (form common metal strainers to cotton gauzes) with different calibre meshes.
Mincing	Tissue is inserted into a canister and manually or mechanically ground to obtain a chop of desired size.
Blending	Tissue is inserted into a canister and reduced to a puree by means of single or multiple blades devices. The blades can be of different materials (from ceramic to metal).
Sedimentation	Tissue remains into a canister (the syringe or others) for the time necessary to obtain a natural gravity sedimentation.
Squeezing	Tissue is collected into a syringe and the piston squeezes the tissue through a weight-mesh-filter inside the same syringe or between two connected canisters.
Tefla-rolling	Tissue is poured onto large (3 × 8-in) pieces of nonadherent Tefla dressing, rolled and kneaded gently for 5 min using a sterile scalpel handle.
Washing	Tissue is washed with saline solution or lactated Ringer solution

Table 3: Current mechanical adipose tissue processing methods

xx) Comparing our three devices

Device	Method	Automation Grade (on a scale of 0-3)	TPT (Until reinjection)	Approval and trademark	Close/ Open system
Rigenera	Washing Sedimentation Centrifugation Mincing Filtration	3	10-12 min	CE trademark	Close
Hy-Tissue SVF	Filtration Emulsification Centrifugation	Device 2; Procedure 3	14-15 min	CE trademark	Close
Hy-Tissue Nanofat	Emulsification Filtration Centrifugation	3	10-12 min	CE trademark	Close

Table 4: Comparing our three devices according to their automation and processing technique. To highlight the automation degree, we have defined a 0–3 grading scale, with 0 corresponding to a fully automatic device that produces an injectable tissue and 3 to a nonautomatic device, in which processing is manual.

The broad spectrum of pathologies in which fat grafting can be applied requires different types of adipose tissue processing treatments. The type of treatment must optimise the tissue based on the final grafting site to improve regenerative efficacy. While initially, the fat tissue was considered a simple filler for the expansion of soft tissue, with the passage of time and the discovery of its properties, it assumed the role of an accurate regenerative material.

The ability of the injected adipose tissue to increase the stem properties of a tissue/structure probably makes fat grafting the primary anti-ageing regenerative technique today. In parallel to the considerations on the regenerative properties of this tissue, numerous reviews have also developed concerning the biological role of the injected tissue within the damaged structures. In the past, Rigotti et al. (2007) suggested that the basis of the therapeutic mechanism consists of a mesenchymalization effect operated by the stem component of the adipose tissue that involves several phases, the first of which are the recall of liquid and angiogenesis.

At the same time, considerations have been made on the role of stem cells in the healing process (which represent a minimal part of the injected tissue) and stem niches in which stem cells are maintained in their molecular and cellular microenvironment.

From the need to adapt the tissue to be injected to the different pathological conditions to be treated and to the other grafting districts, an effort was made by the international scientific community to obtain increasingly effective and safe preparations for the patient and, at the same time, adaptable to different conditions.

The combination of different processing techniques changes the final composition of the tissue to be reinjected. For this reason, and given that the works found in the literature adopt comparison techniques that are not always comparable, it is impossible to indicate one or more processing methods, such as the optimal methods, to be preferred to the others.

Comparing the devices, the negative data that emerge are that these tools are not automatic. None of the devices analysed even reach level 1 on the scale used in this study. This means more significant intervention by the operators, a greater possibility that mistakes are made, the tissue is damaged, and more substantial quantities of the final injectable tissue are lost. Apart from the Rigenera device, which has been classified as a level 2 device, all the other devices and procedures have been classified as level 3. Nevertheless, despite having the same classification, the variability of the processing methods makes them very different. The results of the 17-g centrifugation carried out with the Adipopimer are undoubtedly different from those of 400-g centrifugation (e.g., Hy Tissue SVF and Rigenera). Manual centrifugations (e.g., GID700 and Revolve) differ further. In the latter case, moreover, differences in the processing results can be noted based on the same operator performing the centrifugation, in terms of applied force and consequent speed reached invariance of the applied force and resulting maintenance of the rotation speed. In these cases, there is no variability related only to the automation of centrifugation.

Similar considerations can be made for all manual emulsification procedures (e.g., Hy Tissue SVF, Lipogems, and Puregraft), for which the variance linked to the operator and his experience is indisputable. This means that all these devices and the same device used by different people can produce a highly variable quality of injectable tissue.

At present, fat grafting techniques present a relatively broad spectrum of approaches. They are obtaining significant therapeutic results and allowing us to get biological data that were previously unthinkable. The extension of the therapeutic indications has favoured the proliferation of methods for processing fat, often still under study, refinement, and optimisation.

Considering the diffusion of the fat grafting method and the technical variables described, a confrontation of the scientific community is necessary. For each pathology, the optimal processing conditions must be identified, and the operating

standards of the various devices must be defined. This last aspect would allow a more straightforward comparison of existing devices and new future devices. Undoubtedly, the scientifically consolidated data is that tissue regeneration through the insertion of autologous stem niches allows a real restitution ad integrum and not a simple repair.

Other available devices which were not compared in our studies:

-LipoCube™ Nano (LipoCube, London, United Kingdom),
-MicroFat systems (Kluter Medical SL, Seville, Spain),
-Nano Fat Processing Set (Xelpov Surgical, Rochester, Michigan, USA),
-Nano Fat Transfer Processing Set (HK Surgical, San Clemente, California, USA),
-Tulip NanoTransfer Set™
-Single-Use Transfer™ (Tulip Medical Products, San Diego, California, USA).
-Aquavage (M.D. Resource Corp., Livermore, California, USA),
-Fat Collection Canister (HK Surgical, San Clemente, California, USA), -LipoCollector® (Human Med AG, Schwerin, Deutschland),
-Tissu-Trans® FILTRON® (Shippert Medical Technologies, Centennial, Colorado, US

3. Enzymatic isolation and characterisation of SVF and its application

The gold standard Vs new collagenases

In aesthetic medicine and reconstructive surgery, post-harvest fat processing aims to eliminate contaminants, including cellular debris, free oil, and other non-viable components of the lipoaspirate, such as hematogenous cells. One of the significant fibrous components of animal extracellular connective tissue is collagen, which must be degraded before fat grafting. Collagenase type I (an endopeptidase from *Clostridium histolyticum* is a crude collagenase preparation capable of cleaving native collagen in the triple helix region under physiological conditions *in vivo* and *in vitro,* which is used for the isolation of adipocytes, hepatocytes, and cells from the lung, epithelium, and adrenal tissue the isolation of primary cells or tissue dissociation, however, at present days there is a specific prohibition (within European Union and some other countries) on type 1 collagenase due to its destructive activity which tends to disrupt the regenerative component of the stromal vascular fraction, and this generates a need to have another similar enzyme that can replace the former & preserve specific membrane proteins by maintaining its regenerative potential. In our study, we are trying to optimise and propose a new collagenase (Fidia Pharmaceuticals, Italy) of which the adipose tissue treatment results are comparable to the existing type 1 collagenase and of the enzyme Liberase (Sigmaaldrich) digested product, which might keep more intact cells and take less time to process the fat.

In reconstructive surgery, autologous fat is used for fat grafting to augment adipose tissue volume (i.e., as filler). There is almost no chance of allergic or foreign body reaction; moreover, the plentiful source of fat, which is easily obtainable, inexpensive, repeatable, biocompatible, with low donor-site morbidity, makes it possible the closest to the ideal filler [208]. Enzymatic digestion using collagenase is the conventional processing method to isolate adipose SVF, which is thought to be the main element for the induction of adipogenesis. However, there are different processes (enzymatic, mechanical for adipose tissue digestion). Type 1 collagenase allows isolating the maximum number of nucleated cells per gram of lipoaspirate from all existing fat-digestion procedures, giving >80% viable cells [209, 210]. The SVF is not only composed of adipose-resident stromal cells but is home to macrophages, preadipocytes, endothelial progenitor cells, and vascular cells. However, being a crude-production enzyme, collagenase type -1 has been proven to adversely affect

the product after fat digestion by disrupting cells and not maintaining cell integrity. As a result, many countries, especially in the European Union, have restricted its use, which generates a need to produce another enzyme that can act similarly to collagenase type 1 but protect the cell membrane integrity and include viable nucleated cells [212]. Herein, we focus on using a new collagenase for fat grafting techniques (Fidia Pharmaceuticals, Italy) to harvest SVF enriched with integrated nuclear viable cells before fat grafting. We have compared the product obtained after Coll-I and FC digestion with another digested product obtained from Liberase. Liberase [TM] contains highly purified Collagenase I and Collagenase II. These two collagenase isoforms are blended in a precise ratio and with a medium concentration of Thermolysin, a non-clostridial neutral protease.

xxi) Materials and Methods

Adipose tissue collection

Fat samples were collected from 11 patients going through liposuction. Informed consent was taken from all of them before the collection of pieces. Around 30 ml of lipoaspirate was collected from the abdominal area of each donor with a cannula of 11G, six holes, and a 20 ml Vac-Lock syringe. Fat was transported in an adiabatic container to the laboratory of the University of Verona and processed within 18 hours from harvest.

Enzymatic digestion of fat

Collagenase type 1 digestion

Adipose tissue samples, i.e., lipoaspirates, were processed (digested) using the enzymatic method (as reported in Dai pre et al.) with type 1 collagenase (GIBCO life technology, USA) solution at the concertation of 1 mg/ml, i.e., 0.005 gm of Collagenase type 1 powder and 0.1 gm of Bovine Serum Albumin (BSA, 2%) suspended in 5 ml of Balanced Salt Solution of Hank (HBSS) at 37 °C for 45 min. After the incubation in the shaking incubator, the complete medium was added to neutralise the enzymatic action, followed by centrifugation at 7000 rpm for 7 min at RT. The supernatant was discarded, and the pellet was diluted with complete medium (Dulbecco Minimum Essential Medium, DMEM from Sigmaaldrich, Italy with 10% of FBS, 0.5% of amphotericin B, and 1% of a mixture of penicillin/streptomycin 1:1 both from GIBCO Life Technology, Italy, and used for further experiments, i.e., cell growth, CFU assay, Viability test, etc.

Fidia Collagenase and Liberase digestion

The second portion of lipoaspirate (5 ml) was digested simultaneously with 5 ml of the new Collagenase named 'Fidia collagenase' (Fidia pharmaceuticals, Italy) solution at 0.5x, 1x and 2x concentration (i.e., 0.016% and 0.32% of Fidia collagenase, respectively mixed with 0.1 gm of BSA {2%} diluted into 5 ml of PBS) and incubated for 45 min (1x and, 2x concentration), 90 min (1x concentration) and 20 min (2x concentration) to compare and optimise the best result. The third portion was digested with 5 ml of the 1x Liberase solution (i.e., 5 gm of powder liberase {Sigmaaldrich} diluted into 25 ml of PBS and then divided into five portions (5 ml each) with an incubation period of 45 min at RT in shaking incubator)

After the incubation period with different incubation periods, 5 ml of complete culture medium was added to neutralise the enzymatic action, and the sample was centrifuged at 7000 rpm for 7 min. After centrifugation, the supernatant was discarded, and the pellet was resuspended with 1 ml of complete culture medium and processed the same way as the type 1 collagenase digestion.

Viability assay, Cell culture, and expansion

After all three collagenases at p0 (passage 0), collected cells were put on a burker chamber and counted using Trypan Blue exclusion assay using a CytoSMART counter (Automated Image-Based Cell Counter, version 1.5.0.16380, CytoSMART Technologies B.V, Eindhoven, Netherlands. Around 5,00,000 cells from the end product after digestion were plated in a 25 cm^2 flask with a complete culture medium and incubated at 37 °C and 5% CO2. The medium was first changed after 72h and, successively, every 48h. At confluence, cells were detached by incubating them with trypsin-EDTA 1% (GIBCO Life Technology, Monza, Italy) at 37 °C for 5 min and re-plated in a 75 cm^2 flask. Next, most of the rest of the cells were mixed with another 4 ml of complete medium, plated into a 25 cm2 flask, and cultured inside an incubator maintaining 37°C and 5 % CO_2**.** After 72h, the media was changed, followed by changing every 48h. This way, the cells were cultured and expanded until p4 for the further experiment, and at last growth curve of the cells was compared among the three different enzymes.

CFU assay

Five to seven thousand cells from the p0 (passage 0) were plated inside a 6-well plate with cover glass into triplicate for the colony-forming unit assay. They were cultured until 7-10 days with media change every two days, and at the end of the experiment, colonies were counted using toluidine blue. Further, the number of colonies from the enzymes were compared.

Treatment of collagenases on expanded cells

Cells cultured until p4 were then detached using 0.25% trypsin (Trypsin-phenol red, GIBCO^{TM}), and the viability was checked similarly as explained before with the trypan blue method (pre-viability). After that, about 250,000 cells were re-digested with all the three kinds of collagenases (Diagram) at two different time points, i.e., 20 min and 30 min, in a shaking incubator at 37 °C. After that, the enzymatic action was neutralised by adding 1 ml of complete media and centrifuged at 7000 rpm for 5 min. The supernatant was discarded, and the pellet was diluted in 1 ml of complete media and counted for viability (post-viability). In this procedure, three different concentrations of Fidia collagenase were considered, i.e., 0.5x, 1x, and 2x. The viability was compared with both the cells from 1x concentration of Collagenase type 1 and Liberase 1x solution after the digestion.

Viability of mixed ASDAS

Three different samples were mixed, and the viability was checked. Collected cells were counted using Trypan Blue exclusion assay using a CytoSMART counter (Automated Image-Based Cell Counter, version 1.5.0.16380, CytoSMART Technologies B.V, Eindhoven, Netherlands.

Cell cytotoxicity assay (MTT)

This assay was performed on expanded cells digested with all three kinds of collagenases to check the viability of the 30 min and 20 min digestion for all three different collagenases. After the viability check with trypan blue by CytoSmart, around 10×10^4 cells were mixed in 100 µl of complete media and were plated in sextuplicate for each enzyme (for Fidia collagenase, three different concentration was considered, i.e., 0.5x, 1x, 2x) inside the wells of a 96-well plate and cultured for 24h inside an incubator, maintaining 37 °C and 5 % CO_2. After the incubation period, the media was removed, and 100 µl of MTT solution (i.e., 10% MTT solution in complete media) was added to each well and incubated for 4 hours in the dark inside the same incubator containing a humified atmosphere, 37°C and 5% CO_2. The MTT solution was removed after the incubation, and 100 µl of DMSO was added to each well to dilute the formazan for 10-15 min on a slowly moving incubator at room temperature. At last, the plate was read with a spectrophotometer

(Chromate, Software version, company) and measured at 570 and 630 nm wavelength.

xxii) Analyzing the product *in vitro*

According to the gold standard enzymatic digestion protocol, Fat (5 ml) samples from N = 11 patients were treated with Collagenase type 1, FC, and Liberase for 45 min at 1x concentration. The number of nucleated cells inside the pellet after type-1 collagenase digestion at p0 was higher than Fidia collagenase (Figure 34. A) but lower than Liberase digestion. In the case of cell yield, the type 1 coll digested cells were considered standard; compared to this, the liberase outlined several cells were more, and FC cells were less (lower table of Figure 34. A). Also, a similar situation was observed for the colony-forming-unit assay (upper two bar charts, Figure 34. B), where the number of colonies for FC digested lipoaspirate was lower than the other two collagenases after two weeks. The lower two bar charts of Figure 34. B comprehend the same result showing the CFU efficiency in percentage. Cell yield (lower graph, Figure 34. C) and proliferative capacity (upper diagram, Figure 34. C) show that cells digested with FC took more days to reach the same number of cells compared to the other two collagenases, i.e., type-1 and Liberase. This means FC digested cells (45 min) take longer to proliferate in vitro compared to the two types of collagenases. The typical multi-well plate for the CFU assay is shown in Figure 34.D and, Figure 34. E is the magnified image of 1 colony from the 12 multi-well culture plates. All the experiments were repeated three times to ensure consistency.

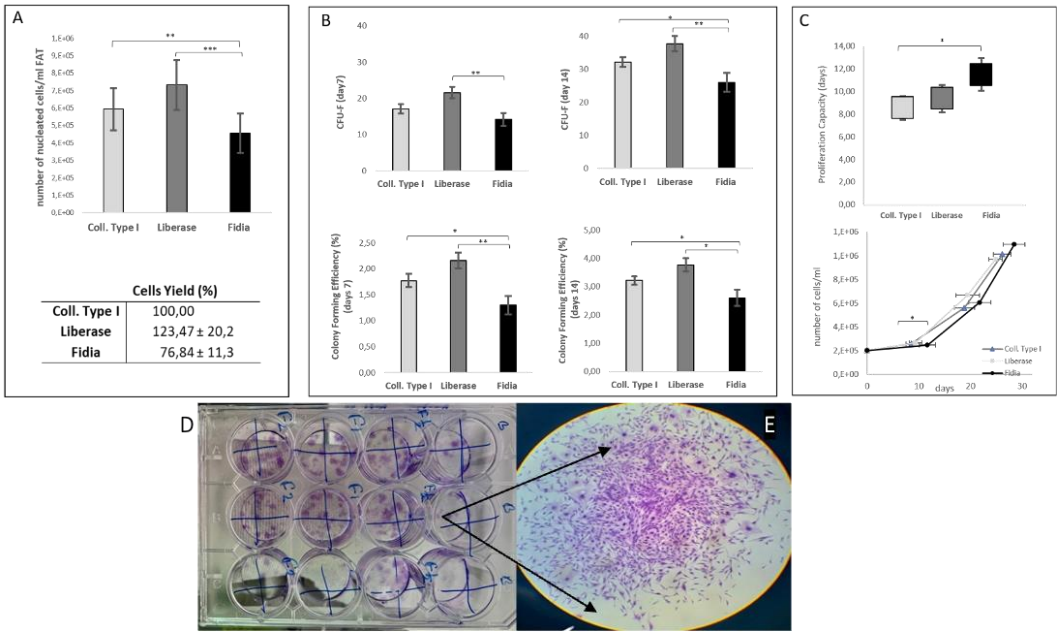

Figure 34. Evaluation of FIDIA Collagenase efficiency using the "gold standard" protocol (1x, 45'); A. Comparison of the number of nucleated cells/ml of fat at P0 among FC, Type 1 and Liberase digested cells; B. Colony-forming unit assay for all the coll digested cells and their efficiency. Percentage of CFU contained in the enzymatically digested pellet. Results are presented as the mean and error bars one standard deviation; C. Proliferative capacity of the digested lipoaspirates until day 14; D. Representative image of a colony-forming unit assay inside 12-Well plates; E. An amplified image of a colony from Figure 1.D, i.e., CFU observed with a light microscope with Toluidine Blue staining (4x magnification)

After digesting the standard protocol, we wanted to see what happens by increasing digestion time, so lipoaspirates from N=5 patients were treated with FC for 90 min at 1x concentration. In contrast, for type 1 and liberase, the time was 45 min. Post digestion, the number of nucleated cells inside the pellet of FC at p0 was almost like that of liberase digested cells and more than type 1 collagenase digested cells (upper bar diagram, Figure 35. A). So, the cell yield shows the same result (lower bar diagram, Figure 35. A). However, after two weeks for the liberase treated cells, the number of colonies was more than FC and type-1 collagenase (Figure 35. B). Also, the growth curve (Figure 35. C) shows that to reach $10x10^6$ cells, the collagenase type-1 and Liberase treated cells took less time than the FC. However, at p0, the cell count was good for the 90-min FC digested cells; in the long term, their growth rate was slower than the other collagenase digested cells.

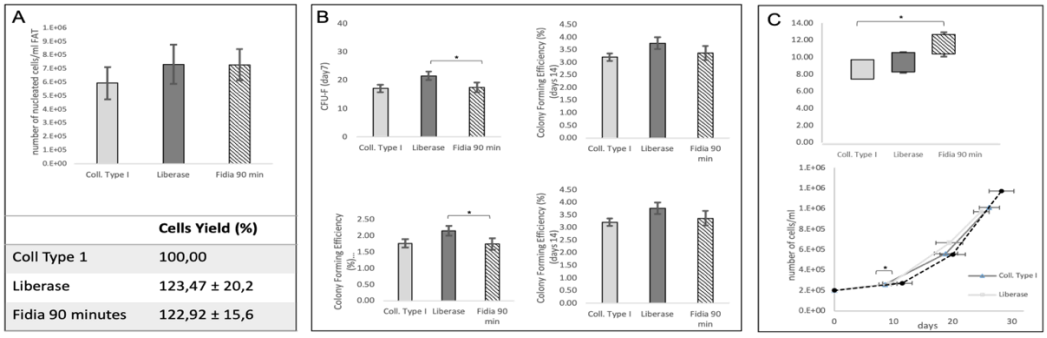

	Cells Yield (%)
Coll Type 1	100,00
Liberase	123,47 ± 20,2
Fidia 90 minutes	122,92 ± 15,6

Figure 35. Evaluation of the efficiency of FC digested cells by increasing the incubation time from 45 min to 90 min at 1x conc; A. Comparison of the number of nucleated cells/ml of fat at P0 among FC (90 min digestion), type 1 and Liberase derived cells (45 min digestion), the lower table of 2. A states the cell yield considering type 1 coll as control; B. Colony-forming unit assay for all the coll digested cells and their efficiency at days 7 and 14. Results are presented as the mean and error bars one standard deviation; C. The lower graph shows the growth and proliferative capacity of the digested lipoaspirates until day 14; FC digested cells took more days to reach confluence (similar number of cells like type 1 and liberase digested)

Fat (5 ml) samples were treated with all three collagenases for 45 min, but the concentration of Fidia collagenase was increased to 2x. The number of cells/ml of fat inside the pellet from FC treated fat at p0 was higher (Figure 36. A) than collagenase type-1 and Liberase treated fat. The cell yield (lower table of 37. A comprehend the same result). The number of colonies and the CFU efficiency after

two weeks derived from the Fidia collagenase treated fat was more than Liberase and type-1 collagenase (Figure 36. B). The FCDC proliferated at a similar rate as the type 1 collagenase, i.e., around day nine, they became confluent.

In contrast, the liberase treated fat-derived cells took a long time to become confluent (36. C). The growth curve of Figure 36. C shows that to reach $10x10^6$ cells, the collagenase type-1 and Liberase treated cells took more time than the FCDC.

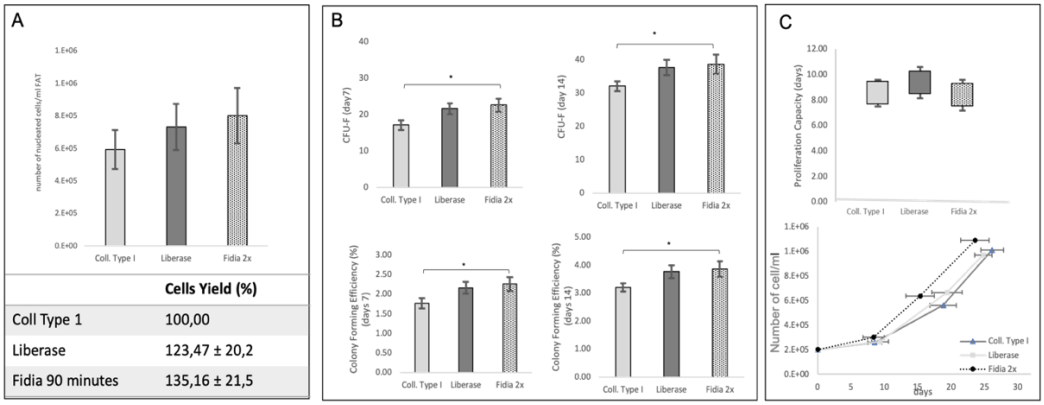

	Cells Yield (%)
Coll Type 1	100,00
Liberase	123,47 ± 20,2
Fidia 90 minutes	135,16 ± 21,5

Figure 36. Evaluation of the efficiency of FC by doubling the enzyme concentration (2x) but keeping 45-minute incubation time; A. Comparison of the number of nucleated cells/ml of fat at P0 among FC, type 1 and Liberase derived cells (45 min digestion), the left lower table of 37. A state the cell yield considering type 1 coll as control; B. Colony-forming unit assay for all the three coll digested cells and their efficiency at day 7 and 14. Results are presented as the mean and error bars one standard deviation; C. The upper graph shows the proliferative capacity, and the lower graph shows the growth rate of the digested lipoaspirates-derived cells until day 14

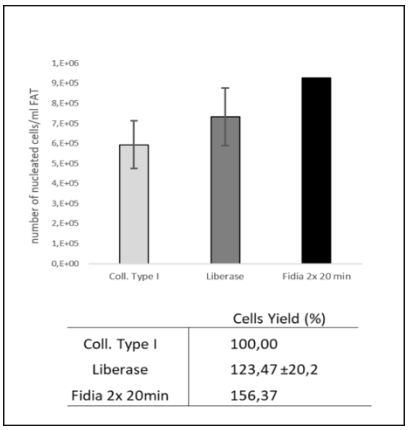

	Cells Yield (%)
Coll. Type I	100,00
Liberase	123,47 ±20,2
Fidia 2x 20min	156,37

Figure 37: Evaluation of the efficiency of FC by doubling the enzyme concentration and decreasing the incubation time to 20-min

To determine whether FC preserves the integrity of the membrane and surface proteins, the expanded ADAS (around 250,000 cells) from passage 4 were digested again with all three collagenases for 30 min. They were checked for viability at p0 with trypan blue (Figure 38. C), followed by growing again to check CFU (2 weeks), MTT test (after 24h) and to observe population doubling time. The number of colonies was the highest for the 2x FCDC, whereas liberase digested cells produced fewer colonies—figure 38. C shows the trypan blue viability test of cells pre- and post-digestion with enzymes at P0. The cells derived after FC digestion were more viable and comparable to the others. MTT was performed to check cell viability, proliferation, and cytotoxicity. The liberase digested cells (Figure 38. F) were also less viable and more toxic than others. However, Fidia 0.5x and 1x were almost similar viable. The colony-forming unit test also showed (Figure 38. A, B) that the cells treated with a 2x concentration of FC gave a maximum number of colonies and efficiency in comparison with the others. The cell proliferation capacity (Figure 38.D) and population doubling time (Figure 38. E) were highest for the liberase digestion, which means FCDC took more time to double than liberase & type 1 digestions. All the results were compared to control (CTR). The differences are all statistically significant vs the CTR.

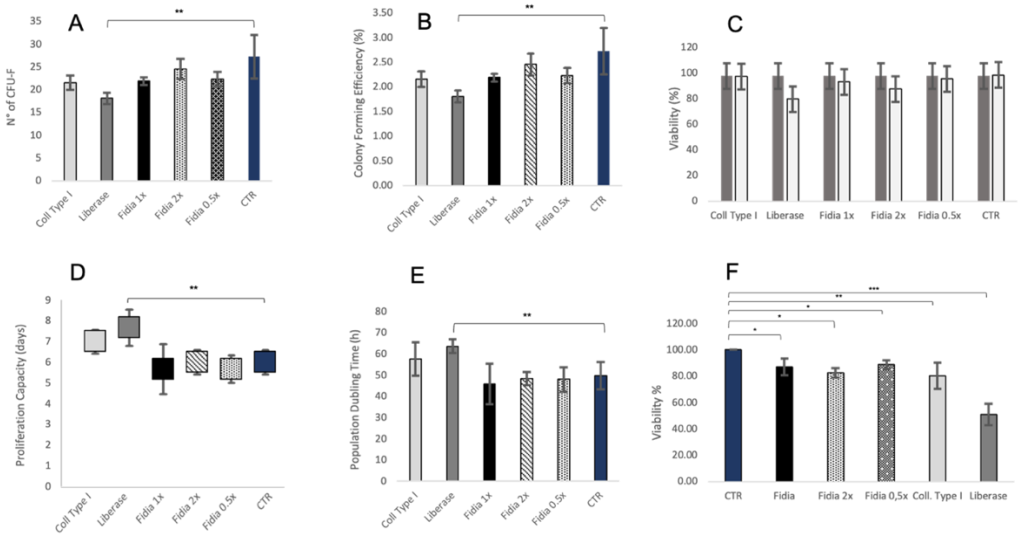

Figure 38. Evaluation of expanded ADAS treated with collagenases for 30 min A. Colony-forming unit assay after 14th day; B. Colony-forming efficiency of the different collagenases after two weeks; C. Trypan Blue viability assay after 30' of digestion of expanded ADAS; D. Proliferation capacity of the expanded cells; E. Population doubling time analysis; F. Cell viability checked with MTT assay for the expanded digested ADAS

Figure 39. A shows the viability of cells with trypan blue after 20-minute digestion of the expanded ADAS. The number of colonies increased for all three concentrations of the FCDC and decreased for the Liberase and type-1 collagenase digestions. For the viability check with trypan blue (Figure 39. C) and MTT (Figure 39. F), the 0.5x and 1x digested cells were more viable. However, the 2x FCDC was a little less viable than the others.

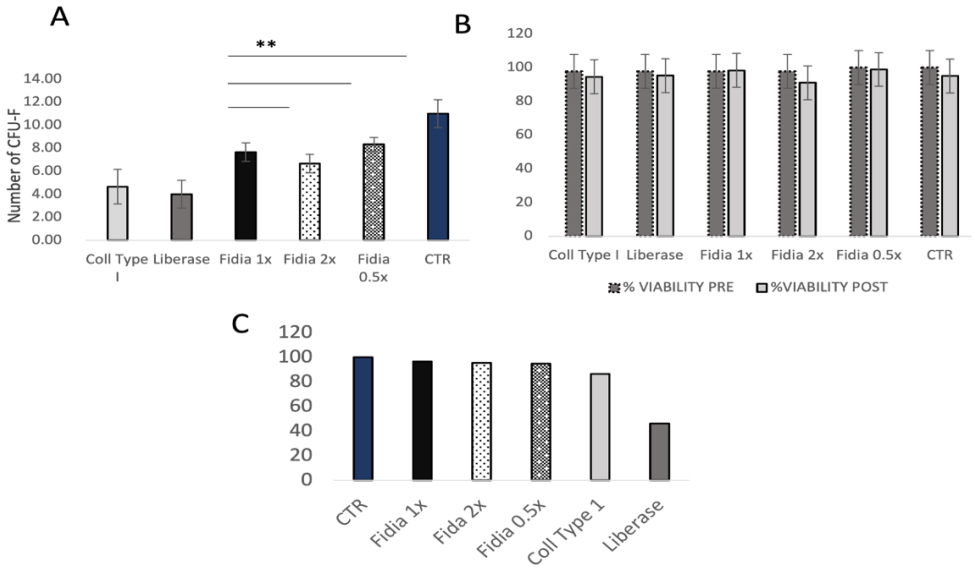

Figure 39. Evaluation of expanded ADAS treated with collagenases for 20 min. Figure A shows the difference among the CFU-F, while Figure B shows the treated cells' pre and post digestion viability. Figure C is the MTT viability test result.

N = 3 patient's lipoaspirate was mixed and was treated with all the three kinds of collagenases; for the Fidia collagenase, three different concentrations (0.5x, 1x, 2x) were considered to compare the result. Figure 39 suggests that the viability was highest for the ADSC was highest for FCDCs than the others, and in the case of Liberase, it was the lowest.

Figure 40. Viability of mixed ADSC; A. The bar represents the actual percentage of viability of cells from mixed ADAS compared to other digestions B. Representative table of the percentage of viability of the cells digested with all three different concentrations of FC, type 1 and Liberase

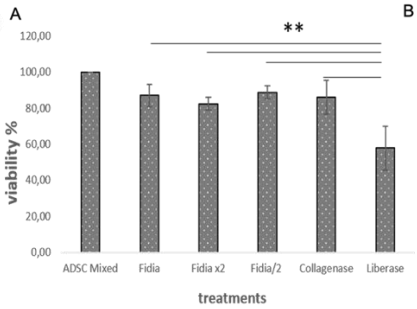

ADSCs Mixed	100,00 ± 0
Fidia	87,07 ± 6,14
Fidia x2	82,40 ± 3,60
Fidia/2	88,80 ± 3,45
Collagenase	85,96 ± 9,33
Liberase	57,87 ± 12,16

The colour generation in the multi-wells after MTT assay was seen clearly in different wells for different enzymes. The table shows that FCDC after 20-minute of type-1 was more viable than that of the 30-min digestion, whereas, in the case of liberase, it was the opposite.

	20 minutes	30 minutes
ADSC Mixed	100,00 ± 0	100,00 ± 0
Fidia	96,45 ± 9,68	87,07 ± 6,14
Fidia x2	95,42 ± 6,23	82,40 ± 3,60
Fidia/2	94,78 ± 10,33	88,80 ± 3,45
Collagenase	86,46 ±14,84	80,31 ± 9,33
Liberase	46,16 ± 6,35	50,99 ± 8,03

Table 5: MTT assay; Viability (%) after 24h

While comparing the MTT viability results, it was observed that viability of the mixed ADSCs was highest for both 20 and 30 mins of digested cells while Liberase treated cells were least viable (Table 5)

4

Discussion

Although the enzymatic method, which has been used for 40 years in the laboratory to isolate cells, is the best method available, it is not compatible with clinics due to the long-lasting procedure and legal restrictions [48, 55-62]. Furthermore, it destroys the stem-cell niche, which is the microenvironment surrounding the stem cell, allowing interactions with neighbouring cells and promoting cell survival, proliferation, and differentiation [63-64]. Many efforts have been made to establish a mechanical method with a yield comparable to collagenase. Unfortunately, so far, none of them has exhibited the same performance. In addition, to use it in clinics, the method must be fast, safe, and standardised. Rigenera® addresses all these requirements. This technology allows the mechanical disaggregation of a small amount of adipose tissue previously harvested from the same patient. Rigenera® technology provides selective filtration, applying a filter of 80 μm, and the product is collected from the reservoir located at the bottom of the Rigenera® device, making it a safe and closed device. The Rigenera® device can be used for various problems, such as ulcers, alopecia, and post-traumatic skin defects [65-70].

The product obtained with this technology consists of fragments of connective tissue (collagen and elastin fibres) and isolated cells (Figure 4), among which mesenchymal-like cells are considered the primary agent responsible for the regenerative potential of the product [37-38]. Therefore, this study was conducted to characterise cell viability, morphology, and immunophenotyping of the mesenchymal-like cells obtained with the Rigenera® device.

We optimised the operating time, demonstrating that, to obtain a higher yield of cells, the best choice is the mechanical disaggregation of adipose tissue for 60 s. Indeed, processing the adipose tissue by the ceramic blades contained in Rigenera® for 60 s, we obtained a higher number of cells with better replication capacity compared to the 30 and 45 s treatments. We hypothesise that a short sample processing time is not enough to produce the proper mechanical disaggregation of fat tissue, allowing only a partial extraction of cells contained within it. These limitations could affect the clinical product's efficiency.

We also proved that Rigenera® treatment does not affect the cell morphology since the cell appearance under the microscope was not altered and was preserved over time (passages higher than the ninth). In addition, when plated in a flask, the cells obtained by the Rigenera® device were able to grow, forming clusters, which is a typical feature of mesenchymal cells, named the colony-forming capacity. Moreover, the differentiation potential of cells extracted with the Rigenera® device towards adipogenic, osteogenic, and chondrogenic lineages was demonstrated.

Unfortunately, the cell yield and, thus, the meantime of confluence was lower than that of the enzymatic method. Still, the replication rate was comparable at higher passages (from the tenth passage). The typical mesenchymal stem cell markers (CD105, CD90, CD73, CD44, and CD29) and the hematopoietic markers (CD45 and CD34) were preserved like the collagenase method over time. Therefore, no alteration in the ASC phenotype was observed.

Moreover, an average expression of the MUSE-SSEA3 antigen was detected. MUSE cells are a subpopulation of mesenchymal stem cells, double-positive for the mesenchymal marker CD105 and the pluripotency marker stage-specific embryonic antigen-3 (SSEA-3), discovered by Kuroda in 2010 [41]. They are known to be pluripotent, i.e., they can differentiate into cells belonging to the three germ layers and can endure stress, such as oxygen deprivation. They could be considered the primary agent responsible for regeneration and reparation [41, 42]. Together with multipotent cells, MUSE cells allow a significant advantage in tissue regeneration, as MUSE cells are present in various connective tissues. This provides safety and ethical benefits for clinical applications.

Finally, since surgeons harvest adipose tissues from various anatomical districts [71], we compared the cells' regenerative potential obtained from the thigh and abdomen. Although subcutaneous regions are considered the most appropriate sites to harvest adipose tissue[71,72], we demonstrated the ASC yield (in terms of the number of cells extracted, replicative rate, and number of CFU) from the thigh was higher than that from the abdomen, using the Rigenera® device. In addition, we found that the progenitor cell frequencies (the ability to form colonies) were higher in ASCs extracted from the thigh. These ASCs could produce more colonies containing more significant numbers of cells compared to those from the abdomen. Moreover, the immunophenotypic analysis confirmed that a much higher yield of ASCs was obtained from thigh samples. However, both the samples (thigh and abdomen) expressed a phenotype profile specific for ASC markers.

Moreover, a difference between cells obtained from the thigh and abdomen was appreciable in cell morphology: abdomen cells were flatter and more widely spread in the flask. This large and flat cell morphology is reflected in the lower replication rate (number of cells at confluence) and the more significant time required to reach confluence than cells extracted from the thigh. These results demonstrated the characteristics of senescent cells [73]. These differences could be since the thigh is often a virgin extraction site. The adipose tissue remains more uniform, with a thinner collagen matrix than adipose tissue obtained from the abdomen. This results in a tissue that is easier to process with the Rigenera® device.

Regenerative medicine involves several activities to repair, regenerate, or substitute damaged tissue or organs using *ex vivo* manipulated cells [117]. We wanted to investigate a well-known commercial system (Rigenera®) to obtain

SVF by mechanical disruption of canine adipose tissue without substantial manipulations comparing, in addition to the obtained micrograft to ASCs.

Before the procedure, blood and any cellular debris are removed to depurate the adipose tissue, preventing inflammatory activity, and maintaining graft sustainability via various enzymatic and mechanical techniques. Typically, collagenase enzymatic digestion is the most common and effective method available. However, it is not without limitations.

The enzymatic digestion via collagenase can eradicate the stem-cell niche competent in relating to the surrounding cell environment and enhancing cell viability, expansion, and differentiation [118]. Furthermore, GMP guidelines of the European Parliament and Council (EC Regulation no. 1934/2007) strictly indicate the use of techniques with minimal cell manipulation within a clinical context, thus excluding the adoption of enzymatic methods.

Accordingly, many efforts have been made to develop medical devices able to disaggregate tissue mechanically. The Rigenera® (HBW, Turin, Italy) system presents a disposable, motor-driven sterile device that deserves to be considered [119]. Injectable micrografts are instantly produced and consist of fragments of adipose tissue with a dimension of 80 μm capable of stimulating the regeneration of damaged tissue [119].

This study thus was focused on the *in vitro* characterization between the proposed treatment and the gold standard enzymatic digestion in terms of cell yield, CFE, proliferation capacity, immunophenotyping, multipotency and anti-inflammatory activity. Additionally, adipose tissue samples were harvested from two anatomical regions (the lumbar and the thigh) to evaluate differences in the regenerative potential.

Our results showed that the cell yield, and thus the number of CFU, the proliferation capacity, and the time required by cells to duplicate, were higher for ED cells compared to Rigenera® cells, pointing out the main limitation of the treatment. Nevertheless, this restriction was not due to the Rigenera® technology alone, but as reported in literature [95, 96], all non-enzymatic methods show lower cell recovery than enzymatic methods.
Some authors [96, 120] clarified that the differences might be partly related to the SVF cell site within adipose tissue in the perivascular niche. Similar cell release from the perivascular niche is not commonly observed within the mechanical procedures of SVF isolation since the enzymatic method does not allow for complete disruption of the extracellular matrix due to the use of proteolytic enzymes digesting the extracellular matrix and withal consolidating

the adipose tissue. In light of these findings, the setting and application of an appropriate protocol are imperative.

Besides, in terms of cell yield, a slight difference between cells obtained from the lumbar and the thigh regions was detected from both ED and Rigenera® in favour of the thigh part, most likely attributable to the thigh being a new reserve site regarding extraction and to the uniformity of the adipose tissue and a thinner collagen matrix, consequently yielding more accessible tissue [114]. We confirm how cells extracted via the Rigenera® device may easily differentiate. Results showed the comparable ability of both ED and Rigenera® cells to differentiate to mesodermal lineages through staining with oil red o, Alizarin red and Alcian blue for osteo, adipogenic and chondrogenic recognition, respectively. For this reason, multipotent cells will efficiently regenerate and repair tissue. Moreover, the immunophenotypic analysis attested that cell from Rigenera® was highly positive for the mesenchymal stem cells markers CD73 and CD90, low positive for hematopoietic CD45 and CD34, and negative for MHC class II antibodies, playing a role in immune responses.

Finally, the study did not show statistically significant differences between the lumbar and the tight regions from which samples were collected except for the mentioned cell yield.

Autologous, adipose tissue-derived micrograft, obtained with the Rigenera® technology, represents an innovative approach that introduces an entirely novel concept in regenerative medicine, showing minimal tissue manipulation's safety and potential benefits. The impressive *in vitro* outcomes demonstrated that this technology might be used to restore functionality and relieve pain in dogs with severe OA. Additionally, such a procedure is a straightforward, rapid, and sustainable one-step method (as well as being a minimally invasive and secure option) compared to the enzymatic process, which, albeit consolidated as a method for 40 years, remains inoperable in clinical settings due to the time-consuming applications, legal limitations, and scientific constraints. Our future work will involve an *in vivo* experimental study to perform the dog model's clinical, eco-graphic, and sonographic evaluations.

A relevant aspect of the Hy-Tissue SVF product study was the detection of micro-fragments in the SVF pellet. Indeed, the morphological characterisation of the SVF product revealed the presence of the micro-fragments of connective tissue that preserved part of the original architecture of adipose tissue with multiple cell types but without mature adipocytes. Only a few small adipocytes (probably pre-adipocytes were observed by the SEM microscopy). We also found the presence of

preserved micro-vessels within the micro-fragments with the perivascular niche left unaltered. We believe that the presence of the perivascular cells could represent an essential feature of the Hy-Tissue SVF product since perivascular cells have MSC *in vivo* [139]. Furthermore, Micro-grafts of fat could have a superior therapeutic potential for tissue repair and regeneration compared to enzymatically extracted ADSCs by the enhanced secretory activity of growth factors and cytokines of the cells [140].

Moreover, ADSC in their niche prolong the long-term survival of their ADSC content and induces a long-lasting anti-inflammatory activity [141]. Other authors suggest that endothelial cells and ADSC in the SVF could be advantageous since they can cause proliferative, pro-angiogenic and vasculogenic effects through paracrine mechanisms and cell-cell contact [142-146]. Additionally, the fat of the extracellular matrix plays an essential role in the effectiveness of some indications, such as the healing of chronic and acute wounds promoting the healing by the differentiation of multipotent cells into fibroblasts [147, 148]. Moreover, the employment of autologous micro-fragmented adipose tissue with SVF in patients with knee OA increases the levels of GAG in cartilage, reducing pain and improving movement abilities [142].

To control variables that could affect the cell yield, only a narrow range of ages was included in our study for women. Besides, lipoaspiration was done by the same physician and using the same technique. It is known that intrinsic factors such as anatomic donor site, harvesting technique, and age can affect the cell yield of the SVF product [149-151]. A normal lipoaspirate can yield between 1×10^5 up to 1×10^6 nucleated cells/ml processed lipoaspirate [152-157], which represents a high variability, probably due to the nature and complexity of adipose tissue and intrinsic factors. Besides, the yield of ADSC from an enzymatic digestion process can be between 1–5% of the total nucleated cells, depending on the donor site [158]. However, we found a high variability between fat samples regarding cell content and yield even controlling these variables.

In our study, we recovered up to 25% of the total stromal vascular fraction (131.200 cell/ml fat) when both fractions (free cells and micro-fragments) were considered, compared to the stromal vascular fraction obtained by enzymatic digestion, suggesting that the process of the Hy-Tissue SVF system was highly efficient for separating nucleated stromal cells. Other mechanical methods produce similar or less nucleated cells yield than Hy-Tissue SVF. For instance, Markarian et al. examined a non-enzymatic procedure with centrifugation that recovered near 10,000 nucleated cells/ml of lipoaspirate [159]. Baptista et al. reported a similar proportion to our results of adherent cells obtained by enzymatic digestion vs the mechanical manual method evaluated (10:1) [160]. Shah et al. evaluated a similar

method using PBS instead of RBC lysis buffer and reported an average of 25,000 ADSC/ml of processed lipoaspirate [161]. Raposio et al. isolated about 125,000 nucleated cells per ml of processed lipoaspirate. About 5% of these cells were probably progenitor cells detected by flux cytometry but not confirmed by CFU-F, which, in turn, is a more reliable technique for identifying multipotent cells [162].

Due to the high variability in methods and results [163], we considered that the most reliable and best comparator were the results obtained for the FAT-ED of each lipoaspirate rather than the results of other described adipose-processing platforms. In our study, the mean CFU-F yield obtained in the SVF was ten times lower compared to CFU-F yield obtained by the enzymatic digestion of fat tissue, which is a reasonable yield value considering that mechanical forces are not efficient for releasing cells attached to their natural matrix niche [164] and that cells can be retained in the phase of condensed adipose tissue (Coleman-like) formed after centrifugation. However, this result does not necessarily imply an inferior potential of mechanical SVF for therapeutic purposes. For instance, the doses of expanded ADSCs used in clinical trials are much higher than any system producing SVF [165, 166.] However, both products (ADSCs and SVF) have shown similar profile improvements in pain, function, stiffness, and quality of life in comparative clinical trials, suggesting that the ADSCs dose is not the most relevant variable for obtaining a therapeutic effect [135, 167]. *In vitro*, ADSCs obtained by mechanical dissociation proved to have immunosuppressive properties like those obtained by enzymatic digestion[168]. In a randomised clinical trial, SVF obtained with the Hy-Tissue SVF kit was an effective treatment for recalcitrant Achilles tendinopathy [169]. The previous study also demonstrated the immunomodulatory potential of SVF in co-culture systems with activated lymphocytes by the reduction of secretion of IL-6.

It is well known that CD34 is a marker of the stromal cell-containing population[128]. In this sense, the detection of CD34+ expression in the free cell fraction of SVF, together with CD73 and CD105, the latter two being classical MSC markers [170], suggests that the free cells of this fraction contain not only nucleated blood cells of hemopoietic origin but also stromal cells. Moreover, in the free cells fraction of SVF, cells are positive for the endothelial marker (CD146). Together with stromal cells, endothelial cells are crucial for the long-term viability and proliferation of MSC [143, 144]. Subsequent studies should be devoted to characterising enzymatic digestion, which probably would have provided a more reliable profile of the total type of cells of the Hy-Tissue SVF product, such as pericytes fraction, which was very low in our analysis.

The main limitations of our study were the small patient population and the no discrimination of peripheral blood cells from the cell's free fraction. However,

considering that the cell-free fraction was around 30% of the total nucleated cell content of SVF and that near 10% were positive for CD34, we estimated that the blood contamination was less than 25% of the whole cells, which in our opinion, is not relevant considering the high variability of the adipose tissue. Finally, although this study characterised the product at a morphological, structural, and cellular level, further application studies aimed to investigate the product's functionality are necessary.

We demonstrated that our experimented innovative device allows the isolation of stromal vascular fraction in free cells and micro-fragments of connective tissue containing stromal cells and extracellular matrix, making this product of potential interest in regenerative medicine.

A histological examination from the Hy-Tissue SVF product confirms the presence of newly formed adipose tissue and micro-vessels. HA1+SVF stimulates *in vivo* adipogenesis after 14 days of injection, whereas HA1 were reabsorbed within seven days. HA2 were reabsorbed within seven days. HA2+SVF stimulates *in vivo* adipogenesis after 14-30 days from the injection. Histological examination confirms the presence of newly formed adipose tissue interposed with the collagen matrix.

No evidence was found of newly formed adipose tissue after 14 days from the injection of HA+ASC (Figure 26, top left). But mice injected with only HAs were shown to have some fat like signs as ‘dense white’ form, which was confirmed when a spot (Red box, Figure 26) was analysed and was compared with literature. The subcutaneous injection of micro-fragments of connected adipose tissue enriched with SVF (product of Hy-Tissue SVF kit) promotes *in vivo* adipogenesis. Hyaluronic acid supports adipogenic stimulation *in vivo* and stimulates adipogenic differentiation *in vitro*. No evidence of newly formed adipose tissue was found after HA+ASC. HA3+SVF stimulates *in vivo* adipogenesis after seven days from the injection. HA3 was reabsorbed within seven days. Histological examination confirms the presence of newly formed adipose tissue and micro-vessels.

Nanofat is a well-described and straightforward procedure that allows the injection of small adipose tissue volumes. The product obtained is an emulsion fat rich in viable cells avoiding expansion or enzymatic treatments. The emulsification procedure reduces the size of adipose fragments harvested by liposuction, by a delicate filtration, obtaining an immediately injectable product [199]. Thanks to its fluid consistency, surgeons promoted nanofat for face treatments, rejuvenation, volume restoration, wrinkles, hypertrophic and atrophic scars, and defects correction [178-181].

Hy-Tissue Nanofat is a new, simple system that drastically reduces adipose tissue processing time and guarantees regenerative units' survival. The device reduces the size of the fat micro-fragments obtained after emulsification by shuffling the lipoaspirates 30 times between two connected syringes and filtering the emulsified adipose tissue through a membrane of 120 µm. In this study, a deep characterisation has been performed, and the abundance of regenerative cells has been described.

Morphological analysis of the fat emulsion shows the presence of lipid droplets of different dimensions, mainly ranging between 60 and 100 µm, making the product easy to inject into the desired location with high precision and suitable for injection under challenging times areas with thin skin.

In vitro results obtained with the Hy-Tissue Nanofat system have been compared with the results obtained through enzymatic digestion (collagenase type I), considered the standard gold technique to purify mesenchymal stem cells [200-201], and with the enzymatic digestion of filtered emulsion. Specifically, this last procedure was performed to evaluate the total amount of regenerative units, in terms of mesenchymal stem cells, that contribute to the tissue remodelling, rejuvenation and regeneration, describing the real regenerative potential of the Hy-Tissue Nanofat product.

We were studying the Hy-Tissue nanofat device, and we saw that the cellular yield of the Hy-Tissue Nanofat product resulted in about 8% (N-ASC), which increased by 29% after the enzymatic digestion of the emulsion (N-ED-ASC), suggesting that the system was highly efficient for extracting nucleated cells. Indeed, the number of N-ED-ASC resulted in $1.25x10^5 \pm 4.65\ x10^4$ cells employing 10 ml of lipoaspirate not so far from the results obtained in Tonnard et al. 2013 [175] for 100 ml of lipoaspirates.
Subsequently, duplication and clonogenic assays have been performed to characterise units presented into the Hy-Tissue Nanofat product. N-ASC's growth rate and clonogenic capability resulted lower than ED-ASC, which agrees with cellular yield results since mechanical emulsification is not as efficient as an enzymatic procedure to extract cells from their collagen matrix [193, 202]. Nevertheless, comparing the CFU-F assay of N-ED-ASC with N-ASC, the colony yield increased 11-times. It is only 2.6 times lower than CFU-F obtained with ED-ASC, reproducing the real clonogenic potential of the Hy-Tissue Nanofat product.

Previous studies established that $CD34^+$ cells represent a stem cell population with higher proliferative capacity. According to the literature, the immunophenotypic analysis of N-ASC reveals 3.37 ± 1.67% of CD34+ expressing markers. Tonnard et al. have reported 4.5 to 6.5% of $CD34^+$ cells in nanofat product. Moreover, a non-statistically significant difference has been noted between the treatments. When

cultured, cells acquired a mesenchymal solid stem cell phenotype, increasing the expression of specific surface markers (CD73, CD105 and CD 29) and confirming phenotype maintenance. N-ASC have also been tested for the capacity to differentiate in three mesenchymal cell types: adipocytes, osteocytes, and chondrocytes. The differentiation ability was evaluated after 5 and 10 days from specific media induction. N-ACS can efficiently differentiate starting from the 5th day, underling a higher differentiative potential comparable with cells enzymatically extracted. Usually, the uptake of lipid droplets, a marker of adipogenic differentiation, is revealable between 10 and 14 days after media stimulation [175, 182, 192, 193], while the calcification and proteoglycan matrix formation are detectable after 21 days [182, 192, 193].
In addition, N-ASC were immunophenotypically analysed for SEEA3 expression as a specific marker for a subpopulation of mesenchymal stem cells called MUSE cells [194-198, 203]. These cells are composed of pluripotent mesenchymal stem cells, able to migrate in damaged areas, as described in different preclinical and clinical models [204-206]. The results showed that N-ASC expressed 25.5 ± 6.5% of SEEA3 marker, while ED-ASC was 0.5 ± 0.2%. This difference might be due to mechanical manipulation of fat tissue since MUSE cells are mainly expressed after severe cellular stress conditions [192, 197]. These cells differentiate in numerous tissues, not only of mesenchymal origin, in a short time and could support the results obtained with differentiation assay. The use of fat emulsion enriched MUSE cells in regenerative medicine could represent a novel aspect, increasing the treatment efficacy and the recovery time. A deeper analysis is necessary to understand the mechanism that undergoes high differentiative potential and MUSE expression.

These results indicate Hy-Tissue Nanofat as a rapid, standardised, efficient system able to produce fat-emulsion rich in viable, proliferative, and multipotent ASC.

We have optimised these three devices (Rigenera, Hy-Tissue SVF and Hy-Tissue nanofat) to produce the re-injectable product from adipose tissue for autologous fat grafting. Products from all these devices have a positive result *in vitro*. However, the device 'nanofat' took comparatively less time to give us the re-injectable effect, and the handling was more accessible too.

Adipose tissue is unique as a source of MSCs. Historically, the fat was relegated to energy storage and structural supportive roles. However, enzymatic dissociation and centrifugation of adipose, yielding a single-cell suspension, called the stromal vascular fraction (SVF), allowed the characterisation of its cellular components, including the adipose-specific MSC: the adipose-derived stromal cell (ASC) [220]. One gram of adipose tissue obtained with minimally invasive liposuction yields approximately 5000 putative stem cells, which is 500 times greater than the number of stem cells isolated from 1 g of BM [221]. Thus, adipose offers autologous

mesenchymal progenitors with multilineage differentiation potential in unrivalled quantity, accessibility, and expandability. In 1964, Martin Rodbell described the first enzymatic dissociation of murine adipose tissue into a single-cell suspension. Since then, many studies have demonstrated reproducible collagenase digesting and isolating cellular fractions either intact (and subsequently minced) or aspirated with tumescent liposuction. The uncultured SVF consists of leukocytes, erythrocytes, endothelial cells, perivascular cells, a particular interest, putative stem, and progenitor cells.

Spindle-shaped cells attach and expand when the heterogeneous SVF cells are cultured in plastic. These cells, selected by plastic adherence, are ASCs [218.] Previous studies have reported using the enzymatic digestion of lipoaspirate material to separate the SVF from adipocytes before using both the SVF and adipocytes as part of the autologous graft. Typically, the enzymatically isolated SVF is added to adipocytes that have not been enzymatically digested (a reserved portion of lipoaspirate). Still, reports have described the use of collagenase-digested adipocytes as part of the graft.

In their practice using collagenase-digested adipocytes to surgically correct infraorbital dark circles, collagenase digestion of the adipose tissue increased the contouring ability of the fat graft by making it a 'more liquid filler' they reported safe and productive results. Although SVF/ adipocytes harvested from collagenase-digested lipoaspirate is not currently approved by the United States Food and Drug Administration (FDA), collagenase has gained acceptance in the treatment of Dupuytren contracture and Peyronie disease. Furthermore, with the increasing use of enhanced fat grafting, specifically in large volume reconstructions and in cases with patients who have minimal adiposity, it will be essential to study the effect of collagenase digestion on the adipocytes. In such circumstances, it may be necessary to use all the fat harvested from the patient, including that used to obtain SVF, to have adequate volume for grafting. Future studies on collagenase-digested adipocytes and SVF may provide grounds for FDA approval of collagenase-isolated SVF and adipocytes in fat grafts.

The *in vitro* effect of collagenase digestion on adipocytes and SVF for both human and murine adipose tissue.[40] We found that increasing the duration of collagenase digestion is detrimental to both the SVF and the adipocytes, causing decreases in the viability of both interstitial cells (which comprise the SVF compartment) and adipocytes. Collagenase digestion affected both adipocyte and interstitial cell viability in a dose- and time-dependent manner. For human tissue, the viability of adipocytes and SVF was significantly decreased when collagenase digestion times exceeded 50 min. Although our *in vitro* studies were the first to indicate the potentially detrimental effects of collagenase digestion on SVF and adipocytes, it is imperative to consider the impact of collagenase digestion on *in vivo* graft

survival. To our knowledge, no studies have examined the effect of collagenase digestion on *in vivo* graft survival.

Tissue regeneration includes delivering specific types of cells or cell products to injured tissues or organs to restore tissue and organ function. Stem cell therapy has drawn considerable attention since transplantation of stem cells can overcome the limitations of autologous transplantation of a patient's tissues; however, it is not perfect for treating diseases.

Our objective of this experiment was to standardise an enzyme (FC) which, after digestion, maintain the surface protein of the cells similar or better than the typical Collagenase type-1 and Liberase (Company name of Liberase that we used) and preserves the natural regenerative content of ADAS by maintaining the intact cell membrane within a short period and easy to be used.

In this study with new collagenase, we demonstrated that the product obtained after the further Fidia Collagenase digestion could be compared to the existing two other collagenases because it has isolated live and proliferative adipose-derived mesenchymal stem cells, which could replace the type 1 collagenase. Furthermore, it also has the potential to be promising in aesthetic and regenerative medicine, which enhances its possible use for autologous fat grafting to be used by plastic surgeons in their medical purposes.

Ethics statement

Written consent was taken from all the patients undergoing liposuction to avail the adipose tissue for our experiment.

Bibliography

1. Birbrair A, Zhang T, Wang ZM, Messi ML, Enikolopov GN, Mintz A, Delbono O, Role of pericytes in skeletal muscle regeneration and fat accumulation, Stem Cells and Development 22 (16), 2298–314, 2013.

2. Carlson BM, Principles of Regenerative Biology, Elsevier Inc. p. 400, 2007.

3. Gabor MH, Hotchkiss RD, Parameters governing bacterial regeneration and genetic recombination after fusion of Bacillus subtilis protoplasts, Journal of Bacteriology, 137 (3), 1346–53, 1979

4. Hussein Abdelhay El-Sayed Kaoud (June 6th, 2018). Introductory Chapter: Concepts of Tissue Regeneration, Tissue Regeneration, IntechOpen, 2018 (https://www.intechopen.com/chapters/61159)

5. Rippa AL, Kalabusheva EP, Vorotelyak EA. Regeneration of Dermis: Scarring and Cells Involved. Cells; 8(6):607, 2019

6. Driskell, R.R, Lichtenberger, B.M, Hoste, E.; Kretzschmar, K.; Simons, B.D.; Charalambous, M.; Ferron, S.R.; Herault, Y. Pavlovic, G. Ferguson-Smith, A.C., et al. Distinct fibroblast lineages determine dermal architecture in skin development and repair. Nature 504, 277–281 2013.

7. Sorrell, J.M.; Caplan, A.I. Fibroblast heterogeneity: More than skin deep. J. Cell Sci., 117, 667–675, 2004

8. Sorrell, J.M.; Baber, M.A.; Caplan, A.I. Clonal characterisation of fibroblasts in the superficial layer of the adult human dermis. Cell Tissue Res, 327, 499–510, 2007

9. Rognoni, E.; Gomez, C.; Pisco, A.O.; Rawlins, E.L.; Simons, B.D.; Watt, F.M.; Driskell, R.R. Inhibition of β-catenin signalling in dermal fibroblasts enhances hair follicle regeneration during wound healing. Development, 143, 2522–2535, 2016

10. Woodley, D.T. Distinct fibroblasts in the papillary and reticular dermis: Implications for wound healing. Dermatol. Clin, 35, 95–100, 2017

11. Xue, M.; Jackson, C.J. Extracellular matrix reorganization during wound healing and its impact on abnormal scarring. Adv. Wound Care (New Rochelle), 4, 119–136, 2015

12. Kruglikov, I.L.; Scherer, P.E. Dermal adipocytes: From irrelevance to metabolic targets? Trends Endocrinol. Metab., 27, 1–10, 2016

13. Festa, E.; Fretz, J.; Berry, R.; Schmidt, B.; Rodeheffer, M.; Horowitz, M.; Horsley, V. Adipocyte lineage cells contribute to the skin stem cell niche to drive hair cycling. Cell, 146, 761–771, 2011

14. Matsumura, H.; Engrav, L.H.; Gibran, N.S.; Yang, T.M.; Grant, J.H.; Yunusov, M.Y.; Fang, P.; Reichenbach, D.D.; Heimbach, D.M.; Isik, F.F. Cones of skin occur where hypertrophic scar occurs. Wound Repair Regen., 9, 269–277, 2001

15. Marangoni, R.G.; Korman, B.D.; Wei, J.; Wood, T.A.; Graham, L.V.; Whitfield, M.L.; Scherer, P.E.; Tourtellotte, W.G.; Varga, J. Myofibroblasts in murine cutaneous fibrosis originate from adiponectin-positive intradermal progenitors. Arthr. Rheumatol., 67, 1062–1073, 2015

16. Plikus, M.V.; Guerrero-Juarez, C.F.; Ito, M.; Li, Y.R.; Dedhia, P.H.; Zheng, Y.; Shao, M.; Gay, D.L.; Ramos, R.; His, T.C.; et al. Regeneration of fat cells from myofibroblasts during wound healing. Science, 355, 748–752, 2017

17. Suszynski TM, Sieber DA, Van Beek AL, Cunningham BL. Characterization of adipose tissue for autologous fat grafting. Aesthet Surg J., 35(2), 194-203, 2015

18. Khorasani M, Janbaz P. Clinical evaluation of autologous fat graft for facial deformity: a case series study. J Korean Assoc Oral Maxillofac Surg., 47(4), 286-290, 2021

19. Gentile P., Casella D., Palma E., Calabrese C. Engineered Fat Graft Enhanced with Adipose-Derived Stromal Vascular Fraction Cells for Regenerative Medicine: Clinical, Histological and Instrumental Evaluation in Breast Reconstruction. J. Clin. Med., 8, 504, 2019

20. Yuan Y., Zhang S., Gao J., Lu F. Spatial structural integrity is important for adipose regeneration after transplantation. Arch. Dermatol. Res., 307(8), 693–704, 2015

21. Özkaya Ö., Egemen O., Barutça S.A., Akan M. Long-term clinical outcomes of fat grafting by low-pressure aspiration and slow centrifugation (Lopasce technique) for different indications. J Plast Surg Hand Surg., 47(5), 394–398, 2013

22. Philips B.J., Marra K.G., Rubin J.P. Adipose stem cell-based soft tissue regeneration. Expet Opin. Biol. Ther., 12(2), 155–16, 2012

23. Coleman S.R., Saboeiro A.P. Primary breast augmentation with fat grafting. Clin. Plast. Surg., 42(3), 301–306, 2015

24. Smith P., Adams W.P., Lipschitz A.H. Autologous human fat grafting: effect of harvesting and preparation techniques on adipocyte graft survival. Plast. Reconstr. Surg., 117(6), 1836–1844, 2006

25. Barzelay A., Levy R., Kohn E. Power-assisted liposuction versus tissue resection for the isolation of adipose tissue–derived mesenchymal stem cells: phenotype, senescence, and multipotency at advanced passages. Aesthet. Surg. J, 35(7), NP230–NP240, 2015

26. Keck M., Kober J., Riedl O. Power assisted liposuction to obtain adipose-derived stem cells: impact on viability and differentiation to adipocytes in comparison to manual aspiration. J. Plast. Reconstr. Aesthetic Surg, 67(1), e1–8, 2014

27. Shridharani S., Broyles J., Matarasso A. Liposuction devices: technology update. Med. Dev. Evid. Res.,7,241, 2014

28. Chung M.T., Zimmermann A.S., Paik K.J. Isolation of human adipose-derived stromal cells using laser-assisted liposuction and their therapeutic potential in regenerative medicine. Stem Cells Transl Med.2(10), 808–817, 2013

29. Yin S., Luan J., Fu S., Wang Q., Zhuang Q. Does water-jet force make a difference in fat grafting? In vitro and in vivo evidence of improved lipoaspirate viability and fat graft survival. Plast. Reconstr. Surg.135(1):127–138, 2015

30. Mazzola, R.F.; Cantarella, G.; Torretta, S.; Sbarbati, A.; Lazzari, L.; Pignataro, L. Autologous fat injection to face and neck: From soft tissue augmentation to regenerative medicine. Acta Otorhinolaryngol., 31, 59–69, 2011

31. Conti, G.; Bertossi, D.; Dai Prè, E.; Cavallini, C.; Scupoli, M.T.; Ricciardi, G.; Parnigotto, P.; Saban, Y.; Sbarbati, A.; Nocini, P. Regenerative potential of the Bichat fat pad determined by the quantification of multilineage differentiating stress enduring cells. Eur. J. Histochem., 62, 271–277, 2018

32. Rigotti, G.; Marchi, A.; Galiè, M.; Baroni, G.; Benati, D.; Krampera, M.; Pasini, A.; Sbarbati, A. Clinical Treatment of Radiotherapy Tissue Damage by Lipoaspirate Transplant: A Healing Process Mediated by Adipose-Derived Adult Stem Cells. Plast. Reconstr. Surg., 119, 1409–1422, 2007

33. Panettiere, P.; Accorsi, D.; Marchetti, L.; Sgrò, F.; Sbarbati, A. Large-breast reconstruction using fat graft only after prosthetic reconstruction failure. Aesthet. Plast. Surg., 35, 703–708, 2011

34. Jimi, S.; Kimura, M.; De Francesco, F.; Riccio, M.; Hara, S.; Ohjimi, H. Acceleration mechanisms of skin wound healing by autologous micrograft in mice. Int. J. Mol. Sci., 18, 1675, 2017

35. De Francesco, F.; Guastafierro, A.; Nicoletti, G.; Razzano, S.; Riccio, M.; Ferraro, G.A. The selective centrifugation ensures a better in vitro isolation of ASCs and restores a soft tissue regeneration in vivo. Int. J. Mol. Sci., 18, 1038, 2017

36. Charles-de-Sá, L.; Gontijo-de-Amorim, N.F.; Maeda Takiya, C.; Borojevic, R.; Benati, D.; Bernardi, P.; Sbarbati, A.; Rigotti, A. Antiaging treatment of the facial skin by fat graft and adipose-derived stem cells. Plast. Reconstr. Surg., 135, 999–1009, 2015

37. Hass, R.; Kasper, C.; Böhm, S.; Jacobs, R. Different populations and sources of human mesenchymal stem cells (MSC): A comparison of adult and neonatal tissue-derived MSC. Cell Commun. Signal., 9, 12, 2011

38. Rigotti, G.; Marchi, A.; Sbarbati, A. Adipose-Derived mesenchymal stem cells: Past, present, and future. Aesthet. Plast. Surg. 2009, 33, 271–273, 2009

39. Dai, R.; Wang, Z.; Samanipour, R.; Koo, K.L.; Kim, K. Adipose-derived stem cells for tissue engineering and regenerative medicine applications. Stem. Cells Int., 2016, 6737345, 2016

40. Chamberlain, G.; Fox, J.; Ashton, B.; Middleton, J. Concise Review: Mesenchymal Stem Cells: Their Phenotype, Differentiation Capacity, Immunological Features, and Potential for Homing. Stem. Cells, 25, 2739–2749, 2007

41. Kuroda, Y.; Kitada, M.; Wakao, S.; Nishikawa, K.; Tanimura, Y.; Makinoshima, H.; Goda, M.; Akashi, H.; Inutsuka, A.; Niwa, A.; et al. Unique multipotent cells in adult human mesenchymal cell populations. Proc. Natl. Acad. Sci., 107, 8639–8643, 2010

42. Wakao, S.; Kitada, M.; Kuroda, Y.; Shigemoto, T.; Matsuse, D.; Akashi, H.; Tanimura, Y.; Tsuchiyama, K.; Kikuchi, T.; Goda, M.; et al. Multilineage-differentiating stress-enduring (Muse) cells are a primary source of induced pluripotent stem cells in human fibroblasts. Proc. Natl. Acad. Sci., 108, 9875–9880, 2011

43. Wakao, S.; Akashi, H.; Kushida, Y.; Dezawa, M. Muse cells, newly found non-tumorigenic pluripotent stem cells, reside in human mesenchymal tissues. Pathol. Int. 2014, 64, 1–9, 2014

44. Coleman, S.R. Structural fat grafts: The ideal filler? Clin. Plast. Surg., 28, 111–119, 2001

45. Coleman, S.R. Structural fat grafting: More than a permanent filler. Plast. Reconstr. Surg., 118, 108S–120S, 2006

46. Lafontan, M. Historical perspectives in fat cell biology: The fat cell as a model for the investigation of hormonal and metabolic pathways. Am. J. Physiol. Cell Physiol. 2012, 302, C327–C359, 2012

47. De Francesco, F.; Mannucci, S.; Conti, G.; Dai Prè, E.; Sbarbati, A.; Riccio, M. A non-enzymatic method to obtain a fat tissue derivative highly enriched in adipose stem cells (ASCs) from human lipoaspirates: Preliminary results. Int. J. Mol. Sci., 19, 2061, 2018

48. Bianchi, F.; Maioli, M.; Leonardi, E.; Olivi, E.; Pasquinelli, G.; Valente, S.; Mendez, A.J.; Ricordi, C.; Raffaini, M.; Tremolada, C.; et al. A new nonenzymatic method and device to obtain a fat tissue derivative highly enriched in pericyte-like elements by mild mechanical forces from human lipoaspirates. Cell Transplant., 22, 2063–2077, 2013

49. Senesi, L.; De Francesco, F.; Farinelli, L.; Manzotti, S.; Gagliardi, G.; Papalia, G.F.; Riccio, M.; Gigante, A. Mechanical and Enzymatic procedures to isolate the stromal vascular fraction from adipose tissue: Preliminary results. Front. Cell Dev. Biol., 7, 88, 2019

50. Aronowitz, J.A.; Lockhart, R.A.; Hakakian, C.S. Mechanical versus enzymatic isolation of stromal vascular fraction cells from adipose tissue. SpringerPlus, 4, 713, 2015

51. Condè-Green, A.; Gontijo De Amorim, N.F.; Pitanguy, I. Influence of decantation, washing and centrifugation on adipocyte and mesenchymal stem cell content of aspirated adipose tissue: A comparative study. J. Plast. Reconstr. Aesthet. Surg., 63, 1375–1381, 2010

52. Oberbauer, E.; Steffenhagen, C.; Wurzer, C.; Gabriel, C.; Redl, H.; Wolbank, S. Enzymatic and non-enzymatic isolation systems for adipose tissue-derived cells: Current state of the art. Cell Regen., 4, 7, 2015

53. Tremolada, C.; Colombo, V.; Ventura, C. Adipose Tissue and Mesenchymal Stem Cells: State of the Art and Lipogems®Technology Development. Curr. Stem. Cell Rep., 2, 304–312, 2016

54. Maioli, M.; Rinaldi, S.; Santaniello, S.; Castagna, A.; Pigliaru, G.; Delitala, A.; Bianchi, F.; Tremolada, C.; Fontani, V.; Ventura, C. Radioelectric asymmetric conveyed fields and human adipose-derived stem cells obtained with a nonenzymatic method and device: A novel approach to multipotency. Cell Transplant. 2014, 23, 1489–1500, 2014

55. Peroni, D.; Scambi, I.; Pasini, A.; Lisi, V.; Bifari, F.; Krampera, M.; Rigotti, G.; Sbarbati, A.; Galiè, M. Stem molecular signature of adipose-derived stromal cells. Exp. Cell Res., 314, 603–615, 2008

56. Raposio, E.; Ciliberti, R.G. Clinical use of adipose-derived stem cells: European legislative issues. Ann. Med. Surg. 2017, 24, 61–64, 2017

57. Casadei, A.; Epis, R.; Ferroni, L.; Tocco, I.; Gardin, C.; Bressan, E.; Sivolella, S.; Vindigni, V.; Pinton, P.; Mucci, G.; et al. Adipose tissue regeneration: A state of the art. BioMed. Res. Int. 2012.

58. Pfaff, M.; Wu, W.; Zellner, E.; Steinbacher, M.D. Processing technique for lipofilling influences adipose-derived stem cell concentration and cell viability in lipoaspirate. Aesthet. Plast. Surg., 38, 224–229,2014

59. Cleveland, E.C.; Albano, N.J.; Hazen, A. Roll, Spin, Wash, or Filter? Processing of Lipoaspirate for Autologous Fat Grafting: An Updated, Evidence-Based Review of the Literature. Plast. Reconstr. Surg., 136, 706–713, 2015

60. Strong, A.L.; Cederna, P.S.; Rubin, J.P.; Coleman, S.R.; Levi, B. The Current State of Fat Grafting: A Review of Harvesting, Processing, and Injection Techniques. Plast. Reconstr. Surg., 136, 897–912, 2015

61. Condé-Green, A.; Wu, I.; Graham, I.; Chae, J.J.; Drachenberg, C.B.; Singh, D.P.; Holton, L., 3rd; Slezak, S.; Elisseeff, J. Comparison of 3 Techniques of Fat Grafting and Cell-Supplemented Lipotransfer in Athymic Rats: A Pilot Study. Aesthet. Surg. J., 33, 713–721, 2013

62. Rose, J.G., Jr.; Lucarelli, M.J.; Lemke, B.N.; Dortzbach, R.K.; Boxrud, C.A.; Obagi, S.; Patel, S. Histologic comparison of autologous fat processing methods. Ophthal. Plast. Reconstr. Surg., 22, 195–200, 2006

63. Condé-Green, A.; Baptista, L.S.; de Amorin, N.F.; de Oliveira, E.D.; da Silva, K.R.; Pedrosa Cda, S.; Borojevic, R.; Pitanguy, I. Effects of centrifugation on cell composition and viability of aspirated adipose tissue processed for transplantation. Aesthet. Surg. J. 2010, 30, 249–255, 2010

64. Morrison, S.J.; Spradling, A.C. Stem cells and niches: Mechanisms that promote stem cell maintenance throughout life. Cell, 132, 598–611, 2008

65. Juhyun, O.H.; Lee, Y.D.; Wagers, A.J. Stem cell aging: Mechanisms, regulators and therapeutic opportunities. Nat. Med., 20, 870–880, 2014

66. De Francesco, F.; Romano, M.; Zarantonello, L.; Ruffolo, C.; Neri, D.; Bassi, N.; Giordano, A.; Zanus, G.; Ferraro, G.A.; Cillo, U. The role of adipose stem cells in inflammatory bowel disease: From biology to novel therapeutic strategies. Cancer Biol. Ther., 17, 889–898, 2016

67. Rodriguez, Y.; Baena, R.; D'Aquino, R.; Graziano, A.; Trovato, L.; Aloise, A.C.; Ceccarelli, G.; Cusella, G.; Pelegrine, A.A.; Lupi, S.M. Autologous Periosteum-Derived Micrografts and PLGA/HA Enhance the bone formation in sinus lift augmentation. Front. Cell Dev. Biol., 5, 87, 2017

68. De Francesco, F.; Graziano, A.; Trovato, L.; Ceccarelli, G.; Romano, M.; Marcarelli, M.; Cusella De Angelis, M.G.; Cillo, U.; Riccio, M.; Ferraro, G.A. A regenerative approach with dermal micrografts in the treatment of chronic ulcers. Stem. Cell Rev. Rep., 13, 139–148. 2017

69. Svolacchia, F.; De Francesco, F.; Trovato, L.; Graziano, A.; Ferraro, G.A. An innovative regenerative treatment of scars with dermal micrografts. J. Cosmet. Dermatol., 15, 245–253, 2016

70. Ceccarelli, G.; Gentile, P.; Marcarelli, M.; Balli, M.; Ronzoni, F.L.; Benedetti, L.; Cusella De Angelis, M.G. In vitro and in vivo studies of alar-nasal cartilage using autologous micro-grafts: The use of the rigenera protocol in the treatment of an osteochondral lesion of the nose. Pharmaceuticals, 10, 53, 2017

71. Dubey, N.K.; Mishra, V.K.; Dubey, R.; Deng, Y.H.; Tsai, F.C.; Deng, W.P. Revisiting the Advances in Isolation, Characterization and Secretome of Adipose-Derived Stromal/Stem Cells. Int. J. Mol. Sci., 19, 2200, 2018

72. Bellini, E.; Grieco, M.P.; Raposio, E. A journey through liposuction and liposculture: Review. Ann. Med. Surg, 24, 53–60, 2017

73. Terzi, M.Y.; Izmirli, M.; Gogebakan, B. The cell fate: Senescence or quiescence. Mol. Biol. Rep, 43, 1213–1220, 2016

74. Paster, E.R.; LaFond, E.; Biery, D.N.; Iriye, A.; Gregor, T.P.; Shofer, F.S.; Smith, G.K. Estimates of prevalence of hip dysplasia in Golden Retrievers and Rottweilers and the influence of bias on published prevalence figures. J. Am. Vet. Med. Assoc., 226, 387–392, 2005

75. Smith, G.K.; Paster, E.R.; Powers, M.Y.; Lawler, D.F.; Biery, D.N.; Shofer, F.S.; McKelvie, P.J.; Kealy, R.D. Lifelong diet restriction and radiographic evidence of osteoarthritis of the hip joint in dogs. J. Am. Vet. Med. Assoc. 2006, 229, 690–693, 2006

76. Moreau, M.; Rialland, P.; Pelletier, J.P.; Martel-Pelletier, J.; Lajeunesse, D.; Boileau, C.; Beauchamp, G. Tiludronate treatment improves structural changes and symptoms of osteoarthritis in the canine anterior cruciate ligament model. Arthritis Res. Ther., 13, R98, 2011

77. Comblain, F.; Serisier, S.; Barthelemy, N.; Balligand, M.; Henrotin, Y. Review of dietary supplements for the management of osteoarthritis in dogs in studies from 2004 to 2014. J. Vet. Pharmacol. Ther., 39, 1–15, 2016

78. Cave, N.J.; Bridges, J.P.; Cogger, N.; Farman, R.S. A survey of diseases of working farm dogs in New Zealand. N. Z. Vet. J.,56, 305–312, 2009

79. Bonnett, B.N.; Egenvall, A.; Olson, P.; Hedhammar, A. Mortality in insured Swedish dogs: Rates and causes of death in various breeds. Vet. Rec., 141, 40–44, 1997

80. Proschowsky, H.F.; Rugbjerg, H.; Ersboll, A.K. Mortality of purebred and mixed-breed dogs in Denmark. Prev. Vet. Med., 58,63–74, 2003

81. Malm, S.; Fikse, F.; Egenvall, A.; Bonnett, B.N.; Gunnarsson, L.; Hedhammar, A.; Strandberg, E. Association between radiographic assessment of hip status and subsequent incidence of veterinary care and mortality related to hip dysplasia in insured Swedish dogs. Prev. Vet. Med., 93, 222–232. 2010

82. Adams, V.J.; Evans, K.M.; Sampson, J.; Wood, J.L. Methods and mortality results of a health survey of purebred dogs in the U.K. J.Small Anim. Pract., 51, 512–524, 2010

83. Krontveit, R.I.; Nødtvedt, A.; Sævik, B.K.; Ropstad, E.; Skogmo, H.K.; Trangerud, C. A prospective study on canine hip dysplasia and growth in a cohort of four large breeds in Norway (1998–2001). Prev. Vet. Med., 97, 252–263, 2010

84. Henrotin, Y.; Sanchez, C.; Balligand, M. Pharmaceutical and nutraceutical management of canine osteoarthritis: Present and future perspectives. Vet. J., 170, 113–123, 2005

85. Tobias, K.M.; Johnston, S.A. Veterinary Surgery: Small Animal; Saunders: Philadelphia, PA, USA, 2012.

86. Rychel, J.K. Diagnosis, and treatment of osteoarthritis. Top. Companion Anim. Med., 25, 20–25, 2010

87. Mortellaro, C.M.; Miolo, A. Approccio medico combinato all'artrosi nel cane. Veterinaria, 18, 9–19, 2004

88. Dini, F.; Tambella, A.M.; Marchegiani, A.; Sisti, V.M.; Villanacci, C.; Ubaldi, F.; Palumbo Piccionello, A.; Scrollavezza, P. Comparative evaluation of two physiotherapy rehabilitation treatments for osteoarthritis in the dog. In Proceedings of the VII International Symposium on Veterinary Rehabilitation and Physical Therapy, Vienna, Austria, 15–18 August, Volume 154, 2012

89. Phillips, M.; Bhandari, M.; Grant, J.; Bedi, A.; Trojian, T.; Johnson, A.; Schemitsch, E. A systematic review of current clinical practice guidelines on intra-articular hyaluronic acid, corticosteroid, and Platelet-Rich Plasma injection for Knee Osteoarthritis: An international perspective. Orthop. J. Sport Med., 9, 23259671211030272, 2021

90. De Francesco, F.; Gravina, P.; Busato, A.; Farinelli, L.; Soranzo, C.; Vidal, L.; Zingaretti, N.; Zavan, B.; Sbarbati, A.; Riccio, M.; et al. Stem Cells in autologous microfragmented adipose tissue: Current perspectives in osteoarthritis disease. Int. J. Mol. Sci., 22, 10197, 2021

91. Gerson, S.L. Mesenchymal stem cells: No longer second class marrow citizens. Nat. Med., 5, 262–264, 1999

92. Wakitani, S.; Goto, T.; Pineda, S.J.; Young, R.G.; Mansour, J.M.; Caplan, A.I.; Goldberg, V.M. Mesenchymal cell-based repair of large, full-thickness defects of articular cartilage. J. Bone Jt. Surg., 76, 579–592, 1994

93. Palumbo Piccionello, A.; Riccio, V.; Senesi, L.; Volta, A.; Pennasilico, L.; Botto, R.; Rossi, G.; Tambella, A.M.; Galosi, L.; Marini, C.; et al. Adipose micro-grafts enhance tendinopathy healing in ovine model: An in vivo experimental perspective study. Stem Cells Transl. Med., 10, 1544–1560, 2021

94. De Francesco, F.; Tirino, V.; Desiderio, V.; Ferraro, G.; D'Andrea, F.; Giuliano, M.; Libondi, G.; Pirozzi, G.; De Rosa, A.; Papaccio,G. Human CD34/CD90 ASCs are capable of growing as sphere clusters, producing high levels of VEGF and forming capillaries.PLoS ONE, 4, e6537, 2009

95. De Francesco, F.; Ricci, G.; D'Andrea, F.; Nicoletti, G.F.; Ferraro, G.A. Human adipose stem cells: From bench to bedside. Tissue Eng. Part B Rev., 21, 572–584, 2015

96. Nicoletti, G.F.; De Francesco, F.; D'Andrea, F.; Ferraro, G.A. Methods and procedures in adipose stem cells: State of the art and perspective for translation medicine. J. Cell. Physiol., 230, 489–495, 2015

97. Ferraro, G.A.; De Francesco, F.; Nicoletti, G.; Paino, F.; Desiderio, V.; Tirino, V.; D'Andrea, F. Human adipose CD34+CD90+ stem cells and collagen scaffold constructs grafted in vivo fabricate loose connective and adipose tissue. J. Cell. Biochem., 114, 1039–1049, 2013

98. De Francesco, F.; Mannucci, S.; Conti, G.; Dai Prè, E.; Sbarbati, A.; Riccio, M. A Non-enzymatic method to obtain a fat tissue derivative highly enriched in adipose stem cells (ASCs) from human lipoaspirates: Preliminary results. Int. J. Mol. Sci., 19, 2061, 2018

99. Senesi, L.; De Francesco, F.; Farinelli, L.; Manzotti, S.; Gagliardi, G.; Papalia, G.F.; Riccio, M.; Gigante, A. Mechanical and Enzymatic procedures to isolate the stromal vascular fraction from adipose tissue: Preliminary results. Front. Cell Dev. Biol., 7, 88, 2019

100. Panchal, J.; Malanga, G.; Sheinkop, M. Safety and Efficacy of percutaneous injection of lipogems micro-fractured adipose tissue for osteoarthritic knees. Am. J. Orthop., 47, 11, 2018

101. Naldini, G.; Sturiale, A.; Fabiani, B.; Giani, I.; Menconi, C. Micro-fragmented adipose tissue injection for the treatment of complex anal fistula: A pilot study accessing safety and feasibility. Tech. Coloproctol, 22, 107–113, 2018

102. Ceserani, V.; Ferri, A.; Berenzi, A.; Benetti, A.; Ciusani, E.; Pascucci, L.; Bazzucchi, C.; Coccè, V.; Bonomi, A.; Pessina, A.; et al. Angiogenic and anti-inflammatory properties of micro-fragmented fat tissue and its derived mesenchymal stromal cells. Vasc. Cell 2016, 8, 3.

103. Al-Ghadban, S.; Bunnell, B.A. Adipose tissue-derived stem cells: Immunomodulatory effects and therapeutic potential. Physiology 2020, 35, 125–133.

104. Polly, S.S.; Nichols, A.E.C.; Donnini, E.; Inman, D.J.; Scott, T.J.; Apple, S.M.; Were, S.R.; Dahlgren, L.A. Adipose-derived stromal vascular fraction and cultured stromal cells as trophic mediators for tendon healing. J. Orthop. Res. 2019, 37, 1429–1439.

105. Bellei, B.; Migliano, E.; Tedesco, M.; Caputo, S.; Papaccio, F.; Lopez, G.; Picardo, M. Adipose tissue-derived extracellular fraction characterization: Biological and clinical considerations in regenerative medicine. Stem Cell Res. Ther. 2018, 9, 207.

106. Pak, J.; Lee, J.H.; Pak, N.; Pak, Y.; Park, K.S.; Jeon, J.H.; Jeong, B.C.; Lee, S.H. Cartilage regeneration in humans with adipose tissue-derived stem cells and adipose stromal vascular fraction cells: Updated status. Int. J. Mol. Sci. 2018, 19, 2146.

107. Raposio, E.; Ciliberti, R. Clinical use of adipose derived stem cells: European legislative issues. Ann. Med. Surg. 2017, 24, 61–64.

108. Oberbauer, E.; Steffenhagen, C.; Wurzer, C.; Gabriel, C.; Redl, H.; Wolbank, S. Enzymatic and non-enzymatic isolation systems for adipose tissue-derived cells: Current state of the art. Cell Regen. 2015, 4, 7.

109. Purpura, V.; Bondioli, E.; Graziano, A.; Trovato, L.; Melandri, D.; Ghetti, M.; Marchesini, A.; Cusella De Angelis, M.G.; Benedetti, L.; Ceccarelli, G.; et al. Tissue characterisation after a new disaggregation method for skin micro-grafts generation. J. Vis. Exp. 2016, 109, e53579.

110. Mancarelli, M.; Trovato, L.; Novarese, E.; Riccio, M.; Graziano, A. Rigenera protocol in the treatment of surgical wound dehiscence. Int. Wound J. 2017, 14, 277–281.

111. De Francesco, F.; Graziano, A.; Trovato, L.; Ceccarelli, G.; Romano, M.; Marcarelli, M.; Cusella De Angelis, M.G.; Cillo, U.; Riccio, M.; Ferraro, G.A. A regenerative approach with dermal micrografts in the treatment of chronic ulcers. Stem Cell Rev. 2017, 13, 139–148, Erratum in Stem Cell Rev. 2017, 13, 149.

112. Svolacchia, F.; De Francesco, F.; Trovato, L.; Graziano, A.; Ferraro, G.A. An innovative regenerative treatment of scars with dermal micrografts. J. Cosmet. Dermatol. 2016, 15, 245–253.

113. Rodriguez, Y.; Baena, R.; D'Aquino, R.; Graziano, A.; Trovato, L.; Aloise, A.C.; Ceccarelli, C.; Cusella, G.; Pelegrine, A.A.; Lupi, S.M. Autologous periosteum-derived micrografts and PLGA/HA enhance the bone formation in sinus lift augmentation. Front. Cell Dev. Biol. 2017, 5, 87.

114. Ceccarelli, G.; Gentile, P.; Marcarelli, M.; Balli, M.; Ronzoni, F.L.; Benedetti, L.; Cusella De Angelis, M.G. In vitro and in vivo studies of alar-nasal cartilage using autologous micro-grafts: The use of the rigenera protocol in the treatment of an osteochondral lesion of the nose. Pharmaceuticals 2017, 10, 53.

115. Riccio, M.; Marchesini, A.; Zingaretti, N.; Carella, S.; Senesi, L.; Onesti, M.G.; Parodi, P.C.; Ribuffo, D.; Vaienti, L.; De Francesco, F. A multicentre study: The use of

micrografts in the reconstruction of full-thickness posttraumatic skin defects of the limbs-a whole innovative concept in regenerative surgery. Stem Cells Int. 2019, 2019, 5043518.

116. Dai Prè, E.; Busato, A.; Mannucci, S.; Vurro, F.; De Francesco, F.; Riccio, V.; Solito, S.; Biswas, R.; Bernardi, P.; Riccio, M.; et al. Comparison of Adipose Stem cells harvested from abdomen and thigh extracted non-enzymatically. Int. J. Sci. Mol. 2020, 21, 3081.

117. Mao, A.S.; Mooney, D.J. Regenerative medicine: Current therapies and future directions. Proc. Natl. Acad. Sci. USA 2015, 24, 14452–14459.

118. Aronowitz, J.A.; Lockhart, R.A.; Hakakian, C.S. Mechanical versus enzymatic isolation of stromal vascular fraction cells from adipose tissue. SpringerPlus 2015, 4, 713.

119. Astarita, C.; Arora, C.L.; Trovato, L. Tissue regeneration: An overview from stem cells to micrografts. J. Int. Med. Res. 2020, 48, 300060520914794.

120. Condé-Green, A.; Rodriguez, R.L.; Slezak, S.; Singh, D.P.; Goldberg, N.H.; McLenithan, J. Comparison between Stromal Vascular Cells' Isolation with Enzymatic Digestion and Mechanical Processing of Aspirated Adipose Tissue. Plast. Reconstr. Surg. 2014, 134, 54.

121. Rojas-Ortega, M.; Cruz, R.; Vega-López, M.A.; Cabrera-González, M.; Hernández-Hernández, J.M.; Lavalle-Montalvo, C.; Kouri, J.B. Exercise modulates the expression of IL-1β and IL-10 in the articular cartilage of normal and osteoarthritis-induced rats. Pathol. Res. Pract. 2015, 211, 435–443.

122. Chinetti-Gbaguidi, G.; Bouhlel, M.A.; Copin, C.; Duhem, C.; Derudas, B.; Neve, B.; Noel, B.; Eeckhoute, J.; Lefebvre, P.; Seckl, J.R.; et al. Peroxisome proliferator-activated receptor- γ activation induces 11β-hydroxysteroid dehydrogenase type 1 activity in human alternative macrophages. Arterioscler. Thromb. Vasc. Biol. 2012, 32, 677–685.

123. Planat-Benard, V.; Varin, A.; Casteilla, L. MSCs and inflammatory cells crosstalk in regenerative medicine: Concerted actions for optimized resolution driven by energy metabolism. Front. Immunol. 2021, 12, 626755.

124. Luque-Campos, N.; Bustamante-Barrientos, F.A.; Pradenas, C.; Garcia, C.; Araya, M.J.; Bohaud, C.; Contreras-Lopez, R.; Elizondo- Vega, R.; Djouad, F.; Luz-Crawford, P.; et al. The Macrophage response is driven by mesenchymal stem cell-mediated metabolic reprogramming. Front. Immunol. 2021, 12, 624746.

125. Longobardi, L.; Jordan, J.M.; Shi, X.A.; Renner, J.B.; Schwartz, T.A.; Nelson, A.E.; Barrow, D.A.; Kraus, V.B.; Spagnoli, A. Associations between the chemokine biomarker CCL2 and knee osteoarthritis outcomes: The Johnston County Osteoarthritis Project. Osteoarthr. Cartil. 2018, 26, 1257–1261.

126. Zuk, P.A.; Zhu, M.; Ashjian, P.; De Ugarte, D.A.; Huang, J.I.; Mizuno, H.; Alfonso, Z.C.; Fraser, J.K.; Benhaim, P.; Hedrick, M.H. Human adipose tissue is a source of multipotent stem cells. Mol. Biol. Cell 2002, 13, 4279–4295.

127. Bora, P.; Majumdar, A.S. Adipose tissue-derived stromal vascular fraction in regenerative medicine: A brief review on biology and translation. Stem Cell Res. Ther. 2017, 8, 145.

128. Bourin, P.; Bunnell, B.A.; Casteilla, L.; Dominici, M.; Katz, A.J.; March, K.L.; Redl, H.; Rubin, J.P.; Yoshimura, K.; Gimble, J.M. Stromal cells from the adipose tissue-derived stromal vascular fraction and culture expanded adipose tissue-derived stromal/stem cells: A joint statement of the International Federation for Adipose Therapeutics and Science (IFATS) and the International Society for Cellular Therapy (ISCT). Cytotherapy 2013, 15, 641–648.

129. Majors, A.K.; Boehm, C.A.; Nitto, H.; Midura, R.J.; Muschler, G.F. Characterization of human bone marrow stromal cells with respect to osteoblastic differentiation. J. Orthop. Res. 1997, 15, 546–557.

130. Shang, Q.; Bai, Y.; Wang, G.; Song, Q.; Guo, C.; Zhang, L.; Wang, Q. Delivery of Adipose-Derived Stem Cells Attenuates Adipose Tissue Inflammation and Insulin Resistance in Obese Mice Through Remodeling Macrophage Phenotypes. Stem Cells Dev. 2015, 24, 2052–2064.

131. Kotani, T.; Masutani, R.; Suzuka, T.; Oda, K.; Makino, S.; Ii, M. Anti-inflammatory and antifibrotic effects of intravenous adipose-derived stem cell transplantation in a mouse model of bleomycin-induced interstitial pneumonia. Sci. Rep. 2017, 7, 14608.

132. Prasai, A.; El Ayadi, A.; Mifflin, R.C.; Wetzel, M.D.; Andersen, C.R.; Redl, H.; Herndon, D.N.; Finnerty, C.C. Characterization of Adipose-Derived Stem Cells Following Burn Injury. Stem Cell Rev. Rep. 2017, 13, 781–792.

133. Lapuente, J.P.; Dos-Anjos, S.; Blázquez-Martínez, A. Intra-articular infiltration of adipose-derived stromal vascular fraction cells slows the clinical progression of moderate-severe knee osteoarthritis: Hypothesis on the regulatory role of intra-articular adipose tissue. J. Orthop. Surg. Res. 2020, 15, 137.

134. Hong, Z.; Chen, J.; Zhang, S.; Zhao, C.; Bi, M.; Chen, X.; Bi, Q. Intra-articular injection of autologous adipose-derived stromal vascular fractions for knee osteoarthritis: A double-blind randomized self-controlled trial. Int. Orthop. 2019, 43, 1123–1134.

135. Pak, J.; Lee, J.H.; Park, K.S.; Park, M.; Kang, L.W.; Lee, S.H. Current use of autologous adipose tissue-derived stromal vascular fraction cells for orthopedic applications. J. Biomed. Sci. 2017, 24, 9.

136. Chu, D.-T.; Nguyen Thi Phuong, T.; Tien, N.L.B.; Tran, D.K.; Minh, L.B.; Thanh, V.V.; Gia Anh, P.; Pham, V.H.; Thi Nga, V. Adipose Tissue Stem Cells for Therapy: An Update on the Progress of Isolation, Culture, Storage, and Clinical Application. J. Clin. Med. 2019, 8, 917.

137. Oberbauer, E.; Steffenhagen, C.; Wurzer, C.; Gabriel, C.; Redl, H.; Wolbank, S. Enzymatic and non-enzymatic isolation systems for adipose tissue-derived cells: Current state of the art. Cell Regen. 2015, 4, 7.

138. Aronowitz, J.A.; Ellenhorn, J.D. Adipose stromal vascular fraction isolation: A head-to-head comparison of four commercial cell separation systems. Plast. Reconstr. Surg. 2013, 132, 932e–939e.

139. Crisan, M.; Yap, S.; Casteilla, L.; Chen, C.W.; Corselli, M.; Park, T.S.; Andriolo, G.; Sun, B.; Zheng, B.; Zhang, L.; et al. A perivascular origin for mesenchymal stem cells in multiple human organs. Cell Stem Cell 2008, 3, 301–313.

140. Vezzani, B.; Shaw, I.; Lesme, H.; Yong, L.; Khan, N.; Tremolada, C.; Péault, B. Higher Pericyte Content and Secretory Activity of Microfragmented Human Adipose Tissue Compared to Enzymatically Derived Stromal Vascular Fraction. Stem Cells Transl. Med. 2018, 7, 876–886.

141. Nava, S.; Sordi, V.; Pascucci, L.; Tremolada, C.; Ciusani, E.; Zeira, O.; Cadei, M.; Soldati, G.; Pessina, A.; Parati, E.; et al. Long-Lasting Anti-Inflammatory Activity of Human Microfragmented Adipose Tissue. Stem Cells Int. 2019, 2019, 5901479.

142. Hudetz, D.; Boric´, I.; Rod, E.; Jelecˇ, Ž.; Kunovac, B.; Polašek, O.; Vrdoljak, T.; Plecˇko, M.; Skelin, A.; Polancˇec, D.; et al. Early results of intra-articular micro-fragmented lipoaspirate treatment in patients with late stages knee osteoarthritis: A prospective study. Croat. Med. J. 2019, 60, 227–236.

143. Kolbe, M.; Xiang, Z.; Dohle, E.; Tonak, M.; Kirkpatrick, C.J.; Fuchs, S. Paracrine effects influenced by cell culture medium and consequences on microvessel-like structures in cocultures of mesenchymal stem cells and outgrowth endothelial cells. Tissue Eng. Part A 2011, 17, 2199–2212.

144. Liang, T.; Zhu, L.; Gao, W.; Gong, M.; Ren, J.; Yao, H.; Wang, K.; Shi, D. Coculture of endothelial progenitor cells and mesenchymal stem cells enhanced their proliferation and angiogenesis through PDGF and Notch signaling. FEBS Open Bio 2017, 7, 1722–1736.

145. Loibl, M.; Binder, A.; Herrmann, M.; Duttenhoefer, F.; Richards, R.G.; Nerlich, M.; Alini, M.; Verrier, S. Direct cell-cell contact between mesenchymal stem cells and endothelial progenitor cells induces a pericyte-like phenotype in vitro. Biomed. Res. Int. 2014, 2014, 395781.

146. Ge, Q.; Zhang, H.; Hou, J.; Wan, L.; Cheng, W.; Wang, X.; Dong, D.; Chen, C.; Xia, J.; Guo, J.; et al. VEGF secreted by mesenchymal stem cells mediates the differentiation of endothelial progenitor cells into endothelial cells via paracrine mechanisms. Mol. Med. Rep. 2018, 17, 1667–1675.

147. Hyldig, K.; Riis, S.; Pennisi, C.P.; Zachar, V.; Fink, T. Implications of Extracellular Matrix Production by Adipose Tissue-Derived Stem Cells for Development of Wound Healing Therapies. Int. J. Mol. Sci. 2017, 18, 1167.

148. Zhou, Z.Q.; Chen, Y.; Chai, M.; Tao, R.; Lei, Y.H.; Jia, Y.Q.; Shu, J.; Ren, J.; Li, G.; Wei, W.X.; et al. Adipose extracellular matrix promotes skin wound healing by inducing

the differentiation of adipose-derived stem cells into fibroblasts. Int. J. Mol. Med. 2019, 43, 890–900.

149. Vilaboa, S.D.A.; Navarro-Palou, M.; Llull, R. Age influence on stromal vascular fraction cell yield obtained from human lipoaspirates. Cytotherapy 2014, 16.

150. Fadel, L.; Viana, B.R.; Feitosa, M.L.; Ercolin, A.C.; Roballo, K.C.; Casals, J.B.; Pieri, N.C.; Meirelles, F.V.; Martins Ddos, S.; Miglino, M.A.; et al. Protocols for obtainment and isolation of two mesenchymal stem cell sources in sheep. Acta Cir. Bras. 2011, 26, 267–273.

151. Mojallal, A.; Auxenfans, C.; Lequeux, C.; Braye, F.; Damour, O. Influence of negative pressure when harvesting adipose tissue on cell yield of the stromal-vascular fraction. Biomed. Mater. Eng. 2008, 18, 193–197.

152. Aronowitz, J.A.; Lockhart, R.A.; Hakakian, C.S. Mechanical versus enzymatic isolation of stromal vascular fraction cells from adipose tissue. SpringerPlus 2015, 4, 713.

153. Trivisonno, A.; Di Rocco, G.; Cannistra, C.; Finocchi, V.; Torres Farr, S.; Monti, M.; Toietta, G. Harvest of superficial layers of fat with a microcannula and isolation of adipose tissue-derived stromal and vascular cells. Aesthetic Surg. J. 2014, 34, 601–613.

154. Jang, Y.; Koh, Y.G.; Choi, Y.J.; Kim, S.H.; Yoon, D.S.; Lee, M.; Lee, J.W. Characterization of adipose tissue-derived stromal vascular fraction for clinical application to cartilage regeneration. Vitr. Cell. Dev. Biol. Anim. 2015, 51, 142–150.

155. Aust, L.; Devlin, B.; Foster, S.J.; Halvorsen, Y.D.; Hicok, K.; du Laney, T.; Sen, A.; Willingmyre, G.D.; Gimble, J.M. Yield of human adipose-derived adult stem cells from liposuction aspirates. Cytotherapy 2004, 6, 7–14.

156. Rodriguez, J.; Pratta, A.S.; Abbassi, N.; Fabre, H.; Rodriguez, F.; Debard, C.; Adobati, J.; Boucher, F.; Mallein-Gerin, F.; Auxenfans, C.; et al. Evaluation of Three Devices for the Isolation of the Stromal Vascular Fraction from Adipose Tissue and for ASC Culture: A Comparative Study. Stem Cells Int. 2017, 2017, 9289213.

157. Doi, K.; Tanaka, S.; Iida, H.; Eto, H.; Kato, H.; Aoi, N.; Kuno, S.; Hirohi, T.; Yoshimura, K. Stromal vascular fraction isolated from lipo-aspirates using an automated processing system: Bench and bed analysis. J. Tissue Eng. Regen. Med. 2013, 7, 864–870.

158. Jurgens, W.J.; Oedayrajsingh-Varma, M.J.; Helder, M.N.; Zandiehdoulabi, B.; Schouten, T.E.; Kuik, D.J.; Ritt, M.J.; van Milligen, F.J. Effect of tissue-harvesting site on yield of stem cells derived from adipose tissue: Implications for cell-based therapies. Cell Tissue Res. 2008, 332, 415–426.

159. Markarian, C.F.; Frey, G.Z.; Silveira, M.D.; Chem, E.M.; Milani, A.R.; Ely, P.B.; Horn, A.P.; Nardi, N.B.; Camassola, M. Isolation of adipose-derived stem cells: A comparison among different methods. Biotechnol. Lett. 2014, 36, 693–702.

160. Baptista, L.S.; do Amaral, R.J.; Carias, R.B.; Aniceto, M.; Claudio-da-Silva, C.; Borojevic, R. An alternative method for the isolation of mesenchymal stromal cells derived from lipoaspirate samples. Cytotherapy 2009, 11, 706–715.

161. Shah, F.S.; Wu, X.; Dietrich, M.; Rood, J.; Gimble, J.M. A non-enzymatic method for isolating human adipose tissue-derived stromal stem cells. Cytotherapy 2013, 15, 979–985.

162. Raposio, E.; Caruana, G.; Bonomini, S.; Libondi, G. A novel and effective strategy for the isolation of adipose-derived stem cells: Minimally manipulated adipose-derived stem cells for more rapid and safe stem cell therapy. Plast. Reconstr. Surg. 2014, 133, 1406–1409.

163. Veronese, S.; Dai Prè, E.; Conti, G.; Busato, A.; Mannucci, S.; Sbarbati, A. Comparative technical analysis of lipoaspirate mechanical processing devices. J. Tissue Eng. Regen. Med. 2020, 14, 1213–1226.

164. Goldberg, S. Mechanical/physical methods of cell disruption and tissue homogenization. Methods Mol. Biol. 2008, 424, 3–22.

165. Song, Y.; Du, H.; Dai, C.; Zhang, L.; Li, S.; Hunter, D.J.; Lu, L.; Bao, C. Human adipose-derived mesenchymal stem cells for osteoarthritis: A pilot study with long-term follow-up and repeated injections. Regen. Med. 2018, 13, 295–307.

166. Pers, Y.M.; Rackwitz, L.; Ferreira, R.; Pullig, O.; Delfour, C.; Barry, F.; Sensebe, L.; Casteilla, L.; Fleury, S.; Bourin, P.; et al. Adipose Mesenchymal Stromal Cell-Based Therapy for Severe Osteoarthritis of the Knee: A Phase I Dose-Escalation Trial. Stem Cells Transl. Med. 2016, 5, 847–856.

167. Yokota, N.; Hattori, M.; Ohtsuru, T.; Otsuji, M.; Lyman, S.; Shimomura, K.; Nakamura, N. Comparative clinical outcomes after intra-articular injection with adipose-derived cultured stem cells or noncultured stromal vascular fraction for the treatment of knee osteoarthritis. Am. J. Sports Med. 2019, 47, 2577–2583.

168. Chaput, B.; Bertheuil, N.; Escubes, M.; Grolleau, J.L.; Garrido, I.; Laloze, J.; Espagnolle, N.; Casteilla, L.; Sensebé, L.; Varin, A. Mechanically Isolated Stromal Vascular Fraction Provides a Valid and Useful Collagenase-Free Alternative Technique: A Comparative Study. Plast. Reconstr. Surg. 2016, 138, 807–819.

169. Usuelli, F.G.; Grassi, M.; Maccario, C.; Vigano, M.; Lanfranchi, L.; Alfieri Montrasio, U.; de Girolamo, L. Intratendinous adipose- derived stromal vascular fraction (SVF) injection provides a safe, efficacious treatment for Achilles tendinopathy: Results of a randomized controlled clinical trial at a 6-month follow-up. Knee Surg. Sports Traumatol. Arthrosc. 2018, 26, 2000–2010.

170. Maleki, M.; Ghanbarvand, F.; Reza Behvarz, M.; Ejtemaei, M.; Ghadirkhomi, E. Comparison of mesenchymal stem cell markers in multiple human adult stem cells. Int. J. Stem Cells 2014, 7, 118–126.

171. Grünherz, L.; Sanchez-Macedo, N.; Frueh, F.S.; McLuckie, M.; Lindenblatt, N. Nanofat applications: from clinical esthetics to regenerative research. Curr. Opin. Biomed. Eng. 2019, 10, 174–180, doi:10.1016/j.cobme.2019.07.002

172. Eto, H.; Kato, H.; Suga, H.; Aoi, N.; Doi, K.; Kuno, S.; Yoshimura, K. The Fate of Adipocytes after Nonvascularized Fat Grafting. Plast. Reconstr. Surg. 2012, 129, 1081–1092, doi:10.1097/PRS.0b013e31824a2b19.

173. Gir, P.; Brown, S.A.; Oni, G.; Kashefi, N.; Mojallal, A.; Rohrich, R.J. Fat Grafting. Plast. Reconstr. Surg. 2012, 130, 249–258, doi:10.1097/PRS.0b013e318254b4d3.

174. Kato, H.; Mineda, K.; Eto, H.; Doi, K.; Kuno, S.; Kinoshita, K.; Kanayama, K.; Yoshimura, K. Degeneration, Regeneration, and Cicatrization after Fat Grafting: Dynamic Total Tissue Remodeling during the First 3 Months. Plast. Reconstr. Surg. 2014, 133.

175. Tonnard, P.; Verpaele, A.; Peeters, G.; Hamdi, M.; Cornelissen, M.; Declercq, H. Nanofat Grafting. Plast. Reconstr. Surg. 2013, 132, 1017–1026, doi:10.1097/PRS.0b013e31829fe1b0.

176. Lindenblatt, N.; van Hulle, A.; Verpaele, A.M.; Tonnard, P.L. The Role of Microfat Grafting in Facial Contouring. Aesthetic Surg. J. 2015, 35, 763–771, doi:10.1093/asj/sjv083.

177. Mesguich Batel, F.; Bertrand, B.; Magalon, J.; François, P.; Velier, M.; Veran, J.; Mallet, S.; Jouve, E.; Sabatier, F.; Casanova, D. Traitement des ridules de la lèvre supérieure par graisse émulsifiée ou « Nanofat » : étude biologique et clinique à propos de 4 cas. Ann. Chir. Plast. Esthétique 2018, 63, 31–40, doi:10.1016/j.anplas.2017.10.004.

178. Gu, Z.; Li, Y.; Li, H. Use of Condensed Nanofat Combined With Fat Grafts to Treat Atrophic Scars. JAMA Facial Plast. Surg. 2018, 20, 128–135, doi:10.1001/jamafacial.2017.1329.

179. Uyulmaz, S.; Sanchez Macedo, N.; Rezaeian, F.; Giovanoli, P.; Lindenblatt, N. Nanofat Grafting for Scar Treatment and Skin Quality Improvement. Aesthetic Surg. J. 2018, 38, 421–428, doi:10.1093/asj/sjx183.

180. Bhooshan, L.S.; Devi, M.G.; Aniraj, R.; Binod, P.; Lekshmi, M. Autologous emulsified fat injection for rejuvenation of scars: A prospective observational study. Indian J. Plast. Surg. 2018, 51, 077–083, doi:10.4103/ijps.IJPS_86_17.

181. Martin, A.; Maladry, D.; Esmaeli, A.; Gaucher, S.; Philippe, H.-J. Fat grafting of hairy areas of head and neck - comparison between lipofilling and nanofat grafting procedures in a cadaveric study. J. Stomatol. Oral Maxillofac. Surg. 2018, 119, 274–278, doi:10.1016/j.jormas.2018.06.011.

182. Wei, H.; Gu, S.-X.; Liang, Y.-D.; Liang, Z.-J.; Chen, H.; Zhu, M.-G.; Xu, F.-T.; He, N.; Wei, X.-J.; Li, H.-M. Nanofat-derived stem cells with platelet-rich fibrin improve facial contour remodeling and skin rejuvenation after autologous structural fat transplantation. Oncotarget 2017, 8, 68542–68556, doi:10.18632/oncotarget.19721.

183. LO FURNO, D.; TAMBURINO, S.; MANNINO, G.; GILIA, E.; LOMBARDO, G.; TARICO, M.S.; VANCHERI, C.; GIUFFRIDA, R.; PERROTTA, R.E. Nanofat 2.0:

Experimental Evidence for a Fat Grafting Rich in Mesenchymal Stem Cells. Physiol. Res. 2017, 663–671, doi:10.33549/physiolres.933451.

184. Rigotti, G.; Marchi, A.; Sbarbati, A. Adipose-Derived Mesenchymal Stem Cells: Past, Present, and Future. Aesthetic Plast. Surg. 2009, 33, 271–273, doi:10.1007/s00266-009-9339-7.

185. Dai, R.; Wang, Z.; Samanipour, R.; Koo, K.; Kim, K. Adipose-Derived Stem Cells for Tissue Engineering and Regenerative Medicine Applications. Stem Cells Int. 2016, 2016, 1–19, doi:10.1155/2016/6737345.

186. Shang, Q.; Bai, Y.; Wang, G.; Song, Q.; Guo, C.; Zhang, L.; Wang, Q. Delivery of Adipose-Derived Stem Cells Attenuates Adipose Tissue Inflammation and Insulin Resistance in Obese Mice Through Remodeling Macrophage Phenotypes. Stem Cells Dev. 2015, 24, 2052–2064, doi:10.1089/scd.2014.0557.

187. Prasai, A.; El Ayadi, A.; Mifflin, R.C.; Wetzel, M.D.; Andersen, C.R.; Redl, H.; Herndon, D.N.; Finnerty, C.C. Characterization of Adipose-Derived Stem Cells Following Burn Injury. Stem Cell Rev. Reports 2017, 13, 781–792, doi:10.1007/s12015-017-9721-9.

188. Kotani, T.; Masutani, R.; Suzuka, T.; Oda, K.; Makino, S.; Ii, M. Anti-inflammatory and antifibrotic effects of intravenous adipose-derived stem cell transplantation in a mouse model of bleomycin-induced interstitial pneumonia. Sci. Rep. 2017, 7, 14608, doi:10.1038/s41598-017-15022-3.

189. Kalinina, N.; Kharlampieva, D.; Loguinova, M.; Butenko, I.; Pobeguts, O.; Efimenko, A.; Ageeva, L.; Sharonov, G.; Ischenko, D.; Alekseev, D.; et al.Characterisationn of secretomes provides evidence for adipose-derived mesenchymal stromal cells subtypes. Stem Cell Res. Ther. 2015, 6, 221, doi:10.1186/s13287-015-0209-8.

190. Charles-de-Sá, L.; Gontijo-de-Amorim, N.F.; Maeda Takiya, C.; Borojevic, R.; Benati, D.; Bernardi, P.; Sbarbati, A.; Rigotti, G. Antiaging Treatment of the Facial Skin by Fat Graft and Adipose-Derived Stem Cells. Plast. Reconstr. Surg. 2015, 135, 999–1009, doi:10.1097/PRS.0000000000001123.

191. Paliwal, S.; Chaudhuri, R.; Agrawal, A.; Mohanty, S. Regenerative abilities of mesenchymal stem cells through mitochondrial transfer. J. Biomed. Sci. 2018, 25, 31, doi:10.1186/s12929-018-0429-1.

192. Dai Prè, E.; Busato, A.; Mannucci, S.; Vurro, F.; De Francesco, F.; Riccio, V.; Solito, S.; Biswas, R.; Bernardi, P.; Riccio, M.; et al. In Vitro Characterization of Adipose Stem Cells Non-Enzymatically Extracted from the Thigh and Abdomen. Int. J. Mol. Sci. 2020, 21, 3081, doi:10.3390/ijms21093081.

193. Busato, A.; De Francesco, F.; Biswas, R.; Mannucci, S.; Conti, G.; Fracasso, G.; Conti, A.; Riccio, V.; Riccio, M.; Sbarbati, A. Simple and Rapid Non-Enzymatic Procedure Allows the Isolation of Structurally Preserved Connective Tissue Micro-Fragments Enriched with SVF. Cells 2020, 10, 36, doi:10.3390/cells10010036.

194. Kushida, Y.; Wakao, S.; Dezawa, M. Muse Cells Are Endogenous Reparative Stem Cells. In; 2018; pp. 43–68.

195. Conti, G.; Zingaretti, N.; Amuso, D.; Dai Prè, E.; Brandi, J.; Cecconi, D.; Manfredi, M.; Marengo, E.; Boschi, F.; Riccio, M.; et al. Proteomic and Ultrastructural Analysis of Cellulite-New Findings on an Old Topic. Int. J. Mol. Sci. 2020, 21, 2077, doi:10.3390/ijms21062077.

196. Conti, G.; Bertossi, D.; Dai Prè, E.; Cavallini, C.; Scupoli, M.T.; Ricciardi, G.; Parnigotto, P.; Saban, Y.; Sbarbati, A.; Nocini, P. Regenerative potential of the Bichat fat pad determined by the quantification of multilineage differentiating stress enduring cells. Eur. J. Histochem. 2018, 62, doi:10.4081/ejh.2018.2900.

197. Fisch, S.C.; Gimeno, M.L.; Phan, J.D.; Simerman, A.A.; Dumesic, D.A.; Perone, M.J.; Chazenbalk, G.D. Pluripotent non-tumorigenic multi-lineage differentiating stress enduring cells (Muse cells): a seven-year retrospective. Stem Cell Res. Ther. 2017, 8, 227, doi:10.1186/s13287-017-0674-3.
198. Simerman, A.A.; Phan, J.D.; Dumesic, D.A.; Chazenbalk, G.D. Muse Cells: Nontumorigenic Pluripotent Stem Cells Present in Adult Tissues—A Paradigm Shift in Tissue Regeneration and Evolution. Stem Cells Int. 2016, 2016, 1–8, doi:10.1155/2016/1463258.

199. Kamat, P.; Frueh, F.S.; McLuckie, M.; Sanchez-Macedo, N.; Wolint, P.; Lindenblatt, N.; Plock, J.A.; Calcagni, M.; Buschmann, J. Adipose tissue and the vascularisation of biomaterials: Stem cells, microvascular fragments and nanofat—a review. Cytotherapy 2020, 22, 400–411, doi:10.1016/j.jcyt.2020.03.433.

200. Peroni, D.; Scambi, I.; Pasini, A.; Lisi, V.; Bifari, F.; Krampera, M.; Rigotti, G.; Sbarbati, A.; Galiè, M. Stem molecular signature of adipose-derived stromal cells. Exp. Cell Res. 2008, 314, 603–615, doi:10.1016/j.yexcr.2007.10.007.

201. Alstrup, T.; Eijken, M.; Bohn, A.B.; Møller, B.; Damsgaard, T.E. Isolation of Adipose Tissue-Derived Stem Cells: Enzymatic Digestion in Combination with Mechanical Distortion to Increase Adipose Tissue-Derived Stem Cell Yield from Human Aspirated Fat. Curr. Protoc. Stem Cell Biol. 2019, 48, e68, doi:10.1002/cpsc.68.

202. Goldberg, S. Mechanical/Physical Methods of Cell Disruption and Tissue Homogenization. In; 2008; pp. 3–22.

203. Wakao, S.; Kitada, M.; Kuroda, Y.; Shigemoto, T.; Matsuse, D.; Akashi, H.; Tanimura, Y.; Tsuchiyama, K.; Kikuchi, T.; Goda, M.; et al. Multilineage-differentiating stress-enduring (Muse) cells are a primary source of induced pluripotent stem cells in human fibroblasts. Proc. Natl. Acad. Sci. 2011, 108, 9875–9880, doi:10.1073/pnas.1100816108.

204. Yamasaki, T.; Wakao, S.; Kawaji, H.; Koizumi, S.; Sameshima, T.; Dezawa, M.; Namba, H. Genetically Engineered Multilineage-Differentiating Stress-Enduring Cells as Cellular Vehicles against Malignant Gliomas. Mol. Ther. - Oncolytics 2017, 6, 45–56, doi:10.1016/j.omto.2017.06.001.

205. Yabuki, H.; Wakao, S.; Kushida, Y.; Dezawa, M.; Okada, Y. Human Multilineage-differentiating Stress-Enduring Cells Exert Pleiotropic Effects to Ameliorate Acute Lung Ischemia–Reperfusion Injury in a Rat Model. Cell Transplant. 2018, 27, 979–993, doi:10.1177/0963689718761657.

206. Mahmoud, E.E.; Kamei, N.; Shimizu, R.; Wakao, S.; Dezawa, M.; Adachi, N.; Ochi, M. Therapeutic Potential of Multilineage-Differentiating Stress-Enduring Cells for Osteochondral Repair in a Rat Model. Stem Cells Int. 2017, 2017, 1–8, doi:10.1155/2017/8154569.

207. Martinello, T.; Bronzini, I.; Maccatrozzo, L.; Iacopetti, I.; Sampaolesi, M.; Mascarello, F.; Patruno, M. Cryopreservation Does Not Affect the Stem Characteristics of Multipotent Cells Isolated from Equine Peripheral Blood. Tissue Eng. Part C Methods 2010, 16, 771–781, doi:10.1089/ten.tec.2009.0512

208. Bellini E, Grieco MP, Raposio E. The science behind autologous fat grafting. Ann Med Surg (Lond). 2017;24:65-73. Published 2017 Nov 10. doi:10.1016/j.amsu.2017.11.001

209. Aronowitz JA, Ellenhorn JDI. Adipose stromal vascular fraction isolation: a head-to-head comparison of four commercial cell separation systems. Plast Reconstr Surg. 2013 Dec;132(6):932e-939e. doi: 10.1097/PRS.0b013e3182a80652. PMID: 24281640.

210. Dai Prè, E.; Busato, A.; Mannucci, S.; Vurro, F.; De Francesco, F.; Riccio, V.; Solito, S.; Biswas, R.; Bernardi, P.; Riccio, M.; Sbarbati, A. In Vitro Characterization of Adipose Stem Cells Non-Enzymatically Extracted from the Thigh and Abdomen. Int. J. Mol. Sci. 2020, 21, 3081. https://doi.org/10.3390/ijms21093081

211. Busato A, De Francesco F, Biswas R, Mannucci S, Conti G, Fracasso G, Conti A, Riccio V, Riccio M, Sbarbati A. Simple and Rapid Non-Enzymatic Procedure Allows the Isolation of Structurally Preserved Connective Tissue Micro-Fragments Enriched with SVF. Cells. 2020 Dec 29;10(1):36. doi: 10.3390/cells10010036. PMID: 33383682; PMCID: PMC7824313.

212. Olenczak, Jonathan B. MD*; Seaman, Scott A. PhD†; Lin, Kant Y. MD*; Pineros-Fernandez, Angela MD*; Davis, Catherine E.‡; Salopek, Lisa S. LVT, RLATG*; Peirce, Shayn M. Ph.D.*†; Cottler, Patrick S. Ph.D.* Effects of Collagenase Digestion and Stromal Vascular Fraction Supplementation on Volume Retention of Fat Grafts, Annals of Plastic Surgery: June 2017 - Volume 78 - Issue 6S - p S335-S342

213. Kølle SF, Fischer-Nielsen A, Mathiasen AB, et al. Enrichment of autologous fat grafts with ex-vivo expanded adipose tissue-derived stem cells for graft survival: a randomised placebo-controlled trial. Lancet. 2013;382:1113–1120.

214. Trojahn Kølle SF, Oliveri RS, Glovinski PV, et al. Importance of mesenchymal stem cells in autologous fat grafting: a systematic review of existing studies. J Plast Surg Hand Surg. 2012;46:59–68.

215. Coleman SR. Structural fat grafting: more than a permanent filler. Plast Reconstr Surg. 2006;118:108S–120S.

216. Seaman SA, Tannan SC, Cao Y, et al. Differential effects of processing time and duration of collagenase digestion on human and murine fat grafts. Plast Reconstr Surg. 2015;136:189e–199e.

217. Kwon SG, Kwon YW, Lee TW, Park GT, Kim JH. Recent advances in stem cell therapeutics and tissue engineering strategies. Biomater Res. 2018 Dec 19;22:36. doi: 10.1186/s40824-018-0148-4. PMID: 30598836; PMCID: PMC6299977.

218. Stem Cells Derived From Fat, James C. Brown, Adam J. Katz, Principles of Regenerative Medicine, Chapter 19, 295-305

219. Caplan A.I., Sorrell J.M.: The MSC curtain that stops the immune system. Immunol Lett 2015; 168: pp. 136-139.

220. Zuk P.A., et. al.: Human adipose tissue is a source of multipotent stem cells. Mol Biol Cell 2002; 13: pp. 4279-4295.

221. Fraser J.K., et. al.: Fat tissue: an underappreciated source of stem cells for biotechnology. Trends Biotechnol 2006; 24: pp. 150-154